UNIVERSITÀ DEGLI STUDI
DI MILANO

PhD in Experimental, Clinical and Pharmacological Sciences

Department of Pharmacological and Biomolecular Sciences

XXXIII Cycle

BIO/14

A mechanistic approach to synaptic plasticity and cognition: synaptic stabilization of NMDARs through the novel interactor Rabphilin-3A

Candidate: LUCA FRANCHINI

Student Number: R11877

Main Supervisor: Prof. Fabrizio Gardoni

External Co-Supervisor: Prof. Camilla Bellone

PhD Coordinator: Prof. Alberico Luigi Catapano

A.A. 2019/2020

Index

ABSTRACT (English)

The glutamatergic synapse is involved in the modulation of higher brain functions, such as learning and memory processes. The activation of specific subtypes of N-methyl-D-aspartate-type glutamate receptors (NMDARs) located at synapses accounts for different electrophysiological properties of neurotransmission and consequent synaptic plasticity mechanisms. NMDAR subunit composition is relevant for physiological neuronal functions and is often altered in many neurological disorders. In particular, augmented levels of synaptic NMDARs containing the GluN2A subunit can be observed after potentiation of neurotransmission during Long-Term Potentiation (LTP). Several studies revealed that LTP at hippocampal synapses underlies encoding and consolidation of memory.

Rabphilin-3A (Rph3A) was recently characterized as a specific GluN2A intracellular binding partner promoting stabilization of GluN2A containing NMDARs at postsynapses through a trimeric complex with the main postsynaptic scaffolding protein PSD-95. Silencing of Rph3A or disruption of Rph3A/GluN2A/PSD-95 interactions leads to reduction in GluN2A-containing NMDARs due to receptor endocytosis. The modulation of this complex in the striatum of parkinsonian animals showing a dyskinetic behavior was able to restore normal locomotive behavior, indicating Rph3A could represent a new pharmacological target in brain diseases. However, the role of Rph3A in hippocampal functions such as synaptic plasticity and learning and memory has not yet been elucidated. In the present PhD project we aimed to investigate the role of Rph3A/GluN2A/PSD-95 complex in these events applying different stimulation protocols both *in vitro* and *in vivo*. In addition, we investigated the possible interplay between these synaptic complexes and the synapse-to-nucleus messenger Ring Finger Protein 10 (RNF10).

We discovered that Rph3A is present in almost 50% of hippocampal dendritic spines at resting conditions. However, after potentiation of neurotransmission the number of Rph3A positive spines increases, paralleled by augmented formation of Rph3A/GluN2A/PSD-95 trimeric complex. Interference with Rph3A/GluN2A interaction through different experimental approaches leads to failure in LTP induction both at molecular and morphological levels, impairing also hippocampal dependent spatial learning. Dendritic spines displaying Rph3A show higher maturation degree in morphological parameters and recruit more newly-synthetized proteins compared to Rph3A negative ones, suggesting that Rph3A positive spines represent more stable and mature neuronal connections. Furthermore, the molecular motor transporter Myosin-VA was previously described as a binding partner of Rph3A and involved in GluA1-containing AMPA receptors delivery to synapses during synaptic potentiation. Interestingly, a trimeric complex composed by Rph3A/MyoVA/GluA1 is detected in hippocampus and their interaction is increased after cLTP application. Finally, our results show that impairing the synapse-to-nucleus transport of RNF10 during chemical-LTP is

detrimental for Rph3A synaptic localization, indicating the integration of synapse-to-nucleus signals during synaptic plasticity probably impacts on Rph3A postsynaptic functions.

In conclusion, our results suggest that Rph3A postsynaptic role is not only given by the stabilization of GluN2A containing NMDARs accounting for adequate LTP induction and hippocampal learning process, but also for modulation of synaptic responsiveness through the delivery of GluA1-containing AMPA receptors during synaptic potentiation.

ABSTRACT (Italiano)

La sinapsi glutamatergica è coinvolta in funzioni cognitive complesse quali apprendimento e memoria. L'attivazione di specifici sottotipi del recettore N-Metil-D-Aspartato (NMDAR) localizzati in sinapsi è responsabile delle diverse proprietà elettrofisiologiche di neurotrasmissione e dei conseguenti meccanismi di plasticità sinaptica. La composizione del recettore NMDA nelle sue subunità è importante per le fisiologiche funzioni neuronali, ma al contempo si è dimostrata alterata nelle principali patologie del sistema nervoso centrale. In particolare, i livelli sinaptici di recettore NMDA contenente la subunità GluN2A aumentano dopo potenziamento della neurotrasmissione, quale ad esempio il Potenziamento a Lungo Termine (LTP). Diversi studi hanno dimostrato come il fenomeno di LTP alle sinapsi ippocampali sia responsabile del processamento e consolidamento della memoria.

Di recente, Rabphilin-3A (Rph3A) è stata identificata come una specifica partner intracellulare della subunità GluN2A, responsabile della stabilizzazione del recettore NMDA contenente la subunità GluN2A in postsinapsi attraverso un complesso trimerico con la principale proteina scaffolding postsinaptica, PSD-95. Silenziamento dell'espressione genica di Rph3A o interferire con la formazione del complesso Rph3A/GluN2A/PSD-95 determina endocitosi dei recettori NMDA contenenti subunità GluN2A, con conseguente riduzione dei livelli presenti in membrana. La modulazione di questo complesso nello striato di animali parkinsoniani resi discinetici è in grado di ripristinare un normale controllo locomotorio, indicando come Rph3A possa rappresentare un nuovo target farmacologico per patologie cerebrali. Tuttavia, il ruolo di Rph3A nelle funzioni ippocampali come plasticità sinaptica e apprendimento e memoria non è ancora stato investigato. Nel presente progetto di Dottorato, abbiamo investigato il ruolo del complesso Rph3A/GluN2A/PSD-95 in tali eventi applicando diversi protocolli di stimolazione sia in vitro che in vivo. In aggiunta abbiamo indagato un possibile relazione tra questi complessi sinaptici e il mediatore sinapto-nucleare Ring Finger Protein 10 (RNF10).

I nostri risultati hanno dimostrato come la proteina Rph3A sia presente in circa il 50% delle spine dendritiche ippocampali in condizioni basali. Tuttavia, dopo potenziamento della neurotrasmissione il numero di spine Rph3A positive aumenta, in parallelo con la formazione del complesso Rph3A/GluN2A/PSD-95. Interferire con l'interazione Rph3A/GluN2A attraverso diverse procedure sperimentali non consente di indurre le conseguenze molecolari e morfologiche di LTP, determinando anche fallimento nell'apprendimento spaziale ippocampo-dipendente. Le spine dendritiche Rph3A positive dimostrano maggior grado di maturazione in parametri morfologici e arruolano maggior quantità di proteine neosintetizzate, suggerendo come le spine Rph3A positive rappresentino siti di neurotrasmissione più stabili e maturi rispetto alle spine in cui è assente Rph3A. Inoltre il motore-molecolare Miosina-VA (MyoVA) è stato dimostrato interagire con la proteina Rph3A e coinvolto nel trasporto dei recettori AMPA

contenenti la subunità GluA1 nelle spine dendritiche durante il potenziamento sinaptico. Abbiamo rilevato un complesso trimerico formato da Rph3A/GluA1/MyoVA in ippocampo e l'applicazione di cLTP favorisce l'interazione tra le sue componenti. Infine, i nostri risultati mostrano come interferenza con il trasporto sinapto-nucleare di RNF10 durante cLTP sia deleteria per la localizzazione sinaptica di Rph3A, indicando come l'integrazione dei segnali sinapto-nucleari durante plasticità sinaptica probabilmente impatti sulle funzioni postsinaptiche di Rph3A.

In conclusione, i nostri risultati suggeriscono come il ruolo postsinaptico di Rph3A non sia relegato alla sola stabilizzazione dei recettori NMDA contenenti la subunità GluN2A, responsabili di corretta induzione di LTP e processi di apprendimento ippocampali, ma sia anche coinvolta nella modulazione della responsività sinaptica attraverso trasporto sinaptico di recettori AMPA contenenti subunità GluA1 durante il potenziamento sinaptico.

INTRODUCTION

1. The Glutamatergic synapse

L-glutamate (GLUT) is not only an aminoacid important for protein synthesis, but it is also the most common excitatory neurotransmitter used at the Central Nervous System (CNS) synapses.

The glutamatergic synapse is characterized by the presence of a presynaptic neuron able to release glutamate in the synaptic cleft onto a postsynaptic cell. In particular, as shown in Fig. 1, the presynaptic neuron converts at the presynaptic terminal Glutamine into Glutamate via Glutaminase enzyme. Glutamate is then stored in synaptic vesicle through vGLUT transporter; these vesicles are maintained at the Active Zone (AZ) of presynaptic terminal waiting for exocytosis. Action potential reaching the presynaptic terminal activated Ca^{2+}-voltage gated channels which increase Ca^{2+} in presynapse promoting exocytosis. Release of neurotransmitter is also promoted by activation of Protein Kinase A (PKA; Jin et al. 2012).

Once in the synaptic cleft, GLUT diffuses and interacts with both pre and postsynaptic glutamate receptors (GluRs). Depending on ion-channel characteristics or intracellular second messenger activation, GluRs are distinguished in ionotropic receptors (iGluRs) and metabotropic receptors (mGluRs) respectively. At hippocampal glutamatergic postsynapse, we can detect among iGluRs the N-methyl-D-Aspartate receptors (NMDARs) and α-amino-3-hydroxy-5-methyl-4-isoxazolepropionic acid receptor (AMPAR), while among mGluRs in particular mGluR1/5. Glutamate is generally re-uptaken from astrocytes and converted to glutamine which then is delivered to presynaptic terminals.

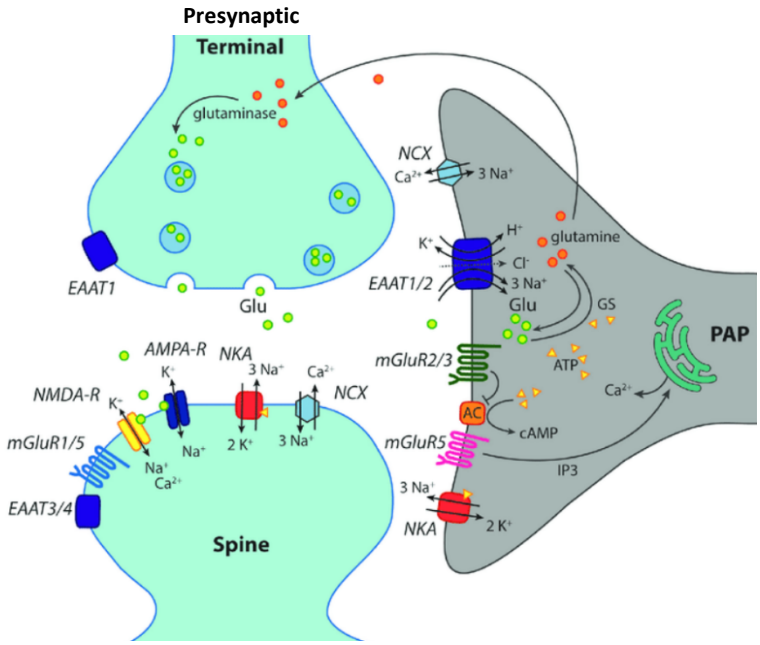

Figure 1. Representative scheme of a tripartite glutamatergic synapse in hippocampus. The picture displays a presynaptic terminal and a postsynaptic spine as well as a perisynaptic astrocyte process (PAP) reaching close to the synaptic cleft. In addition to ionotropic (NMDA, AMPA) and metabotropic (mGluR) receptors for glutamate, glutamate transporters (EAAT1-4) are indicated. Moreover, main mechanisms of ion transport across the plasma membrane, such as the Na + /K +-ATPase (NKA) are schematically shown. GS, glutamine synthase; AC, adenylate cyclase; NCX, Na + /Ca 2+-exchanger. For further explanations and abbreviations: see text.

2. mGluRs

mGluRs are G-protein coupled receptors (GPCRs) consisting of an extracellular N-terminal domain (NTD) with an agonist binding site (ABD), seven transmembrane spanning domains (TD) and an intracellular C-terminal domain (CTD). The CTD couples to an heteromeric G-protein composed of α, β, and γ subunit and is responsible for downstream signaling. During the inactive state, α subunit of G-protein is bound to Guanosine di-phosphate (GDP) which is switched to Guanosine Tri-Phosphate after receptor activation. GTP is then hydrolyzed to GDP leading to phosphorylation of different effectors; in particular the most relevant are Phospholipase C (PLC), Adenyl Cyclase (AC) and ion-channels (Pin, Galvez, & Prézeau, 2003).

The mGluRs widely expressed in the CNS and are encoded by 8 different genes with several splice variants. According to ligand selectivity, G-protein coupling and sequence homology mGluRs are classified in three main groups:

- Group 1 of mGluRs consists of mGluR1-5, which are mostly located postsynaptically and involve PLC activation and MAP kinase phosphorylation.

- Group 2 of mGluRs consists of mGluR2-3, which are present pre- and postsynaptically, inhibiting AC and Calcium (Ca2+) channels while promoting Potassium (K+) channels opening.
- Group 3 of mGluRs consists of mGluR4-6-7-8 widespreaded from retinal cells to cerebellar neurons, with similar signaling to Group 2 of mGluRs (Niswender & Conn, 2010; Pin et al., 2003).

Given these characteristics of mGluRs, they are responsible of neurotransmission modulation both at pre- and postsynaptic sites, leading to increase or reduction in plasma membrane potential.

3. iGluRs

iGluRs are cation-permeable receptors which activation leads to depolarization of the plasma membrane; thus, their effect drives excitatory postsynaptic currents (EPSC) on postsynaptic cells. iGluRs consist of three different classes of receptors such as NMDARs, AMPARs and Kainate receptors (KRs). In particular, the NMDARs and AMPARs will play a major role in the topic of this PhD thesis, thus they will be described in more details compared to other glutamate receptors.

4. AMPA Receptors

AMPARs are heterotetrameric combination of different GluA1-4 subunits, permeable to Sodium (Na+) and/or Ca2+ (Mark L. Mayer, 2017; Wollmuth, 2018). This characteristic is dictated by the presence of a specific GluA2 subunit variant with an Arginine (R; GluA2R) or Glutamine (Q; GluA2Q) at the pore channel. GluA2Q, GluA1, GluA3 and GluA4 constitute calcium-permeable AMPARs; while GluA2R leads to Ca^{2+}-impermeability (Wollmuth, 2018). Ca^{2+}-permeable AMPAR have been associated with excitotoxicity and neurodegeneration (Henley & Wilkinson, 2016). GluA1-A2 subunits are the dominant components of AMPARs at region CA1 of hippocampus (W. Lu et al., 2009). Interestingly, GluA1 subunit displays two phosphorylation residues at CTD such as Serine-845 (S845) and S831, which are relevant for stabilization of the receptor at plasma membrane during synaptic plasticity (Otmakhov et al., 2004).

Fast excitatory currents at glutamatergic synapses are given by AMPAR activation (Malinow & Malenka, 2002). Depending on the magnitude of this event, postsynaptic depolarization can reach the activation threshold for NMDARs, as described later. AMPAR presence at the PSD is modulated by interaction with so called “auxiliary subunits” which are scaffolding proteins affecting also receptor functions. The TARPs family is the most studied “auxiliary subunits” class and stargazing is the prototypical one, promoting AMPAR maintenance in PSD through interaction with Postsynaptic Density protein of 95KDa, PSD-95. Other AMPAR interacting proteins are PICK1 and GRIP which represent scaffolding proteins for receptor stabilization at plasma membrane (Mignogna et al., 2015; Xia, Zhang, Staudinger, & Huganir, 1999).

5. NMDARs

NMDARs display peculiar pharmacological properties, since their pore channel is blocked in resting conditions by Magnesium Ions (Mg2+), which is removed by adequate depolarization giving rise to the ion-flow of Ca2+ and Na+. Given these characteristics, NMDARs have been considered a coincident detector of presynaptic glutamate release and postsynaptic depolarization (Seeburg et al., 1995). NMDARs have been considered exclusively located at the postsynaptic membrane (PSD); however, several studies identified NMDARs in the presynapse ranging from neocortex to hippocampus and cerebellum (Berretta & Jones, 1996; Bidoret, Ayon, Barbour, & Casado, 2009; Casado, Dieudonné, & Ascher, 2000; McGuinness et al., 2010; Siegel et al., 1994; Sjöström, Turrigiano, & Nelson, 2003).

From a cellular point of view, NMDARs are not only located at the PSD but also in extrasynaptic sites, defining different pools of receptors involved in several forms of synaptic plasticity events. Furthermore, synaptic NMDARs are commonly associated to pro-survival signaling and improvement of neurotransmission, while extrasynaptic NMDARs mostly mediate glutamate excitotoxicity and are detrimental for dendritic spine remodeling, also leading to neuronal death (Bell & Hardingham, 2011; G. E. Hardingham & Bading, 2010; Luo, Wu, & Chen, 2011).

Beside the increased Ca^{2+} concentrations given by NMDAR activation, recently also a metabotropic signaling involving not clear “signalosomes” has been been associated with receptor activity independently of ion-flow. This aspect certainly complicates the understanding of this receptor in neuronal functions (Barria & Malinow, 2002; Ferreira et al., 2017; Nong et al., 2003; Vissel, Krupp, Heinemann, & Westbrook, 2001).

NMDARs are tetrameric receptors composed by two obligatory subunits GluN1 combined with two regulatory subunits of GluN2 and/or GluN3 type. In particular the regulatory subunits are expressed in several isoforms as GluN2A-D and GluN3A-B. The combination of two identical regulatory subunits leads to di-heteromeric NMDARs while assembly of two different regulatory subunits to tri-heteromeric NMDARs. Diverse NMDAR subtypes display different pharmacological and intracellular signaling properties (Paoletti, Bellone, and Zhou 2013). Noteworthly, the qualitative and quantitative composition of NMDARs is spatio-temporally regulated and dependent on the brain region considered.

For example, GluN2B-2D and GluN3A-3B subunits are more expressed in early neuronal stages, while GluN2A-2C are more abundant in mature ones redefining the subset of receptors in adult conditions (Akazawa, Shigemoto, Bessho, Nakanishi, & Mizuno, 1994; Monyer, Burnashev, Laurie, Sakmann, & Seeburg, 1994; Sheng, Cummings, Roldan, Jan, & Jan, 1994). In adult hippocampus, neocortex and striatum both GluN2A and GluN2B subunits represent the most abundant synaptic regulatory subunits. However, GluN2A/GluN2B ratio is in favor of GluN2A in hippocampus and neocortex while in the striatum there is an opposite situation with predominant GluN2B (Gardoni and Bellone 2015; Paoletti, Bellone, and Zhou 2013)

General structure of NMDAR subunits

As shown in Fig.2, each subunit of NMDAR can be divided in an extracellular NTD, a TD and an intracellular CTD. On NTD is located the ABD for Glycine (or D-serine, on GluN1 and GluN3 subunits) or Glutamate (on GluN2 subunits) (Johnson & Ascher, 1987). The TD is involved in Mg^{2+} interaction through Asparagine residues located on M2 loop of GluN1 and GluN2 subunits (Wollmuth, Kuner, & Sakmann, 1998). The CTDs of NMDAR subunits display more differences in length and aminoacidic (aa) sequence homology compared to TDs and NTDs (Groc et al., 2006; G. Hardingham, 2019; Stephen F. Traynelis et al., 2010). The biological meanings of GluN-CTDs differences are

i) common and different intracellular protein interactors (G. Hardingham, 2019; Sun et al., 2018);
ii) different phosphorylation sites responsible for fast modulation of receptor activity and trafficking (B. S. Chen & Roche, 2007; Grau et al., 2014; Hawkins et al., 2004).

In particular, CTD phosphorylation residues are involved in receptor recycling and triggering or maintenance of specific synaptic plasticity events (B. S. Chen & Roche, 2007; Grau et al., 2014; B. Li et al., 2002; B. S. Li et al., 2001; Snyder et al., 2001).

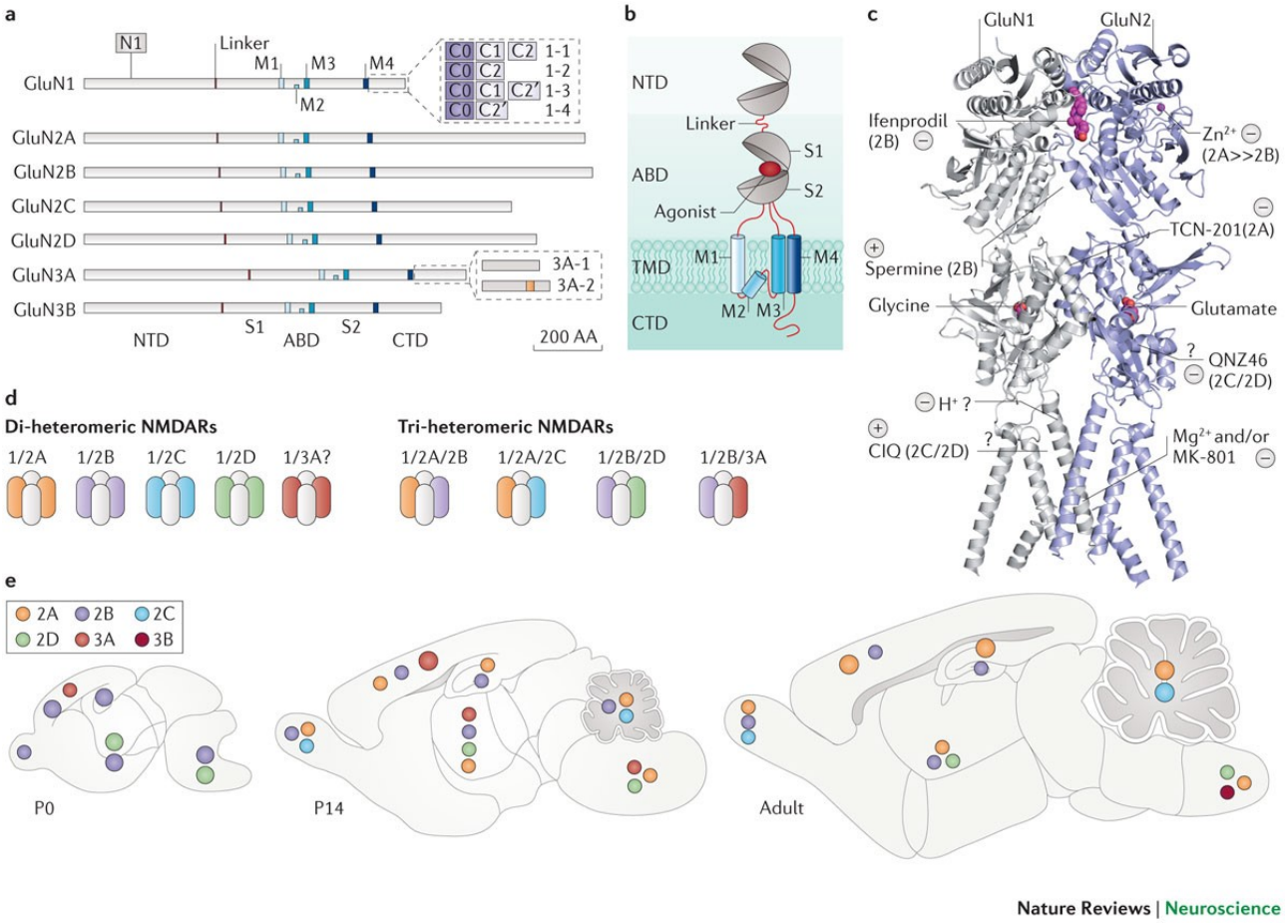

Figure 2. NMDAR subunits display a modular architecture. NMDRs Extracellular harbor with multiple binding sites for small molecules acting as allosteric modulators. A sample of various populations of diheteromeric and tri-heteromeric NMDARs. (Paoletti, Bellone and Zhou, 2013).

6. Dendritic spines and synaptic plasticity

Dendritic spines are bulbous protrusions along dendritic shaft, where excitatory neurotransmission takes place. In particular, dendritic spines display a spine head connected to dendrites through a narrow neck. However, depending on the shape of spines we can distinguish i) mushroom spines, ii) stubby spines, iii) thin spines (K. M. Harris, Jensen, & Tsao, 1992; C. Sala & Segal, 2014).

i) Mushroom spines are considered the more stable and mature type of dendritic spines. They represent a stable connection between neuronal cells and they are characterized by a large spine head, with narrow neck. This is why they are considered as memory spines, due to their higher stability.

ii) Stubby spines are instead characterized by no visible constriction between head and neck. They are mostly detected in early postnatal stages, but are scarce in mature brain.

iii) Thin spines display a longer neck and smaller head compared to mushroom spines. They are also named as “learning spines”, since they can be stabilized to mushroom spines, but also eliminated

depending on type and intensity of stimulation (Kristen M Harris, Jensen, and Tsao 1992; Majewska, Newton, and Sur 2006; Peters and Kaiserman-Abramof 1970, K. M. Harris, Jensen, and Tsao 1992).

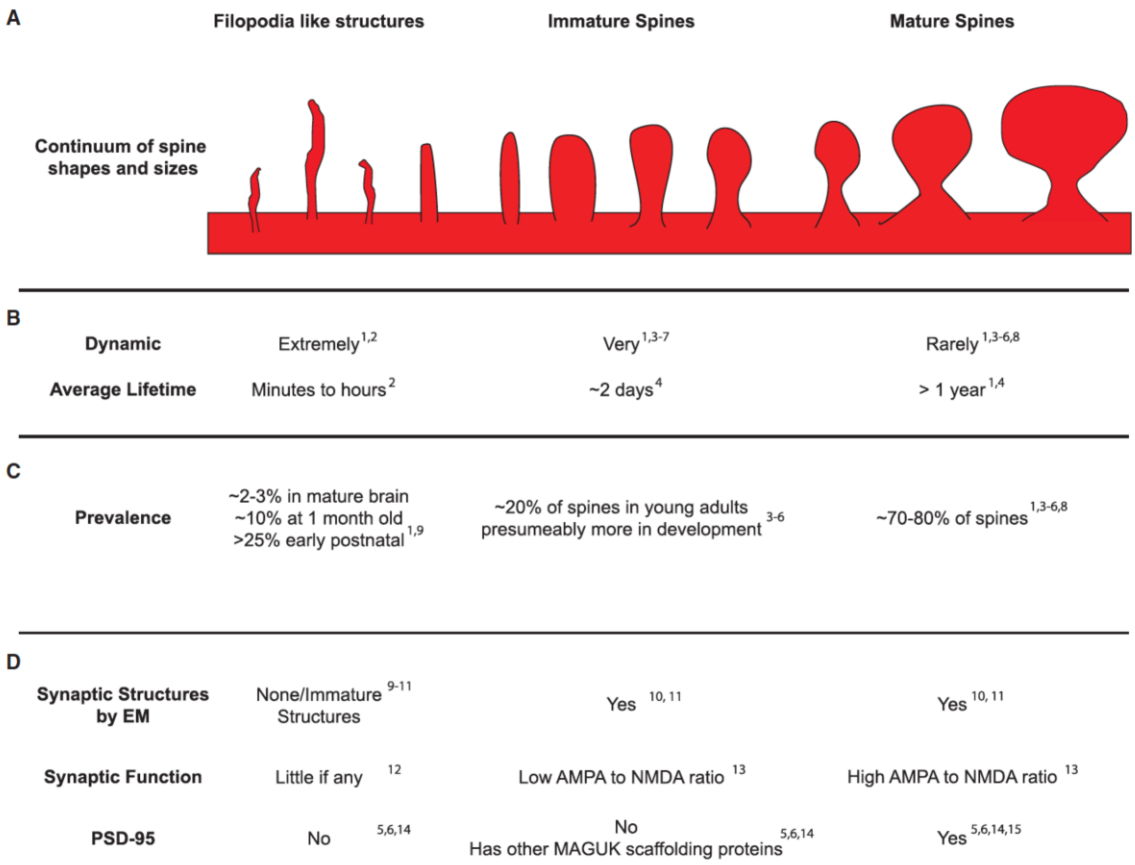

Figure 3. Spines Exist on a Continuum of Morphologies and Functions from Nonfunctional Filopodia-like Structures to Large Mature Spines. (A) Diagram showing continuum of spine shapes. These spines can be grouped into three separate categories, filopodia-like structures, immature spines, and mature spines. Distinguishing between these categories based on morphology is extremely difficult due to the limited resolution of light microscopy. (B) The history of a spine can distinguish between these types. (C) In adults, the majority of spines contain a mature synaptic contact, while 20% are either immature or filopodia like. (D) The three categories of spines are difficult to distinguish based on any one category alone. However, by comparing across several criteria the differences become clearer.

Filopodia are often excluded from dendritic spine classification, since they represent a first attempt to generate dendritic spines and they are characterized by the lowest stability. Filopodia display a long and thin structure without visible spin head; in fact, they are not yet in stable contact with a presynaptic terminal. Filopodia are then turned to “protospine” by connecting to a presynaptic bouton, and then eventually shaped to one of the three other type of spines (Dailey & Smith, 1996; Freire, García-López, & García-Marín, 2010). Dendritic spines are characterized by dynamism in shape and receptor organization occurring in the postsynaptic density (PSD) apposed to the active zone of presynaptic terminal. The PSD region is enriched in

scaffolding and signaling proteins interacting with postsynaptic receptors, such as NMDARs and AMPARs at glutamatergic synapses (Sheng & Sala, 2001).

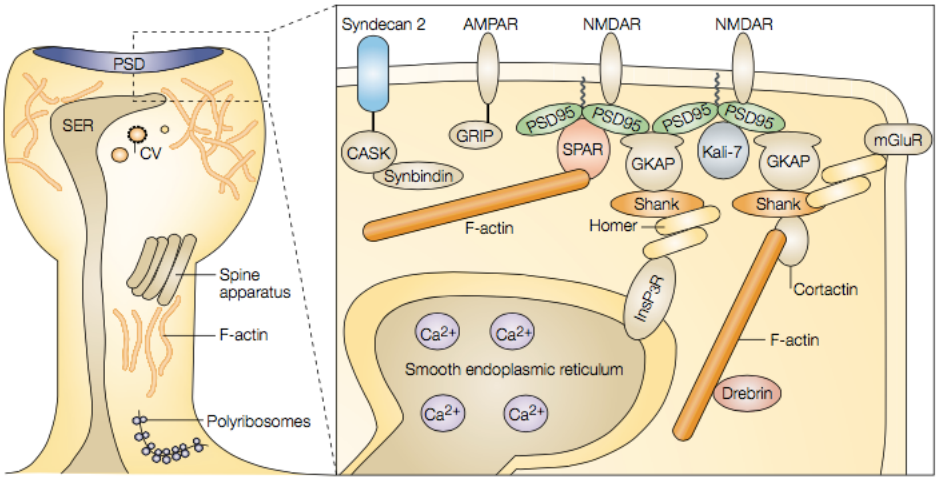

Figure 4. Structure of a mushroom dendritic spine. In dendritic spines we can detected smooth endoplasmic reticulum which extends from dendritic shaft and represents an intracellular source of calcium. Furthermore, Polyribosomes were detected between polyribosomes and spine neck, indicating local protein synthesis occurs in proximity of dendritic spines. In the scheme above, some of the most relevant protein-protein interaction at PSD are depited. The figure is adapted from Hering and Sheng (2001).

During neurodevelopment, neuronal spines are characterized by lower stability rate in spite of higher spine density and filopodia amount. Between adolescence and adulthood, dendritic spines undergo a tight selection and shrinkage, thus only specific neuronal connections are maintained while other are eliminated. The remaining spines are then stabilized to mushroom and thin spines, mostly (Dailey & Smith, 1996; Freire et al., 2010). Among scaffolding proteins, as reported in Fig. 4, PSD-95 represents one the most abundant proteins and it represents a marker of spine stability (E. Kim & Sheng, 2004). In fact, PSD-95 displays 3 PDZ-domains which are used for protein-protein interaction with NMDARs (Kornau, Schenker, Kennedy, & Seeburg, 1995) and AMPARs through TARPs interaction (Tomita, Sekiguchi, Wada, Nicoll, & Bredt, 2006).

Synaptic plasticity is represented by synaptic adaptation mechanisms following specific environmental stimuli. Different mechanisms lead to molecular and structural modifications of the neurotransmission at dendritic spines, which represent the locus of structural and functional synaptic plasticity underling higher brain functions (C. Sala & Segal, 2014). Strengthening of specific synapses, destabilization of others and formation of new ones, underlies the experience-dependent plasticity processes (Bourne & Harris, 2012; Caroni, Donato, & Muller, 2012; Hill & Zito, 2013; Kasai et al., 2010). Therefore, adequate synaptic plasticity mechanisms at dendritic spines are required for elaboration of complex cognitive functions such as learning and memory. The main synaptic plasticity events underling higher brain functions are Long Term Potentiation (LTP) and Long-Term Depression (LTD) promoting different molecular and cellular consequences, as described later.

LTP implies a long lasting increase in neurotransmission with dendritic spine potentiation; while LTD is represented by reduced neurotransmission, accompanied by destabilization of dendritic spines promoting spine shrinkage and retraction (Chidambaram et al., 2019). However, the "Long-Term" definition implies a time dependent feature which should always be considered in experimental studies. Neuroscientists addressed as "Long-Term" events in synaptic plasticity, those consequences maintained from a few hours in vitro, to several hours and days ex vivo and in vivo (Frey & Morris, 1998; Redondo et al., 2010). A common feature of LTP and LTD is the need of intracellular Ca^{2+}, in particular LTP requires higher Ca2+ concentrations compared to LTD (Bear & Malenka, 1994; Lisman, 1989; Malenka & Bear, 2004). However, recently also the spike timing theory proved a different impact on synaptic plasticity, depending on the timing of stimulation and frequency used (Rao-Ruiz, Yu, Kushner, & Josselyn, 2019; Shouval, Bear, & Cooper, 2002)

From a molecular and cellular point of view, early modifications of neurotransmission are allowed by already present sources of enzymes, receptors, scaffolding proteins in situ, which are rearranged to set up the adaptive responses (Frey & Morris, 1998). During early phases of these changes, new components also derive from local pools of mRNA translated to proteins in dendrites and spines (Dieck et al., 2015; Hering & Sheng, 2001) which are then directed to target areas. Blocking protein synthesis during LTP protocols on hippocampal slices does not impair LTP induction but affects LTP maintenance (Frey & Morris, 1998). This observation indicates long lasting changes in synaptic transmission require protein synthesis, in particular the somatic translation supports the initial local one. Overall, these observations indicate a bidirectional communication must exists between synapse and nucleus in order to maintain basal and active states of synapses (Carrano et al., 2019; Dinamarca et al., 2016; Karpova et al., 2013; Marcello, Di Luca, & Gardoni, 2018; Panayotis, Karpova, Kreutz, & Fainzilber, 2015).

From an anatomical point of view, the main brain regions involved learning and memory are neocortex and hippocampus, which display an abundant glutamatergic neuronal population with a few percentage of inhibitory neurons (Bezaire & Soltesz, 2013). Noteworthly, hippocampal connections with other brain regions such as striatum, are relevant for goal-directed and habitual behavior through feedback based learning and memory (Balleine & O'Doherty, 2010; Shohami & Biegon, 2014; Yin & Knowlton, 2006). Interestingly, these circuits are eventually modulated by other type of neurotransmitters such as noradrenaline and dopamine (H. Hu et al., 2007; Seol et al., 2007; Wagatsuma et al., 2017). The most common brain circuit studied for LTP and LTD is the enthorinal cortex(EC)-hippocampal(HP) pathway (Figure 5), which is involved in different forms of learning: from spatial to social memory, fear memory and context recognition (Morris, Garrud, Rawlins, & O'Keefe, 1982; Okuyama, Kitamura, Roy, Itohara, & Tonegawa, 2016; Redondo et al., 2014). As shown in Fig. 5, EC terminals make synapse with granule cells from dentate gyrus (DG) of hippocampus, or encompasses DG directly communicating with mossy fibers of hippocampal CA3 (perforant pathway). From DG information passes in CA3 and then to CA1 via Schaffer collateral from mossy fibers. From CA1 region,

neurotransmission moves to subiculum and/or EC again (Park, Bae, Yoon, & Ko, 2018). Most of the studies on LTP/LTD use ex vivo fresh hippocampal slices. In particular LTP is mimicked by electrophysiological high frequency stimulation (HFS) on Schaffer collateral of CA3-CA1 or theta burst stimulation (TBS), while LTD with low frequency stimulation (LFS).

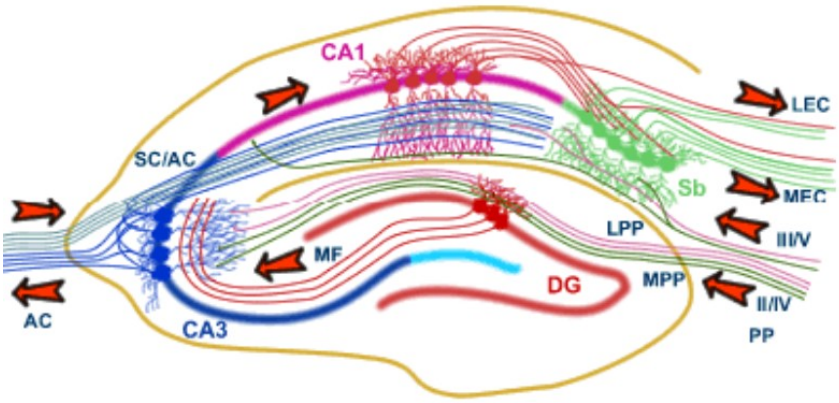

Figure 5. Enthorinal cortex-hippocampal circuitry. Enthorinal cortex divided in medial (MPP) and lateral (LPP) perforant pathways, Dentate Gyrus (DG), Lateral enthorinal cortex (LEC), medial frontal cortex (MFC), subiculum (Sb). (Adapted from http://www.bristol.ac.uk/synaptic/pathways/).

Understanding how the glutamatergic neurotransmission in the brain affects cognition may lead to new pharmacological strategies for several neurological disorders, where learning and memory processes are deficitary (S. Li et al., 2011; Snyder et al., 2005).

Long-Term Depression (LTD)

LTD results from a lower neurotransmission accounting for dendritic spine weakening and is thought to be relevant for removal of memories in adults (Dumas, 2005).

From a molecular perspective, the Ca2+ source for LTD induction may derive from NMDARs during low synaptic transmission, +. However, the involvement of non-NMDARs Ca2+ sources increases in low frequency paired-pulse synaptic stimulation protocols (Huber, Kayser, & Bear, 2000; N. Kemp & Bashir, 1997; Nicola Kemp, McQueen, Faulkes, & Bashir, 2000). In hippocampus, over time there is an increased LTD susceptibility due to a reduction in NMDAR functions (Bodhinathan, Kumar, & Foster, 2010) paralleled by augmented contribution to synaptic plasticity of L-type Ca2+ channels (VDCCs) (Norris, Halpain, & Foster, 1998) and intracellular Ca2+ stores (Kumar & Foster, 2005).

Different protocols for LTD induction can be found in literature, for example, through application of different drugs it is possible to obtain a chemically-induced LTD (cLTD). Application of Group 1 mGluR agonists such as R,S-3,5-dihydroxyphenylglycine (DHPG) (Huber et al., 2000; Huber, Roder, & Bear, 2001; Izumi & Zorumski, 2012) or NMDA in a Mg2+ supplemented medium (Marcello et al., 2013; Oh, Derkach, Guire, & Soderling, 2006). Interestingly, group 1 mGluR dependent LTD is induced in CA1 region of hippocampus (Oliet, Malenka, & Nicoll, 1997); however, these receptors were also reported to prime LTP (A. Cohen, Raymond, & Abraham, 1998; Mellentin, Jahnsen, & Abraham, 2007; Van Dam et al., 2004) and to drive subunit switch of GluN2B to GluN2A in hippocampus itself (Matta, Ashby, Sanz-Clemente, Roche, & Isaac, 2011). A hallmark of LTD process is the removal of AMPARs from PSD (Collingridge, Peineau, Howland, & Wang, 2010).

From a morphological point of view, LTD also influences dendritic spine shape and numbers; in particular, LTD leads to dendritic spine destabilization and shrinkage, with consequence reduction in dendritic spine density (Bastrikova, Gardner, Reece, Jeromin, & Dudek, 2008; Monfils & Teskey, 2004; Zhou, Homma, & Poo, 2004).

Long-Term Potentiation (LTP)

LTP represents a drastic implementation in neurotransmission which may involve both pre and postsynaptic components, by increasing the probability of neurotransmitter release and/or responsiveness of postsynaptic compartment respectively (Malenka & Bear, 2004).

From a molecular point of view at hippocampal glutamatergic synapses, upon neurotransmitter release, AMPARs activation mediates subsequent depolarization promoting NMDARs opening, and the consequent Ca2+ influx triggers a variety of signaling cascades, dependent on the frequency and the intensity of the stimulation. Strengthening of the synapse is induced by insertion of GluA1-containing AMPARs at lateral side of PSD, which are surface stabilized via phosphorylation at Ser-845 (Joiner et al., 2010). In fact, augmented AMPARs in PSD also increase responsiveness to the GLUT released from presynapse, thus resulting in a potentiated neurotransmission (see Figure 6).

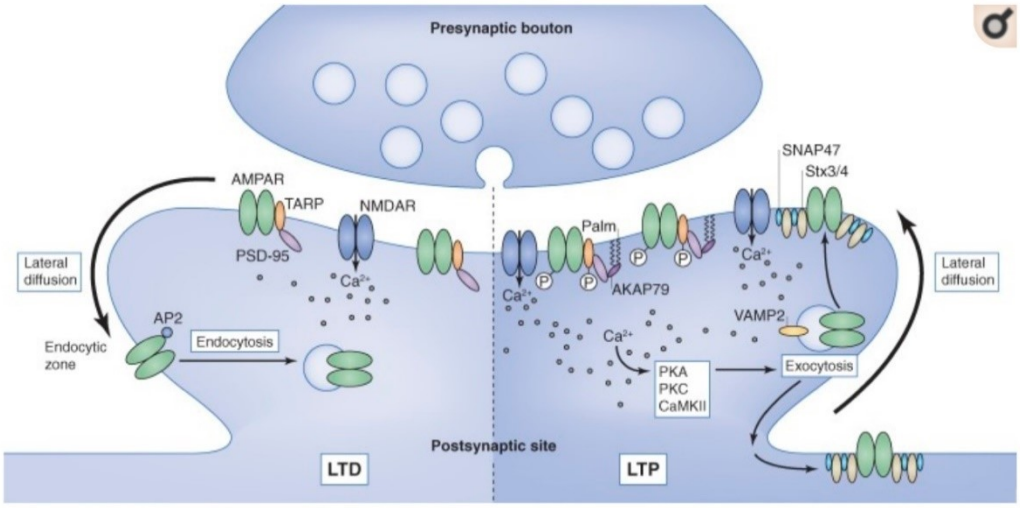

Figure 6. General description of LTD (left) and LTP (right) mechanisms. Depression of synaptic transmission is reflected by low Ca^{2+} influx promoting phosphatase activation AMPAR internalization, and thus reduced responsiveness of postsynapse. LTP is triggered by higher Ca^{2+} concentrations and promotes kinase activation with AMPAR insertion in PSD. (Adapted from Vitureira and Goda 2013).

As shown in Figure 7, iGluRs reorganization at synapses is the result of different biological strategies i) the receptors are rapidly removed by endocytosis, ii) moved from extrasynaptic sites to the PSD and iii) exocited from intracellular pools. In this way, also the composition and the total amount of synaptic NMDARs reflects specific adaptation mechanisms accounting for potentiation of spines (Barria & Malinow, 2002; Bellone & Nicoll, 2007; Grosshans, Calyton, Coultrap, & Browning, 2002).

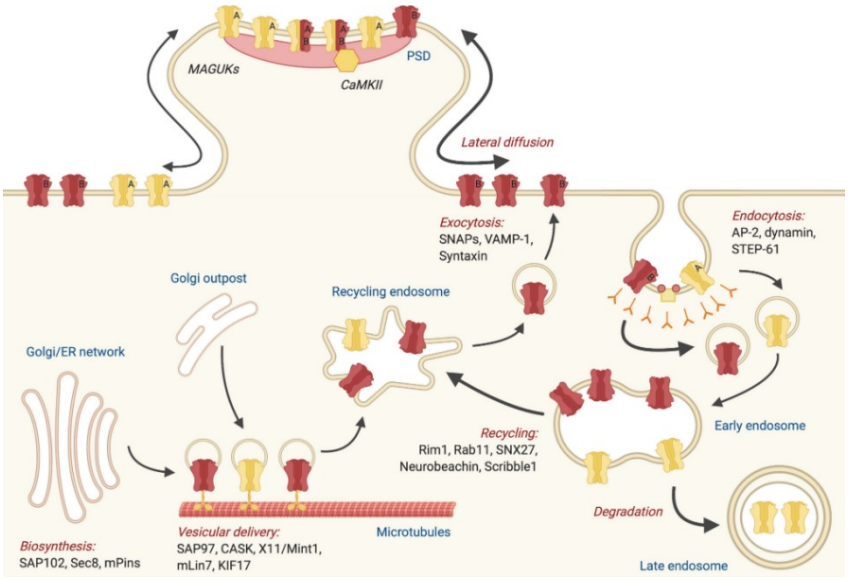

Figure 7. Routes of NMDARs trafficking. NMDARs are moved from lateral side of PSD, eventually exocyted or endocyted. Endosomes derive from Golgi/ER network and are trafficked through molecular motors along microtubule cytoskeleton to target regions. Endosomes are then fused into recycling endosomes, which can be exocyted or converted to late endosomes for degradation. (Adapted from Vieira et al. 2020).

From a structural and morphological point of view, as mentioned for LTD, also LTP affects dendritic spine shape, dimensions and number. In particular, dendritic spine density differently augments over time depending on the biological model considered and the type of stimulation. For example, LTP induction increases spine density in dissociated neuronal slice cultures within 30 minutes (Segal, 2005); while in vivo time-lapse imaging of neocortex reported augmented spine density after 4 days (Knott, Holtmaat, Wilbrecht, Welker, & Svoboda, 2006). Furthermore, activation of synaptic glutamate receptors during LTP promotes increase in dendritic spine head volume (Kopec, Li, Wei, Boehm, & Malinow, 2006; Lang et al., 2004), which is maintained over time through intracellular kinases (Y. Yang, Wang, Frerking, & Zhou, 2008). This occurrence leads to accumulation in PSD of glutamate receptors (Kopec et al., 2006), F-actin (Kramár, Lin, Rex, Gall, & Lynch, 2006), polyribosomes (Ostroff, Fiala, Allwardt, & Harris, 2002) and mitochondria (Z. Li, Okamoto, Hayashi, & Sheng, 2004). Generally, an augmented spine head volume correlates with improved synaptic strength, paralleled by less plasticity, thus providing the explanation of mushroom spines considered as the "memory spines" while thin spine the "learning spines" (Grutzendler, Kasthuri, & Gan, 2002; Trachtenberg et al., 2002).

On in vitro models such as hippocampal primary cultures and ex vivo brain slices it is also possible to induce a chemical LTP (cLTP) through a cocktail of different drugs. Among cLTP protocols, the most frequently employed on hippocampal primary cultures is Glycine application (NMDAR co-agonist) with Bicuculline (GABA A receptor antagonist) and eventually strychnine (sigma receptor antagonist, D. Lim et al. 2018; W. Y. Lu et al. 2001; Mizui et al. 2014). On hippocampal slices mostly a Forskolin/Rolipram cocktail is used to promote cAMP-dependent activation of PKA, which promotes presynaptic release of neurotransmitter (Jin et al., 2012), paralleled by phosphorylation of S845 of GluA1-containing AMPAR, leading to potentiation of neurotransmission (Oh et al., 2006). However, the latter protocol has been also used on hippocampal primary cultures (Franchini et al., 2019; Marcello et al., 2013).

Interestingly, LTP at different hippocampal regions does not always employ NMDAR activation. For example, LTP at CA1 requires NMDARs (Morris, Anderson, Lynch, & Baudry, 1986), on the other hand at mossy fibers in CA3 it does not (Zalutsky & Nicoll, 1990). A seminal research from Morris Richard in 1986 reported that blocking NMDARs through administration of aminophosphonovaleric acid (AP5), completely prevented CA1 hippocampal LTP induction, and hippocampal dependent spatial learning in the Morris Water Maze (MWM) (Morris et al. 1982, 1986). However, in this study scientists did not investigate eventual influence of hippocampal synaptic NMDAR subunit composition accounting for the observed phenotype.

Therefore, over time many efforts have been done to associate specific synaptic plasticity events to synaptic NMDAR subunits, not only in the learning and memory field. Nevertheless, results emerging from the literature are sometimes controversial. In particular, both GluN2A and GluN2B subunits seems to play a role in hippocampal learning and memory tasks (Carrano et al. 2019; Franchini et al. 2019; Kellermayer et al. 2018;

Shipton and Paulsen 2014; Franchini et al. 2020), and this can probably be ascribed to similar and different intracellular interactors of GluN2A and GluN2B subunits, as well as experimental approaches used.

7. Synaptic GluN2A-containing NMDA Receptors

GluN2A subunit pharmacology

GluN2A and GluN2B are by far the most abundant NMDAR regulatory subunits expressed in the mammalian brain (Monyer et al., 1994; Paoletti et al., 2013). GluN2A-containing NMDARs are highly expressed in the adult hippocampus and are more localized at synaptic sites where they are enriched in the PSD compared to extrasynaptic sites (Franchini, Carrano, Di Luca, & Gardoni, 2020; G. E. Hardingham & Bading, 2010; Paoletti et al., 2013)and display a slower mobility compared to other GluN2-containing ones (Groc et al., 2006). Importantly, Synaptic NMDARs mainly mediate pro-survival and synaptic plasticity pathways, associated to maturation of dendritic spines and improved neurotransmission (Luo et al., 2011); whereas extrasynaptic NMDARs are mostly responsible for glutamate excitotoxicity and are detrimental for neuronal functions, often leading to dendritic spine removal and neuronal death (G. E. Hardingham & Bading, 2010; Luo et al., 2011). Furthermore, the balance in synaptic GluN2-type subunits is responsible for adequate glutamatergic neurotransmission, which is altered in several neurological disorders and which is linked to the pathophysiology of brain diseases (Franchini et al., 2020).

The GluN2A subunit is a 1464aa protein encoded by the Glutamate Ionotropic Receptor NMDA Type subunit 2A (GRIN2A) gene in a neurodevelopmental manner and typical of adult neuronal and brain stages, as previously mentioned.

Recently, a GluN2A short isoform was detected in primate and human brains but not in rodents and was shown to assemble with GluN1 subunits leading to functional NMDARs, indicating probably different pools of GluN2A-containing NMDARs in human brain which should be taken into account for future therapeutic strategies involving NMDAR functions (Warming et al., 2019).

GluN2A NTD displays specific residues (H42, H128, K233, and E266) (Fayyazuddin, Villarroel, Le Goff, Lerma, & Neyton, 2000) able to interact with Zinc (Zn^{2+}) ions leading to receptor inhibition and reduced NMDAR currents (N. Chen, Moshaver, & Raymond, 1997; M. L. Mayer & Vyklicky, 1989; Paoletti, Ascher, & Neyton, 1997; Williams, Mason-Parker, Abraham, & Tate, 1998). Furthermore, GluN2A NTD affects receptor structural conformation when subjected to extracellular pH variations, thus providing another peculiar inhibition mechanism. Interestingly, this event was shown to be independent of agonist binding (Banke, Dravid, & Traynelis, 2005) and plasma membrane potential (S. F. Traynelis & Cull-Candy, 1991; Stephen F. Traynelis & Cull-Candy, 1990; Velíšek, Dreier, Stanton, Heinemann, & Moshé, 1994). Most of the studies investigating GluN2A subunit functions in synaptic plasticity exploited the selective antagonist NVP-AM077.

However, what emerges from recent literature is that selectivity towards GluN2A is only 5-10 fold more than GluN2B (Frizelle, Chen, & Wyllie, 2006). Therefore, scientists are now developing Negative Allosteric Modulators (NAM) and Positive Allosteric Modulators (PAM). In particular, the most promising NAMs seem TCN-201 and its derivates (Schreiber et al., 2018; Yi et al., 2016); while among PAMs GNE-5729 displays a better pharmacokinetic profile compared to the ancestor GNE-0723 (Hanson et al., 2020; Villemure et al., 2016; Volgraf et al., 2016).

GluN2A TD displays the M2-loop Asparagine (N) residue involved in Mg2+ interaction at 651 position. Mutation of this residue in Lysine (K) leads to the GluN2A-N651K variant, which displays reduced Mg2+ interaction in spite of low Ca2+ influx, overall indicating a dominant negative variant of GluN2A (ref).

Among GluN2A-CTD phosphorylation sites, Tyrosines (Y) residues such as Y1387 (Salter & Kalia, 2004), Y1105, Y1267 (Zheng, Gingrich, Traynelis, & Conn, 1998) seem to play a role in enhancing receptor activity for example by reducing zinc affinity (Zheng et al. 1998). On the other hand, Y842 seems to be involved in use-dependent receptor endocytosis, with participation of more residues not well identified on the 874-1464 fragment of GluN2A CTD (Vissel et al., 2001). Among other phosphorilation sites, S1232 was shown to enhance receptor activity (B. S. Li et al., 2001; Jian Wang, Liu, Fu, Wang, & Lu, 2003).

The GluN2A-CTD also accounts for lower mobility of the receptor in PSD compared to GluN2B-CTD (Groc et al. 2006), probably depending on different interacting scaffolding proteins involved in receptor trafficking.

GluN2A CTD binding partners

GluN2A CTD displays several interactors some of which are specific for this subunit, while others are in common for example with GluN2B CTD (for review see Sun et al. 2018).The domain of interaction of these proteins on GluN2A CTD is different, but sometimes overlapping, defining a competition for the binding which is also dependent on the active state of the synapse and modulated by synaptic plasticity mechanisms (Franchini et al., 2020). Most of these interactors have been shown to play a role in LTP induction and maintenance.

Among GluN2A binding partners we find i) scaffolding proteins, ii) synapse to nucleus messengers, iii) protein kinases and iv) other proteins.

- scaffolding proteins:

Members of the membrane-associate guanylate kinase (MAGUK) such as Postsynaptic density protein of 95 KDa (PSD-95), PSD-93, SAP102, SAP97 bind to the last 3 aminoacid of GluN2A (1461-1464aa) and promote retention of GluN2A containing NMDARs in PSD (Howard, Elias, Elias, Swat, & Nicoll, 2010; Kornau et al.,

1995; I. A. Lim, Hall, & Hell, 2002; Sheng & Sala, 2001). The Rab-effector protein Rabphilin-3A (Rph3A) binds to 1349-1389aa fragment of GluN2A in association with PSD-95. Interfering with Rph3A-GluN2A-SD-95 protein complex leads to a reduction of synaptic GluN2A receptors (Stanic et al., 2015). Scribble-1 binds to 1458-1464aa sequence of GluN2A and promotes insertion of GluN2A-containing NMDARs via interplay with AP2 (Piguel et al., 2014).

- Synapse to nucleus-messengers:

It is known that signaling cascades initiated at synapses promote immediate and short-term changes in synaptic plasticity. However, long lasting adaptations require synapse-to-nucleus communication in a bidirectional manner. Therefore, recently several synapse-to-nucleus messengers have been investigated (Carrano et al., 2019; Dinamarca et al., 2016; Karpova et al., 2013; Marcello et al., 2018). In particular the synapse-to-nucleus messenger Ring Finger Protein 10 (RNF10) specifically binds to 991-1049aa portion of GluN2A and migrates to the nucleus upon synaptic NMDAR activation or the induction of LTP (Carrano et al., 2019; Dinamarca et al., 2016). PKC-dependent phosphorylation of RNF10 at S31 detaches RNF10 from GluN2A and allows RNF10 binding to importin-α for transport to the nucleus where it probably modulates gene expression relevant neuronal maturation (Carrano et al., 2019). Extracellular Regulated Kinase is downstream both GluN2A- and GluN2B-containing NMDAR signaling and is involved not only in local signaling, but also in synapse to nucleus communication even if not yet was proved to move to the nucleus (Zhai, Ark, Parra-Bueno, & Yasuda, 2013).

- Protein Kinases:

Ca^{2+}/calmodulin-dependent protein Kinase II (CaMKII) is the most abundant protein at the glutamatergic PSD and is activated by Ca^{2+}-Calmodulin complexes driven by NMDAR opening. CaMKII interacts with 1389–1464 domain of GluN2A (F. Gardoni et al., 2001; Fabrizio Gardoni, Bellone, Cattabeni, & Di Luca, 2001) and with different CTD portions of GluN2B subunit (Bayer & Schulman, 2001; S & Colbran RJ, 1998). When this occurs, CaMKII autophosphorylates its autoinhibitory domain in T286, becoming active. The active conformation of CaMKII remains, even when the Ca^{2+} stimulus has subsided, therefore it is also named as “molecular memory” (Braun & Schulman, 1995; Colbran & Brown, 2004). The interaction between GluN2A and this kinase was shown to be in an unphosphorylated state, but it is promoted by autophosphorylation of CaMKII (F. Gardoni et al., 1999). Increased formation of GluN2A/CaMKII complex induces also a disruption of GluN2A/PSD-95 interaction thus leading to a dynamic modification of GluN2A-interacting proteins following NMDAR activation (F. Gardoni et al., 2001). Cyclin-Dependent Kinase 5 (CdK5) binds GluN2A at fragment 1218–1246, regulating receptor recycle and degradation via coordination with the protein AP2 (B. S. Li et al., 2001; Jian Wang et al., 2003). Cdk-5 depepdent phosphorylation at S1232 of GluN2A was shown to be important for LTP maintainance in CA1 region of hippocampus (B. S. Li et al., 2001)

- Other proteins:

Guanine nucleotide exchange factors (GEFs): Brefeldin A-resistant Arf guanine nucleotide exchange factor 2 (BRAG2) binds 1078–1117 fragment of GluN2A CTD and mediates exchange of GDP to GTP at ADP-rybosilation factors (Arf) (Elagabani et al., 2016). However, also BRAG1 is able to interact with synaptic GluN2A-containing NMDAR complex, as reported previously by Sakagami (Sakagami et al., 2008). Ras-guanine nucleotide-releasing factor 2 (Ras-GRF2) is a Ca^{2+}/Calmodulin (CaM) sensor mediating GluN2A-containing NMDAR signaling in mature neurons(S. Li, Tian, Hartley, & Feig, 2006), in fact its expression is developmentally regulated (Tian et al., 2004). Ras-GEF are important mediators of NMDARs late phase signaling, since they involve MAP kinases, ERK1/2 and also CREB phosphorylation which is important for gene expression (Tian et al., 2004). Nevertheless, the domain of interaction between Ras-GRF2 and GluN2A is not known. IQGAP1 serves as a scaffold protein for different signaling pathways involving B-Raf, Cdc42, Rac1, ERK, Lis1 and MEK. IQGAP1 was found to preferentially interact with GluN2A-PSD-95 complexes compared to GluN2B-containing ones, thus indicating a possible signaling interplay through IQGAP1 between different pools of NMDAR (JG, Z, & DB, 2008; Kholmanskikh et al., 2006; Reiner, Sapoznik, & Sapir, 2006; Ryu, Futai, Feliu, Weinberg, & Sheng, 2008). Calmodulin (CaM) interacts with CTD of GluN2A subunit in a calcium-dependent manner at the 875-1029 domain, through interaction with a tryptophan residue (1014), which is critical for protein–protein interaction (Bajaj et al., 2014). Ca^{2+}/Calmodulin complexes have been recently considered as a synapse-to-nucleus messengers of the γCaMKII and γCaMKI signaling, regulating gene expression and higher brain functions (S. M. Cohen et al., 2016; Ma et al., 2014). Bip, is an ER chaperone protein which selective deliveries GluN2A-containing NMDAR at the synapse from the dendritic ER (X. M. Zhang et al., 2015).

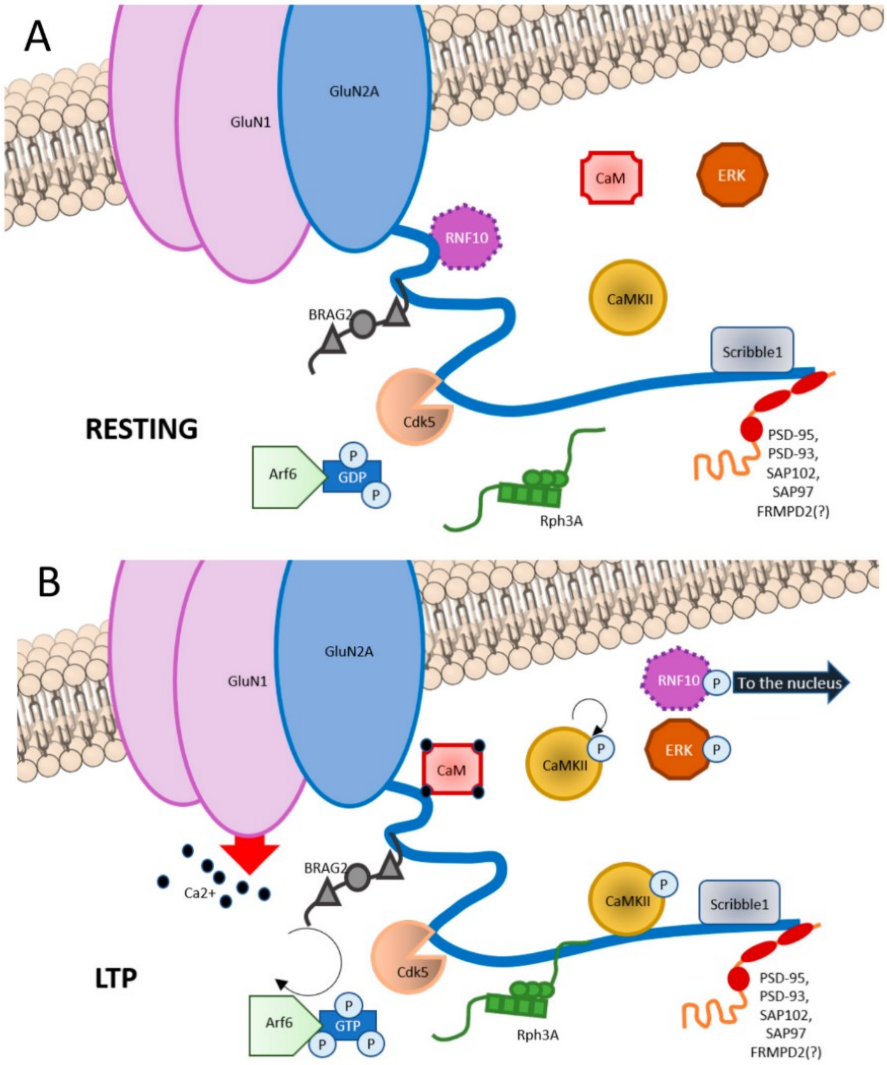

Figure 8. Representative picture of GluN2A-CTD binding partners in resting condition (A) and LTP (B). A) In basal condition, GluN2A CTD binds RNF10 at aa991-1049; BRAG2 at aa1078-1117; Cdk5 at aa1218-1246; CaMKII at aa1389-1464; Scribble1 at 1458-1464; and PSD scaffolding proteins such as PSD-93, PSD-95, SAP102, and SAP97 at aa1461-1464. (**B**) Upon LTP induction, phosphorylation of RNF10 triggers RNF10 detachment and its nuclear translocation. Simultaneously, CaM binds to aa875-1029 of GluN2A. BRAG2 exchanges GDP with GTP to Arf6-GTPase, which is involved is vesicles recycle at the postsynapse, also with Scribble1. Rph3A interaction with GluN2A at aa1349-1389 increases. CaMKII is disinhibited and is recruited at the postsynapse. Ras-ERK downstream cascade is initiated.

GluN2A in physiological synaptic plasticity

GluN2A-containing NMDARs participate to different forms of physiological synaptic plasticity. From a molecular profile, GluN2A levels are rapidly upregulated at synapses after LTP (Barria & Malinow, 2002; Bellone & Nicoll, 2007) as well as in cognitive tasks such as novel object recognition (Cercato et al., 2017) and habituation to new environments (Maria Veronica Baez et al., 2013). This is probably due to trafficking of pre-assembled GluN2A-containing NMDARs located in extrasynaptic sites, or exocyted (see Figure 9). Local

protein synthesis supports GluN2A-containing NMDARs assembly in situ after LTP; lately protein synthesis derived from the soma will direct to target regions more GluN2A-containing NMDARs (María Verónica Baez, Cercato, & Jerusalinsky, 2018) maintaining long lasting changes in neurotransmission.

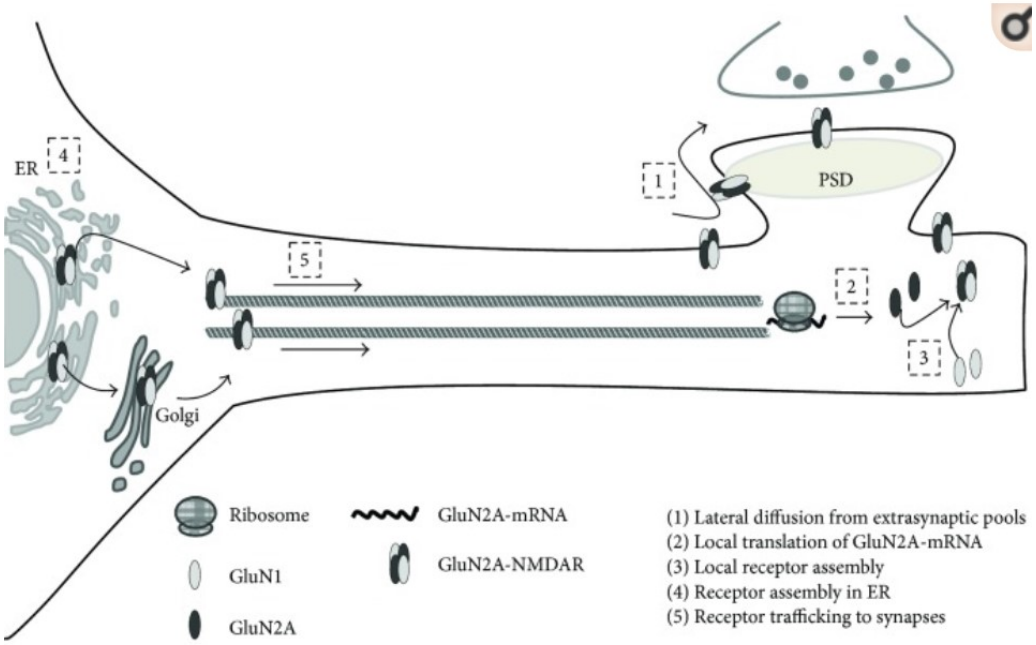

Figure 9. Modulation of GliuN2A-containing NMDARs during synaptic plasticity. After glutamate release and synaptic potentiation, 1) rapidly pre-assembled GluN2A-NMDARs are moved to PSD from extrasynaptic pools, 2-3) local translation promotes replenish of GluN2A-containing NMDARs in situ, 4-5) protein synthesis from the soma allows delivery of GluN2A-containing NMDARs to target spines. (adapted from María Verónica Baez, Cercato, and Jerusalinsky 2018).

Several studies tried to address GluN2A roles in synaptogenesis and synaptic plasticity by pharmacological or genetic approaches. Different experimental approaches have led to controversial results on GluN2A involvement. While early GluN2A overexpression as well as GluN2A CTD expression in organotypic hippocampal cultures is detrimental for dendritic spine growth (Gambrill & Barria, 2011); studies on hippocampal slices with chimeric GluN2A or GluN2B subunits with respective exchanged CTDs knock-in, did not affect synaptogenesis and AMPAR currents (Ryan et al., 2013).

A variety of studies indicate GluN2A functions are important for short-term memory tasks. In particular, reducing GluN2A expression or expressing GluN2A-lacking CTD does not impair spatial learning acquisition in MWM or radial arm maze after several days of training (Bannerman et al., 2008). However, the same experimental approach resulted in impaired short term working memory (Bannerman et al., 2008). Similarly, blocking GluN2A through selective antagonist NVP-AM077 injected intraperitoneally did not alter MWM performance during acquisition and consolidation (Ge et al., 2010); however when infused in CA1 region of hippocampus, NVP-AM077 treatment disrupted the performance in delayed alternation T-maze test (X. H. Zhang, Liu, Yi, Zhuo, & Li, 2013). Interestingly, Neto1 knock-out (KO) mice display lower GluN2A levels and

impaired LTP and poorly perform in spatial object displacement task but not in novel object recognition one, indicating a specific hippocampal impairment (Ng et al., 2009). Regarding fear memory tests, GluN2B subunit seems to be mostly involved in spite of GluN2A (Y. F. Chen et al., 2019; Goodfellow, Abdulla, & Lindquist, 2016; Gupta-Agarwal, Jarome, Fernandez, & Lubin, 2014; Jacobs et al., 2014; Zhan et al., 2018). However, Zhang and colleagues (X. M. Zhang et al., 2015) identified GluN2A synaptic delivery by ER chaperone protein Bip is required for acquisition of fear conditioning.

GluN2A in pathological synaptic plasticity

Some of GluN2A CTD phosphorylation sites are known to be relevant in certain pathological conditions. Phosphorylation at S1232 is promoted by Cdk5 (Li et al. 2001) and interfering with Cdk5 activity during ischemic injury reduces CA1 pyramidal neuronal cell death (Wang et al. 2003). A GluN2A-Y1387 mutation was found in a family displaying autistic features (Lesca et al., 2013), and this residue is well known to be phosphorylated by Src-kinases promoting GluN2A synaptic delivery (Salter & Kalia, 2004).

GluN2A in epilepsy:

Epilepsy is a common disease resulting in abnormal firing of brain circuits. Several drugs are in use for epilepsy treatment, trying to restore a balance in excitation and inhibition at CNS circuitry (Devinsky et al., 2018). Several GRIN2A mutations have been associated with many types of epilepsy-aphasia spectrum (EAS) such as benign epilepsy with centrotemporal spikes (BECTS), the Landau-Kleffner syndrome (LKS) and epileptic encephalopathy with continuous-spike-and-waves-during-slow-wave-sleep (CSWSS) (Carvill et al., 2013; Lemke et al., 2013; Lesca et al., 2013). Among the mutated consequent GluN2A variants, the P552R was detected in a patient reporting intellectual disability and seizures (De Ligt et al., 2012). Interestingly, transfecting hippocampal primary cultures with GluN2A-P552R leads to stimulated-induced excitotoxicity rescued by memantine (Ogden et al., 2017). These observations suggest GluN2A-P552R represents a dominant positive variant of GluN2A, and indeed displays increased agonist potency without impairment in receptor expression and trafficking (Ogden et al., 2017). Noteworthly, also dominant negative variants of GluN2A were associated to epileptic phenotypes such as GluN2A-I148S, R512H, I184T, C436R, R518H, T531M, V85G, D731N (Lemke et al., 2016; Sibarov et al., 2017; Swanger et al., 2016; Xu & Luo, 2018). A dominant negative variant previously mentioned is also GluN2A-N651K, which was reported in epileptic clinical phenotypes (Stephen F. Traynelis et al., 2010).

There are a variety of in vitro and in vivo models of epilepsy, each with specific features which should be taken into account depending on the experimental aim. In fact, studies on different model identified controversial results for the association of GluN2A to the epileptic phenotype. Chen and colleagues in 2007

reported GluN2 antagonism in the pilocarpine and kindling models of epilepsy is able to reduce pathological phenotype. However, only blocking selectively GluN2A subunit epilepsy was reduced as well as seizure-induced mossy-fiber sprouting and the activity dependent Brain-Derived Neurotrophic Factor (BDNF) expression (Q. Chen et al., 2007). In a recent study Hanson and colleagues revealed epileptic phenotype was ameliorated in a model of Dravet syndrome by application of GluN2A selective PAM (Hanson et al., 2020), indicating specific GluN2A involvement in epilepsy is case-specific due to different pathophysiological mechanisms.

GluN2A in neurodevelopmental disorders

NMDAR dysfunction was also associated with neurodevelopmental disorders such as Intellectual Disabilities (ID), characterized by reduced learning and social interaction. Fragile X syndrome (FXS) is an ID often accompanied by autistic features, with a strong genetic component in the pathophysiology. In particular, FXS derives from lack or altered expression of FMR1 gene into Fragile Mental Retardation Protein (FMRP), which binds mRNA (Bagni, Tassone, Neri, & Hagerman, 2012) and regulates its transport (Bassell & Warren, 2008; De Rubeis & Bagni, 2010). Among FMRP target mRNAs altered in FXS, most are related to synaptic compartment such as PSD-95, NMDARs, Shank1-3, Calcium channels, SNAP-25 etc. (Pasciuto & Bagni, 2014). LTP is impaired in CA1 region of hippocampus as well as in other brain regions in FXS animal models (Desai, Casimiro, Gruber, & Vanderklish, 2006; Lauterborn et al., 2007; H. Y. Lee et al., 2011; Meredith, Holmgren, Weidum, Burnashev, & Mansvelder, 2007; Paradee et al., 1999; Zhao et al., 2005). Interestingly, inhibition of GluN2A through different antagonists and NAM as well as deleting GluN2A subunit expression, restored NMDAR dependent LTP in CA1 region these animals (Lundbye, Toft, & Banke, 2018).

GluN2A in Parkinson's Disease and Dystonia

An adequate cortico-striatal communication is necessary for correct motor activity (Fabrizio Gardoni & Bellone, 2015). In Parkinson's disease (PD) there is an impaired basal ganglia communication derived from progressive depletion of dopaminergic neurons from substantia nigra (SN) (Calabresi, Picconi, Tozzi, & Di Filippo, 2007). The striatal synaptic levels of GluN2A is altered by both partial and massive SN degeneration in the 6-hydroxydopamine model of PD. In particular, partial SN degeneration in 6OHDA model results in selective increase of GluN2A levels at spiny projecting neurons (SPN) accompanied by striatal LTP impairment (Paillé et al., 2010). Full-lesion of nigro-striatal communication increases GluN2A/GluN2B ratio paralleled by altered LTD and LTP (Fabrizio Gardoni et al., 2006; Paillé et al., 2010). Interestingly, usage of TAT-cell permeable peptides able to disrupt GluN2A interaction with scaffolding proteins ameliorates motor behavior and electrophysiological properties (Paillé et al., 2010). Another component of neurodegeneration process

in PD is alpha-synuclein (α-syn) accumulation. Noteworthly, α-syn leads to visuo-spatial deficits and impairs LTP at SPNs, without altering LTD (Durante et al., 2019). On hippocampal primary cultures, α-syn oligomers impair LTP in a NMDAR-dependent mechanism (Diógenes et al., 2012). Unfortunately, only symptomatic treatments are available for PD, and among them the gold standard is Levodopa. Levodopa usage leads to immediate benefits but over time these are accompanied by a almost 50% probability of dyskinesia (Levodopa-induced dyskinesia; LID). Of relevance, Levodopa restores electrophysiological properties and LTP/LTD only in not dyskinetic animals (H. Y. Lee et al., 2011; Picconi et al., 2003; Prescott et al., 2014). In order to treat dyskinetic behavior, also Amantadine, a low-affinity NMDAR antagonist, is employed as add-on therapy, due to a role of NMDARs also in this Levodopa treatment consequence. In particular, GluN2A/GluN2B ratio is increased in dyskinetic striatum, and interfering with GluN2A-MAGUK or GluN2A-Rph3A interaction reduces dyskinetic behavior (Fabrizio Gardoni et al., 2012; Stanic et al., 2017).

Synaptic plasticity alterations have also been reported for early-onset generalized torsion dystonia (DYT1) (Quartarone & Hallett, 2013). Noteworthly, in striatum of DYT1 mouse model LTP was recorded in an earlier time window compared to WT, while LTD has not been detected. These alterations indicate an earlier GluN2A expression at SPNs in DYT1 condition (Maltese et al., 2018).

GluN2A role in Alzheimer's disease:

Alzheimer's Disease (AD) is the most common form of dementia age-dependent and associated with deterioration of hippocampus and neocortex areas, with consequent learning and memory deficits. From a molecular point of view, AD is characterized by amyloid-β-1–42 (Aβ1–42) deposits in extracellular plaques (and intracellular neurofibrillary tangles of hyperphosphorylated tau.) Importantly, Aβ1–42 oligomers alter NMDAR functions and are detrimental for LTP, while promoting LTD and dendritic spine loss (Hsieh et al., 2006; J. H. Kim, Anwyl, Suh, Djamgoz, & Rowan, 2001; S. Li et al., 2009). Several studies reported overactivation of extrasynaptic NMDARs in AD leading to excitotoxicity and cell death. This event is given by overload of Ca2+ which can activate death signaling pathway (N. W. Hu, Klyubin, Anwy, & Rowan, 2009; S. Li et al., 2011; Tackenberg et al., 2013). Noteworthly, Aβ1–42 triggers a plethora of detrimental effects on neuronal cells also via GluN2A-containing NMDARs. In particular, Marcello and colleagues observed Aβ1–42 toxicity requires GluN2A-NMDARs and neuronal activity (Marcello et al., 2019); furthermore, Texidó and coworkers assigned GluN2A-containing NMDARs a pivotal role in Ca2+ overload induced by Aβ1–42 (Texidó, Martín-Satué, Alberdi, Solsona, & Matute, 2011). Interestingly, in 2013 Malinow's laboratory observed oligomeric Aβ1–42 induces GluN2B-containing NMDARs synaptic loss and increased GluN2A/GluN2B subunit ratio at synapses (Kessels, Nabavi, & Malinow, 2013). Moreover, GluN2A-containing NMDARs seem to promote dendritic spine loss induced by oligomeric Aβ1–42 (Tackenberg et al., 2013).

8. Rabphilin-3A (Rph3A)

Ras-related protein in brain (Rabs) represent a broad family of molecules involved in vesicle trafficking, exocytosis and sorting. From literature analysis of Rabs, their roles is synaptic transmission seem to be mostly in presynaptic terminals, regulating neurotransmitter vesicle fusion at the active zone; while in the dendritic and synaptic compartment they direct endosomes from/to target membranes. Rabs work as Ras-like small GTPases thus are active in a GTP-bound conformation while are off when GDP is bound. The biological significance of several Rabs is to identify the cellular destiny of vesicles, thus specific Rabs are associated to specific intracellular pathways; and of relevance some are detected only at the presynapse while other are exclusively postsynaptic. To accomplish their functions, Rabs recruit so called "effectors" such as tethering factors, molecular motors and phospholipid modulators (Pylypenko, Hammich, Yu, & Houdusse, 2018).

In particular, among Rab effectors Rabphilin-3A (Rph3A) is abundantly expressed in the brain (rat cerebellum, neuromuscular junction and retina, hippocampus; (Franchini et al., 2019; Mizoguchi et al., 1994; Stanic et al., 2015) and interestingly kidney podocytes (Rastaldi et al., 2003). Rph3A was thought to be exclusively presynaptic involved in docking of neurotransmitter release (Mizoguchi et al., 1994), however our research group identified this protein also in the postsynaptic compartment, bound to GluN2A subunit of NMDARs in PSD (Stanic et al., 2015).

Rph3A: genetic, protein structure and interactors

Rabphilin-3A is a 694 protein of ~78KDa encoded by RPH3A gene, and firstly identified in bovine brain (Shirataki et al., 1993). Genetic locus of RPH3A is human and rat chromosome 12 (NC_000012.12, NC_005111.4 respectively) while in mice on chromosome 5 (NC_000071.6). After its identification, Rph3A was detected in synaptic vesicle and granules of chromaffin cells, suggesting a role in vesicle trafficking and eventually exocytosis (Darchen et al. 1990, 1995; Mollard et al. 1990; Chung et al. 1995; Mizoguchi et al. 1994).

From a structural point of view, as shown in Figure 10, Rph3A polypeptide can be divided into a NTD, C2 domains (C2A and C2B) and a CTD.

As for the NTD, it displays a cysteine rich zinc-finger domain necessary for Rab3-GTPase interaction with 45-170aa sequence (S. H. Chung, Takai, & Holz, 1995; McKiernan, Stabila, & Macara, 1996; Stahl, Von Mollard, Walch-Solimena, & Jahn, 1994), Rab27 (Fukuda, 2003), Rabaptin5 (Ohya, Sasaki, Kato, & Takai, 1998) and α-actinin (Kato et al., 1996). After NTD, there is a linker portion and the C2A and C2B domains at 432-536aa and 554-675aa respectively (Shirataki et al., 1993), which are commonly used to bind phospholipids in a Ca2+-dependent manner, thus their presence in Rph3A accounts for a Ca2+ sensor function of Rph3A in membrane

binding (Fykse, Li, & Südhof, 1995). In particular, deleting one or both C2 domains leads to inhibition of Ca2+-dependent exocytosis (Shirataki et al., 1993). On the other hand, Rab3A seems to be not affected by absence of Rph3A; thus, the C2 domain functions as Ca^{2+} sensors for exocytosis does not appear relevant. Therefore, it was hypothesized Rph3A role is probably associated to extreme physiological transmission (Fukuda, 2003; Schlüter et al., 1999). Rph3A also displays two main characterized residues such as S234 and S274, which are phosphorylated by PKA and CaMKII respectively, leading to a more soluble Rph3A (Fykse et al., 1995; Lonart & Südhof, 1998).

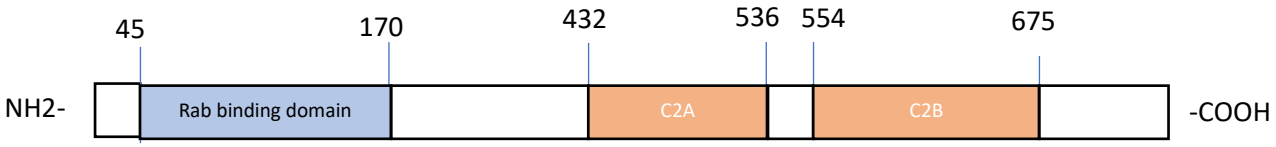

Figure 10. Schematic representation of Rph3A structure. Rph3A display a Rab-binding domain at the N-terminal fragment, followed by a linker region and then two C2 domains (C2A and C2B).

Notably, Rab3 is expressed in 4 isoforms (A-D) which are found at the presynapse and regulate exocytosis. Interestingly, in Rab3A-KO mice model, Rabphilin3A is greatly reduced (C. Li et al., 1994; Schlüter, Schmitz, Jahn, Rosenmund, & Südhof, 2004). Rph3A displays preferential interaction with Rab3A and Rab3C (C. Li et al., 1994). Rabphilin3A-Rab3 affinity is much higher when Rab3A is in a GTP-bound state compared to a GDP one (Geppert & Südhof, 1998). From a functional point of view, Rab3A-GTP was found to inhibit Ca^{2+}-dependent exocytosis in bovine chromaffin cells (PC12), while expression of Rph3A promotes mediators release (S.-H. Chung, Stabila, Macara, & Holz, 1997; Holz, Brondyk, Senter, Kuizon, & Macara, 1994). In accordance with previous studies, Chung and colleagues in 1997 hypothesized Rab3A-GTP interacting with Rph3A at vesicles represents a checkpoint for exocytosis promoting an optimal arrangement of vesicle pools. On a GDP-bound state Rph3A-Rab3 interaction is reduced promoting Ca^{2+} -dependent exocytosis (S.-H. Chung et al., 1997). From these observations, Rph3A seems to play a role in vesicle exocytosis thus interference with its function may result in altered neuronal transmission.

However, opposite conclusions were obtained from a phenotype characterization of Rph3A-KO mouse model (Schlüter et al., 1999), showing no alteration in brain structure and electrophysiological properties and spatial learning of mutant animals. Noteworthly, no significant changes in protein levels relevant for neurotransmission were observed among Rph3A-KO, Rab3A-KO and WT animals (NMDAR R1, PSD-95, RIM, Rab3A/C, synaptophysin etc).

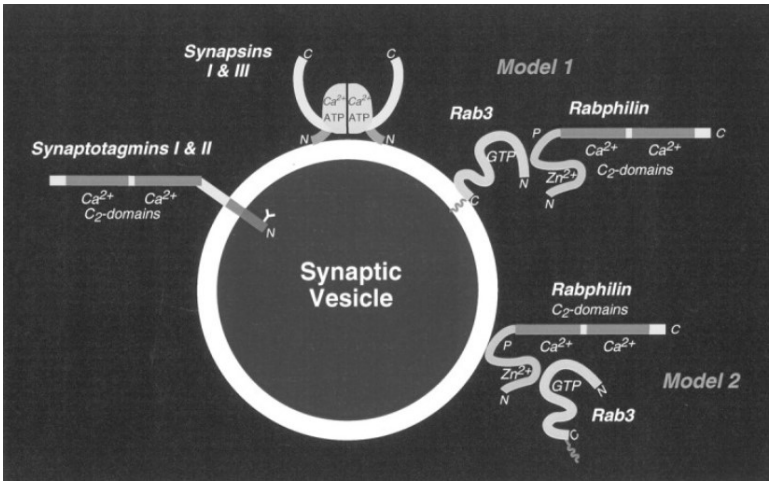

Figure 11. Rapbhilin-3A interaction synaptic vesicles. Rph3A is able to bind synaptic vesicles alone (Model 2) or by interacting with Rab proteins. Adapted from (Schlüter et al., 1999).

An important aspect when studying vesicle trafficking is the redundance of Rab-effectors, so that their single relevance may be unmasked only in specific experimental conditions.

For example, RIM is a well-known Rab-effector protein able also to bind Rab3A and is involved in neurotransmitter release (Persoon et al., 2019), and recently was associated with synaptic delivery of NMDARs through recycling endosomes (Jiejie Wang et al., 2018). Therefore, we cannot exclude compensation mechanisms of other molecules in synaptic transmission when Rph3A functions and presence are impaired (Schlüter et al., 1999). Interestingly, two specific site mutations of RPH3A (p.Arg269Gln and p.Val464Leu) have been detected in a young patient reporting myastenic syndrome (Maselli et al., 2018). Scientists were expecting these mutations to affect Rph3A functions and thus interaction with protein partners involved in neurotransmission at presynapse. Interestingly, only one of the site mutation, p.Arg269Gln, was associated with a decrease in 14-3-3 interaction, but how this correlates with clinical phenotype was not investigated (Maselli et al., 2018).

Rph3A role in exocytosis seems also to involve the actin-cytoskeletal molecular motor MyosinVA (MyoVA). In fact, Brozzi and colleagues in 2012 investigated Rab effecotrs roles at secretory granules in pancreatic cells (MIN6). Vesicles are trafficked at exocytosis regions through molecular motors, for example MyoVA. In particular, MyoVA interacts with Rab27 and both Rab-effectors Granulophilin A and B (GranA/B). Interestingly, interfering with GranA/B binding to MyoVA delocalizes secretory granules and enhances stimulated secretion. This event was driven by a MyoVA binding to Rph3A at its C2A-C2B domains. When also Rph3A-MyoVA interaction was impaired, reduced but still modest stimulated secretion was observed, indicating the lack Rab-effectors may be compensated by other proteins at secretory granules, and defining subset of vesicle pools (Brozzi et al., 2012). Notably, Rph3A seems to be recruited at new formed vesicles. This aspect is in accordance with the previously mentioned role of Rph3A in allowing vesicle maturation

before stimulated secretion (S.-H. Chung et al., 1997). Furthermore, MyoVA was also associated to mRNA transport in dendritic compartment and thus involved in local protein synthesis. In particular, mRNA for local translation are transported as RNA-protein complexes also termed “mRNA granules”, which were shown to contain mRNA-binding proteins, ribosomal RNA, mRNAs and translation factors (Hirokawa, 2006). Noteworthly, MyoVA was found to interact with Translocated in liposarcoma (TLS or FUS) in mouse cortical and hippocampal neurons (Fujii et al., 2005; Yoshimura et al., 2006). TLS is a well-known RNA binding protein associated to RNA granules. Interestingly, TLS is associated to GluN1 subunit of NMDARs in retinal ganglion cell line RGC-5, and interacts with MyoVA in a Ca^{2+} dependent manner (Selamat et al., 2009). In particular, MyoVA-TLS interaction is reduced in by Ca2+ or by depolarization determining a redistribution of GluN1-TLS complexes (Selamat et al., 2009). Noteworthly, Ca2+ modulation of TLS-MyoVA interaction also affects mRNA levels in RNA granules associated to TLS (Yoshimura et al., 2006). Overall, MyoVA seems to play a role in vesicle transport and able to affect local translation of mRNA. However, in these studies Rph3A was not investigated as a possible partner of RNA granules-MyoVA complexes.

Postsynaptic Rph3A function: a stabilizer of GluN2A-containing NMDARs in PSD

Our research group recently identified Rph3A as a potential binding partner of GluN2A through a two-yeast hybrid assay using the C-terminal fragment of GluN2A, thus indicating potential presence of Rph3A also at the postsynapse and in a protein-complex with GluN2A-containing NMDARs.

Rph3A presence at the PSD was confirmed through rat hippocampal fractionation to obtain purified PSDs, but also through EM of dendritic spines from CA1 pyramidal neurons and colocalization of Rph3A and PSD-95 on hippocampal primary cultures (Figure 11).

The interaction between GluN2A and Rph3A resulted from immunoprecipitation (IP) of GluN2A in crude membrane fraction (P2) of rat hippocampus. Notably, Rph3A Notably, among the several partners of Rph3A, MAGUK proteins like SNAP-25 (Ferrer-Orta et al., 2017; J. De Lee et al., 2008) and CASK (Y. Zhang, Luan, Liu, & Hu, 2001) are reported, and a well-known MAGUK member at PSD is PSD-95. Interestingly, IP of PSD-95 also revealed Rph3A and GluN2A presence, indicating the formation of a ternary complex at PSD (Fig.1).

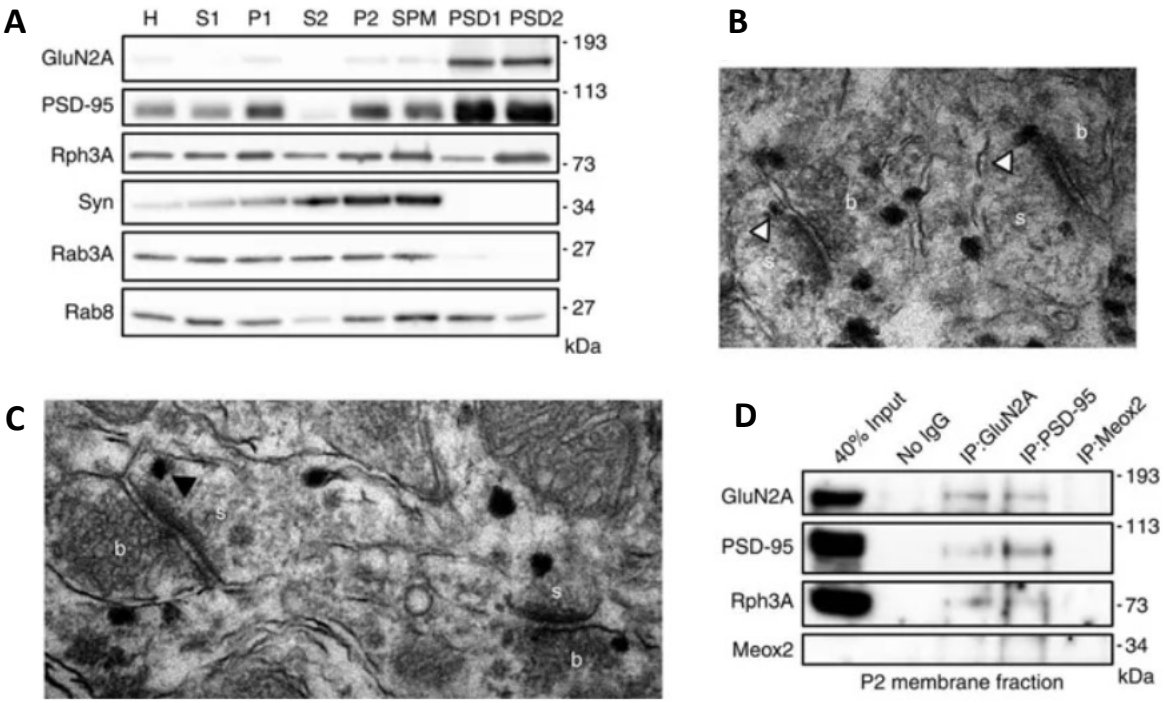

Fig.11. Rph3A is present in the postsynapse and interacts with GluN2A and PSD-95. A) Subcellular expression of GluN2A, PSD-95, Synaptophysin (Syn), Rph3A, Rab3A and Rab8 in rat hippocampus. H, homogenate; S1/2, supernatant 1/2; P1/2, pellet 1/2; SPM, synaptosomal plasma membrane; PSD1/2, postsynaptic density fraction ½. B,C) Immunolabelling of Rph3A in dendritic spines of pyramidal cells in the CA1 stratum radiatum of the hippocampus. Electron microscopy images show that Rph3A is found lateral to the PSD (white arrowheads) and at different positions in dendritic spines (white arrowheads). b, bouton, s, spine. D) Co-immunoprecipitation experiments on rat hippocampal P2 fractions using polyclonal GluN2A, monoclonal PSD-95 and irrelevant monoclonal Meox2 antibodies show that Rph3A is associated with both GluN2A and PSD-95.

Rph3A interaction was specific for GluN2A subunit but not GluN2B as reported in colocalization analysis of eGFP-GluN2A/GluN2B with RFP-Rph3A transfected in COS-7 cells (Fig.12B). The domain of interaction of Rph3A on GluN2A CTD was investigated through GST-binding assay using as a bait different truncated GluN2A CTDs which only shared the 1349-1389aa sequence (Fig.12C). This portion in fact, was not reported to interact with other proteins (Franchini et al. 2020). Rph3A was revealed in all GluN2A CTD baits pull-down, indicating aa in this fragment are responsible for GluN2A-Rph3A interaction. On the other hand, Rph3A domain of interaction with GluN2A was identified as the N-terminal fragment (Rph3A-179; Fig. 12D-E).

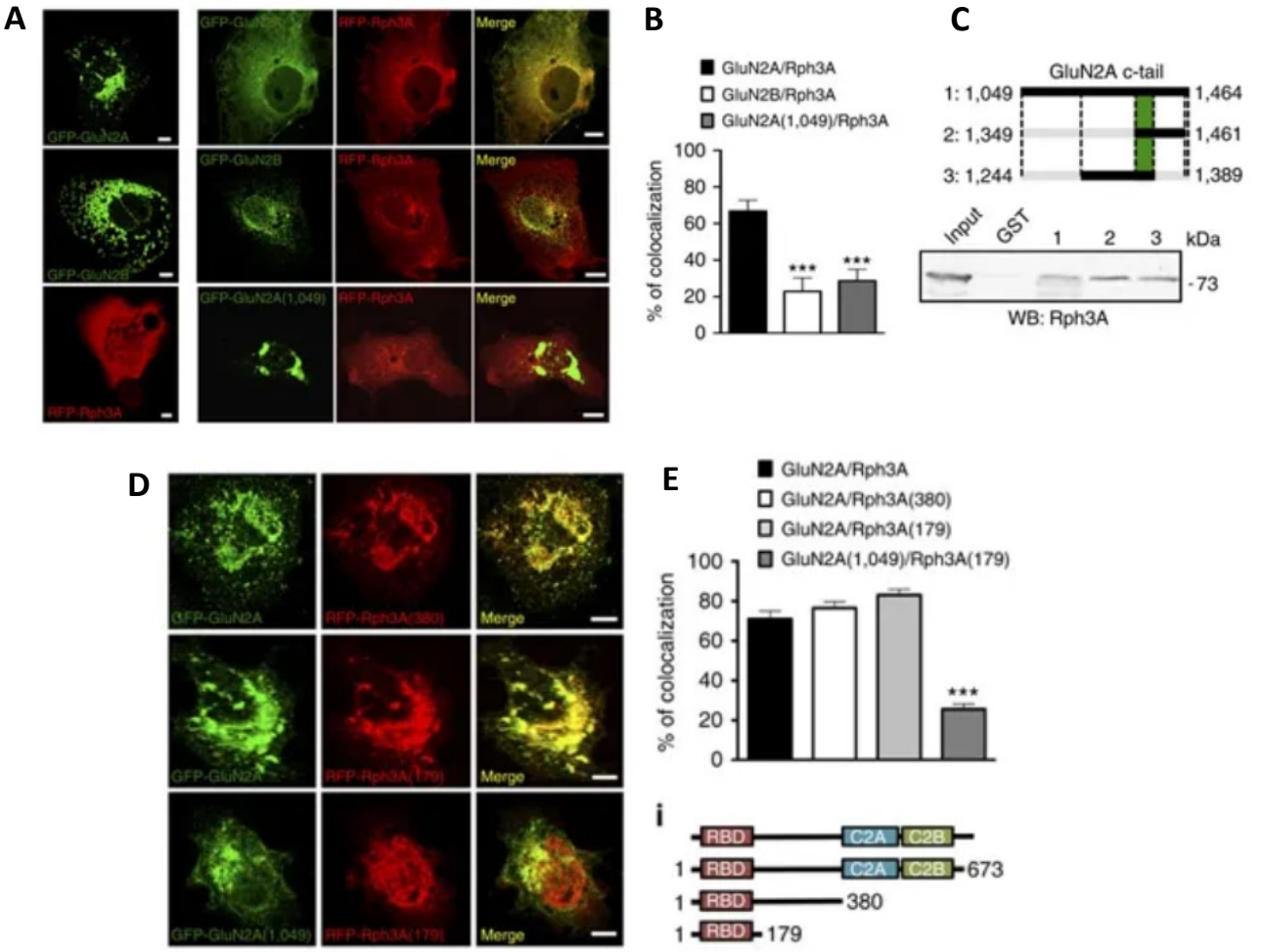

Figure 12. Identification of Rph3A and GluN2A domains of interaction. Confocal imaging of COS7 cells transfected with eGFP-GluN2A (green), eGFP-GluN2B (green) or RFP-Rph3A (red) and cells co-transfected with either eGFP-GluN2A, eGFP-GluN2B and RFP-Rph3A or eGFP-GluN2A(1,049) (green) and RFP-Rph3A. Scale bars, 10 µm. (**b**) Bar graph representing the percentage of co-localization between eGFP-GluN2A and RFP-Rph3A, eGFP-GluN2B and RFP-Rph3A, eGFP-GluN2A(1,049) and RFP-Rph3A. Data are presented as mean±s.e.m., *n*=5–9, ***P<0.001, unpaired Student's *t*-test. (**c**) GST pull-down assay of Rph3A using C-terminal GluN2A GST fusion protein with different sizes on rat brain extracts. 1, GluN2A (1,049–1,464); 2, GluN2A (1,349–1,461); 3, GluN2A (1,244–1,389). D) Confocal imaging of COS7 cells co-transfected with eGFP-GluN2A and RFP-Rph3A(380) (upper panels), eGFP-GluN2A and RFP-Rph3A(179) (middle panels) or eGFP-GluN2A(1,049) and RFP-Rph3A(179) (lower panels). Scale bars, 10 µm. E) Bar graph representing the percentage of co-localization between GluN2A and RFP-Rph3A constructs. Data are presented as mean±s.e.m., n=10, ***P<0.001; one-way ANOVA followed by Tukey post-hoc test, GluN2A(1,049)/Rph3A(179) versus GluN2A/Rph3A, GluN2A(1,049)/Rph3A(179) versus GluN2A/Rph3A(380), GluN2A(1,049)/Rph3A(179) versus GluN2A/Rph3A(179).

Rph3A/PSD-95 interaction resulted from last C-terminal HVSSD residues (Fig.13A-D), which are known to be a consensus motif for PDZ binding (Doyle et al., 1996). Interestingly, Rph3A is able to bind all three PDZ domains of PSD-95, however with higher affinity towards PDZ-3. Noteworthly, GluN2A is already reported to bind PSD-95, thus indicating the existence of a trimeric complex between GluN2A, PSD-95 and Rph3A.

From these results, both shRNA targeting Rph3A expression as well as TAT-cell permeable peptides (CPP; which are also able to cross Blood Brain Barrier in vivo (BBB)) were used to interfere with GluN2A/PSD-95/Rph3A protein complex. More in detail, TAT-9c is a CPP resembling the last 9 aa of Rph3A CTD interacting with PSD-95. TAT-Rph3A-9c efficacy in disruption of Rph3A/PSD-95 interaction was verified by colocalization analysis in COS-7 between Rph3A/PSD-95 and Rph3A/PSD-95/GluN2A (Fig.13A-D), comparing it to TAT-Rph3A-9c without VSSD sequence (TAT-Rph3A(-VSSD)).

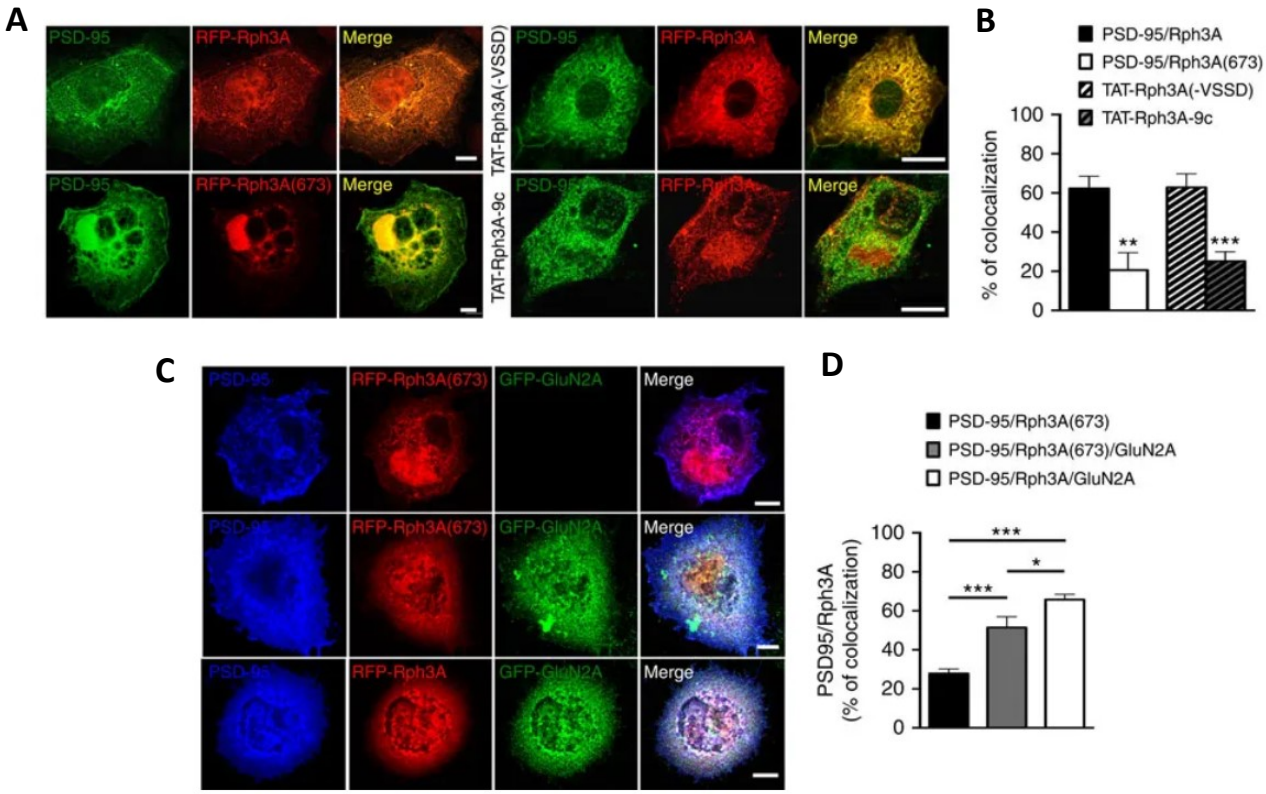

Fig.13 Rph3A last 9aa at CTD are responsible for PSD-95 interaction. Confocal imaging of COS7 cells co-transfected with PSD-95 (green) and RFP-Rph3A (red) in the presence or absence of TAT-Rph3A-9c or TAT-Rph3A(−VSSD), or PSD-95 and RFP-Rph3A(673) (red). Scale bars, 10 µm. (**d**) Bar graph representing the percentage of co-localization between PSD-95 and RFP-Rph3A in the presence or absence of TAT-Rph3A-9c or TAT-Rph3A(−VSSD), and PSD-95 and RFP-Rph3A(673) (*n*=5–10; unpaired Student's *t* test). (**e**) Confocal imaging of COS7 cells co-transfected with PSD-95 (blue), RFP-Rph3A or RFP-Rph3A(673) (red) in the presence or absence of GFP-GluN2A (green). Scale bar, 10 µm. (**f**) The bar graph represents the percentage of co-localization between PSD-95 and RFP-Rph3A constructs (*n*=8; one-way ANOVA followed by Tukey *post-hoc* test). All data are presented as mean±s.e.m., **P*<0.05, ***P*<0.01, ****P*<0.001).

Reducing Rph3A expression through shRph3A reduced specifically GluN2A presence at the postsynapse, without affecting GluN2B presence in PSD (Fig.14A-B). When TAT-2A-40 was applied on hippocampal primary cultures, TAT-2A-40 reduced synaptic levels of GluN2A indicating a destabilization of the receptor protein complex at PSD (Fig.14C-K).

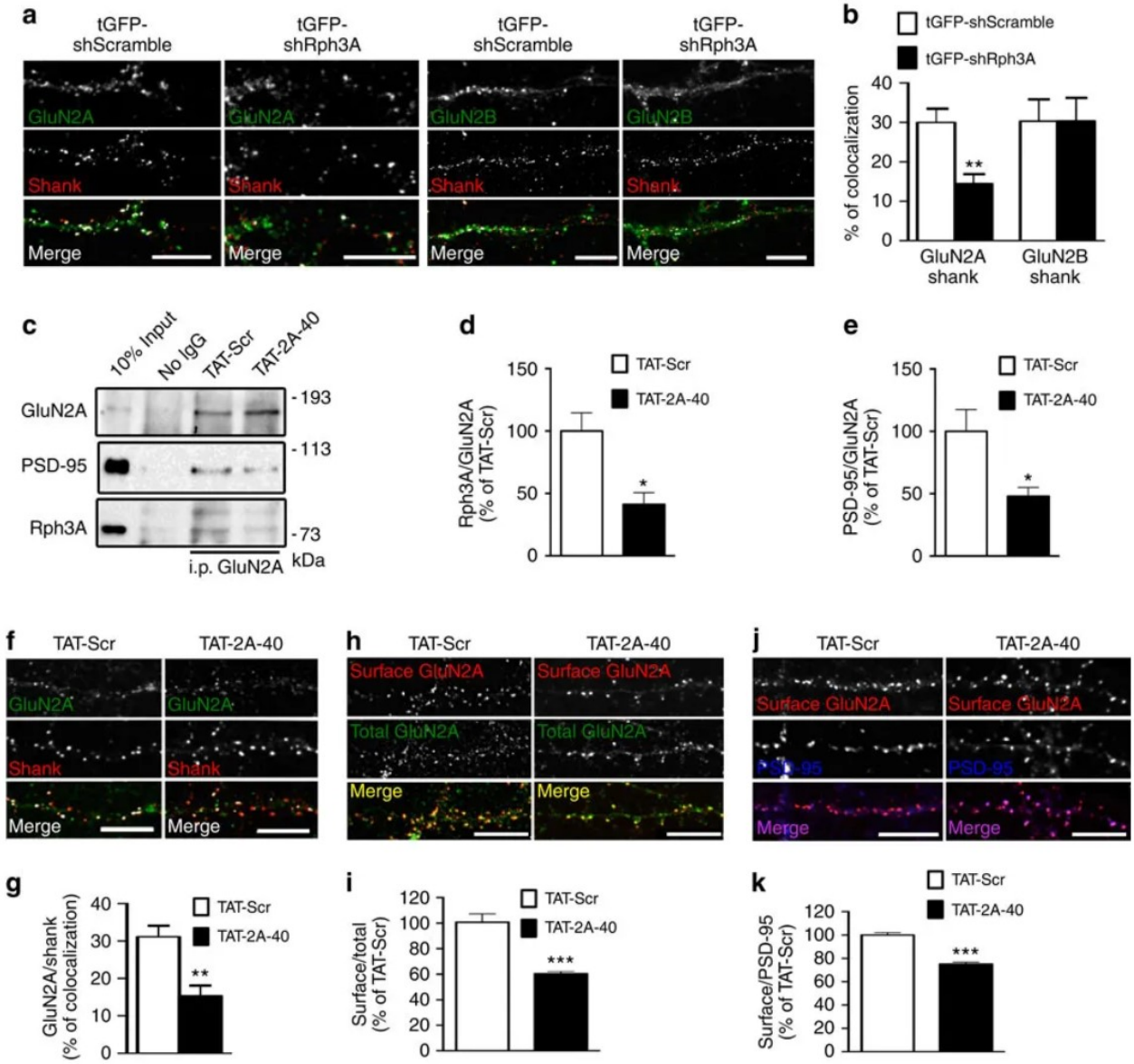

Figure 14. Disruption of Rph3A/GluN2A or Rph3A/PSD-95 interaction reduces GluN2A synaptic levels. A) Fluorescence immunocytochemistry of GluN2A (green) and Shank (red) or GluN2B (green) and Shank in *DIV15* neurons transfected with tGFP-shScramble or tGFP-shRph3A (*DIV9*). (B) Bar graph representing the percentage of co-localization of GluN2A or GluN2B with Shank (*n*=10–19). (C-E) Co-immunoprecipitation of GluN2A with PSD-95 and Rph3A in P2 fractions from primary hippocampal neurons (*DIV15*) treated with TAT-2A-40 10 µM 30 min, showing a reduction of the interaction compared with animals treated with the control peptide TAT-Scr. The bar graphs show Rph3A/GluN2A (D) and PSD-95/GluN2A (E) co-immunoprecipitation expressed as % of TAT-Scr (*n*=4). (F) Fluorescence immunocytochemistry of GluN2A (green) and Shank (red) in *DIV15* neurons treated with TAT-Scr or 10 µM TAT-2A-40 for 30 min. (G) Bar graph representing the percentage of co-localization of GluN2A with Shank (*n*=7–14). (H) Fluorescence immunocytochemistry of surface GluN2A (red) and total GluN2A (green) in *DIV15* hippocampal neurons treated for 30 min with 10 µM TAT-Scr or TAT-2A-40. (i) Bar graph representation of the percentage of integrated density ratio GluN2A surface/total compared with the mean of TAT-Scr (*n*=119–144). (J) Fluorescence immunocytochemistry of surface GluN2A (red) and PSD-95 (blue) in *DIV15* hippocampal neurons treated for 30 min with TAT-Scr or TAT-2A-40 10 µM. (K) Bar graph representation of the percentage of integrated density ratio surface GluN2A/PSD-95 compared with the mean of TAT-Scr (*n*=119–150). All data are presented as mean±s.e.m.; **P*<0.05, ***P*<0.01, ****P*<0.001; unpaired Student's *t* tests. All scale bars represent 10 µm.

We also evaluated TAT-9c activity by analyzing GluN2A/Rph3A/PSD-95 complex presence in vivo by injection TAT-Rph3A-9c i.p.. Furthermore, we treated hippocampal primary cultures with the same peptide, to verify synaptic localization of GluN2A. As shown in Fig.5A-B, TAT-Rph3A-9c led to significant reduction in GluN2A/Rph3A/PSD-95 complex presence in vivo, furthermore impairing GluN2A-containing NMDAR presence in PSD in vitro (Fig.15C-D).

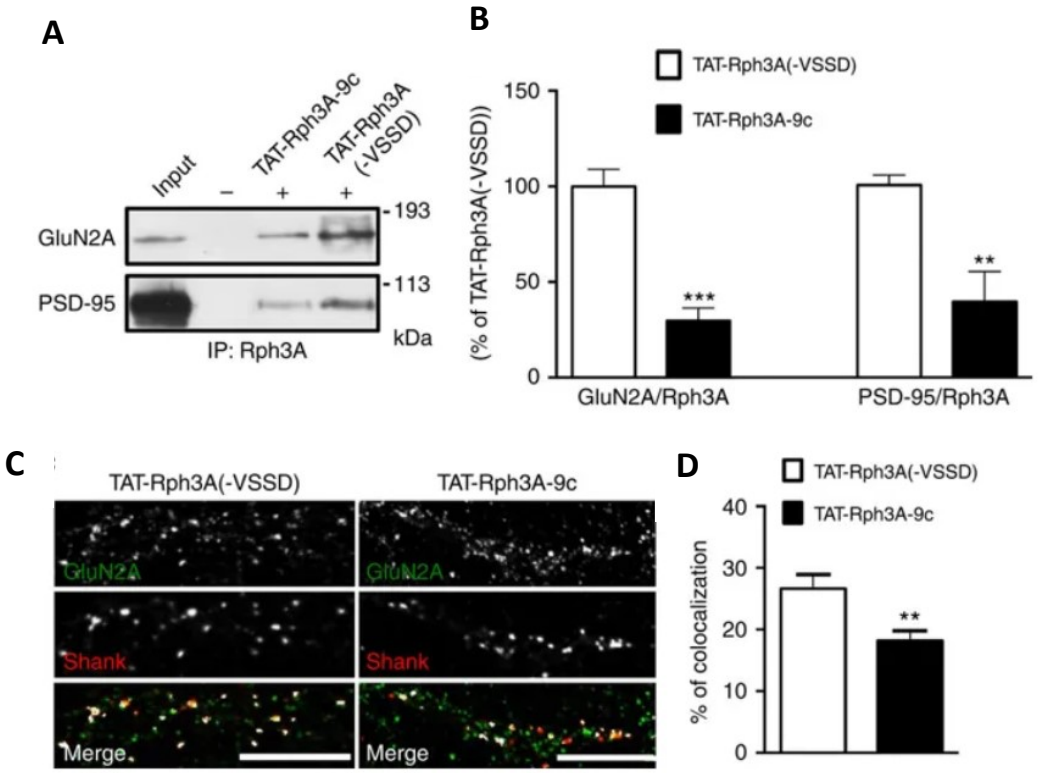

Figure 15. TAT-Rph3A-9c reduces GluN2A/Rph3A/PSD-95 complex and synaptic levels of GluN2A. Co-immunoprecipitation of Rph3A with GluN2A and PSD-95 from P2 fraction from forebrain of mice 2 h after injection with TAT-Rph3A-9c (3 nmol g^{-1}, i.p.) showing a reduction of both interactions compared with mice treated with the control peptide TAT-Rph3A(−VSSD). The bar graphs show GluN2A/Rph3A (left columns) and PSD-95/Rph3A (right columns) co-immunoprecipitation expressed as % of TAT-Rph3A(−VSSD); $^{**}P<0.01$, $n=3$; $^{***}P<0.001$, $n=5$; unpaired Student's *t*-test. (**c**) Fluorescence immunocytochemistry of GluN2A (green) and Shank (red) in DIV15 neurons treated with 10 µM TAT-Rph3A(−VSSD) or TAT-Rph3A-9c for 30 min. Scale bars, 10 µm. (**d**) Bar graph representing the percentage of co-localization of GluN2A with Shank. Data are presented as mean±s.e.m., $n=10$, $^{**}P<0.01$; unpaired Student's *t*-test.

Rph3A/GluN2A interaction is necessary for the synaptic localization of GluN2A-containing NMDARs. However, the reduction observed by TAT-2A-40 treatment could lead to lateral mobilization or endocytosis of the receptor. Therefore, we used live imaging in hippocampal primary cultures to address this point. In particular, we previously transfected primary cultures with SEP-GluN2A and then treated with TAT-2A-40. As

shown in Fig.6A-B, TAT-2A-40 significantly led to reduced SEP-GluN2A fluorescence. However, pretreatment with Dynasore (dynamin inhibitor) prevented this effect (Fig.16C-D).

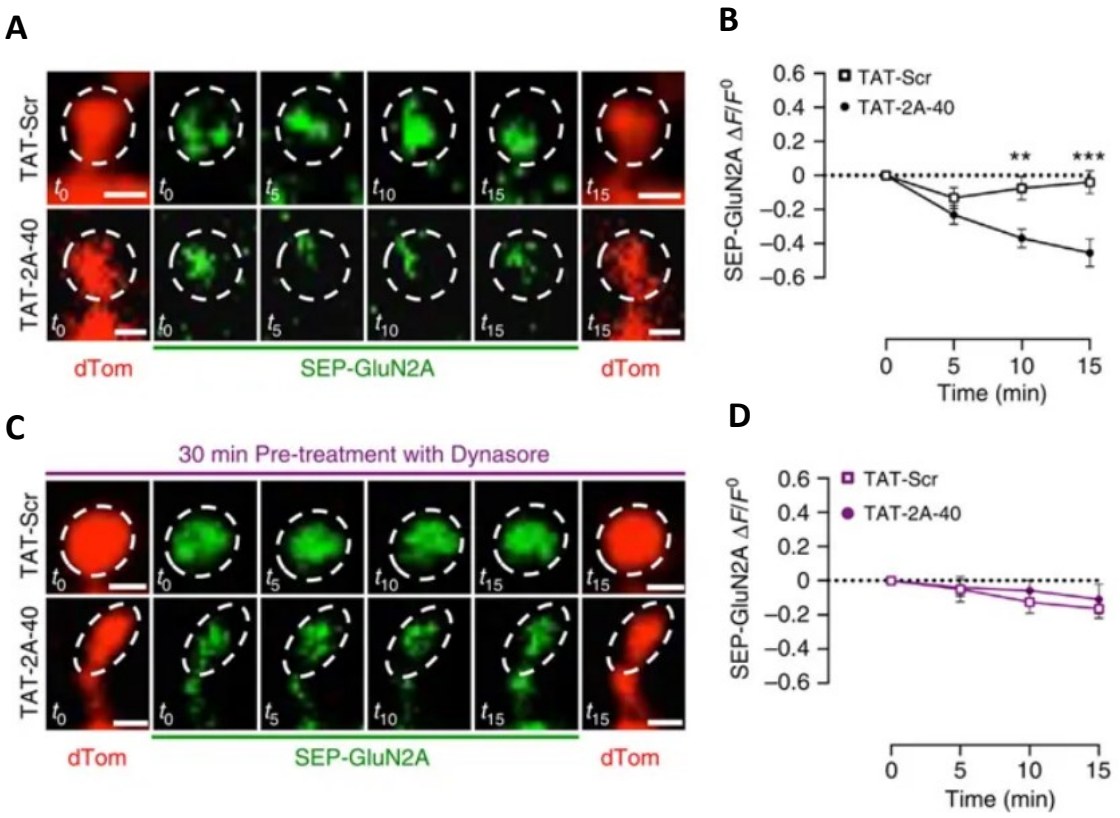

Figure 16. Disruption of Rph3A/GluN2A interaction leads to GluN2A endocytosis. A) Live imaging of *DIV16* hippocampal neurons co-transfected with SEP-GluN2A (green) and dTom (red) after 0 min (t_0), 5 min (t_5), 10 min (t_{10}) and 15 min (t_{15}) of treatment with 10 µM TAT-Scr or TAT-2A-40. Scale bars, 1 µm. (**B**) *XY* graph representing the $\Delta F/F_0$ of SEP-GluN2A over time. Data are presented as mean±s.e.m., n=17–22, $^{**}P$<0.01 and $^{***}P$<0.001; unpaired Student's t-test. C) Live imaging of pre-treated with Dynasore 80 µM for 30 min *DIV16* hippocampal neurons co-transfected with SEP-GluN2A (green) and dTom (red) after 0 min (t_0), 5 min (t_5), 10 min (t_{10}) and 15 min (t_{15}) of treatment with 10 µM TAT-Scr or TAT-2A-40. Scale bars, 1 µm. (D) *XY* graph representing the $\Delta F/F_0$ of SEP-GluN2A over time. Data are presented as mean±s.e.m., n=19–20.

Single cell injection at CA1 pyramidal layer in hippocampal slices of non permeable 2A-40 peptide reduced NMDA EPSCs, but not the amplitude (Figure 17A-D), indicating disruption of Rph3A/GluN2A affects NMDA mediated components of neurotransmission.

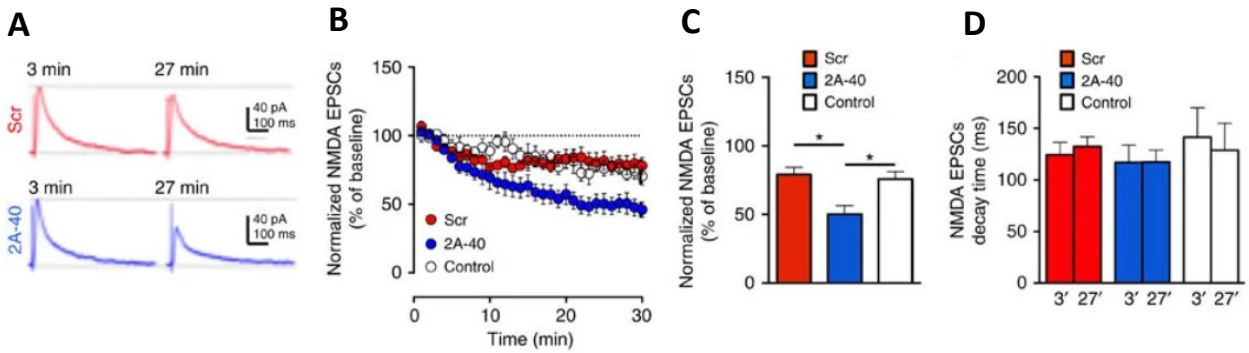

Fig. 17 TAT-2A-40 reduces NMDA EPSC in CA1 region of hippocampus. Sample traces showing the effect of intracellular perfusion of the non-permeable 2A-40 or its scramble peptides on pharmacologically isolated NMDAR-mediated EPSCs (+30 mV) recorded from a CA1 pyramidal cell. Traces represent the average of 6–9 responses with a scale of 40 pA over 100 ms. (**b**) Summary graph illustrating the time course of the effect of 2A-40 or its scramble on the peak amplitude of NMDAR-EPSCs. For comparison, the amplitude of NMDAR-EPSCs in the absence of any peptide in the intracellular solution (open circles) were also plotted (*n*=5–9). (**c**,**d**) Bar graphs summarizing the effect on the amplitude of NMDAR-EPSCs (**c**; Mann–Whitney test) and decay time (**d**) of the peptides (*n*=5–9).

To verify whether also AMPAR currents were affected by Rph3A/GluN2A complex disruption, we electroporated cells in CA1 region of organotypic hippocampal slices with shScramble or shRph3A and then recorded NMDA and AMPAR currents. A significant reduction of NMDA/AMPA currents in shRph3A transfected neurons compared to shScramble was observed, but no alteration of AMPA currents was revealed among experimental groups. Overall electrophysiological analysis indicate interference with GluN2A/PSD-95/Rph3A protein complex affects basal synaptic electrophysiological properties through modification of NMDA mediated currents.

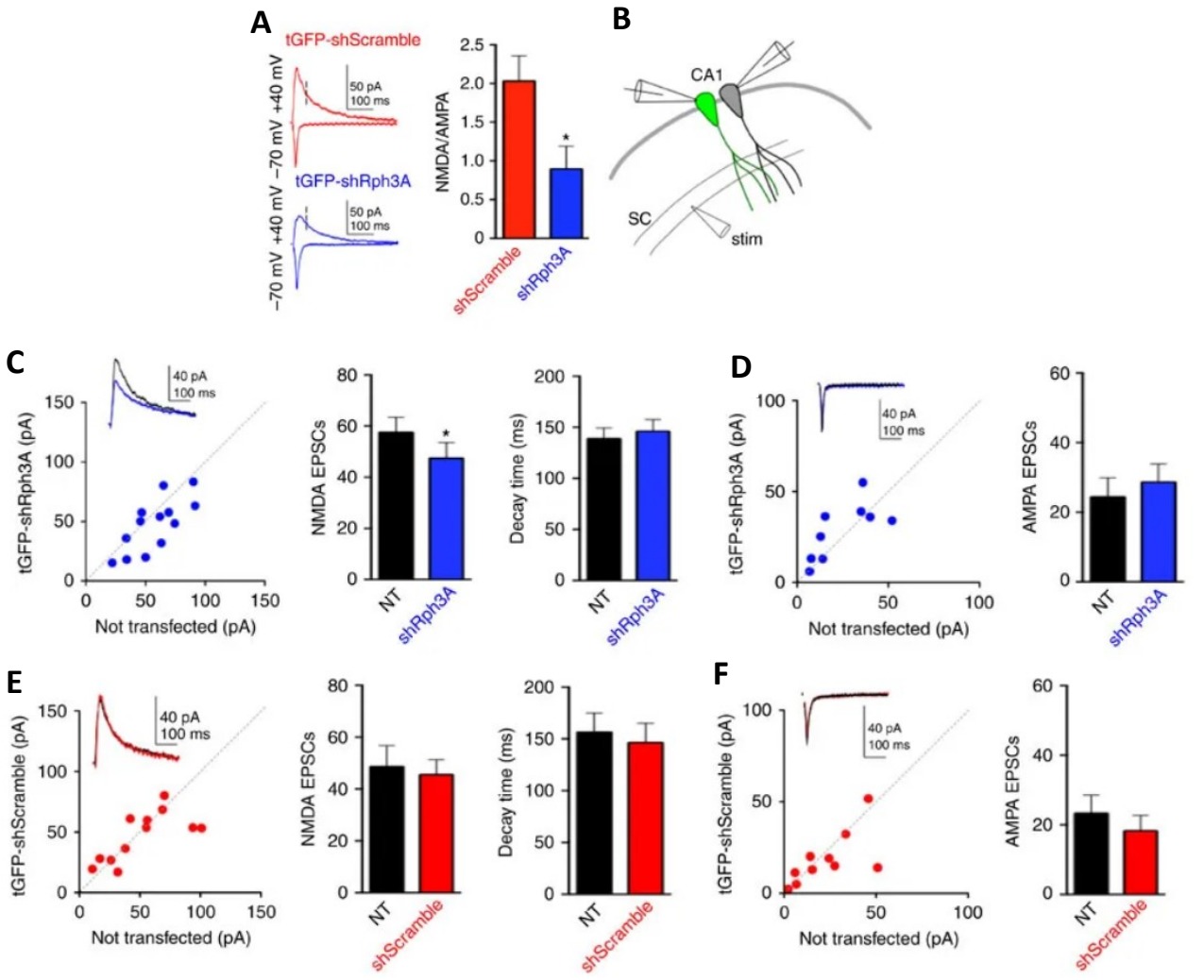

Figure 18. silencing Rph3A selectively affects NMDA mediated component of neurotransmission but not AMPAR currents. A) Sample traces and summary graphs illustrating that transfection of tGFP-shRNA-Rph3A induced a significant reduction in the NMDA/AMPA ratio when compared with cells transfected with tGFP-shRNA-Scramble (tGFP-shRNA-Scramble: 2.03±0.32; *n*=9; tGFP-shRNA-Rph3A: 0.89±0.29, *n*=8; Mann–Whitney test). B) Schematic illustrating paired recordings from neighbouring transfected and non-transfected neurons.C) Sample traces shown in the inset (not transfected (NT): *n*=13; tGFP-shRNA-Rph3A: *n*=13; Mann–Whitney test). D) Amplitude of AMPAR-mediates EPSCs at SC-CA1 (recorded at −70 mV; NT: *n*=9; tGFP-shRNA-Rph3A: *n*=9). E) Transfection with tGFP-shRNA-Scramble did not modify the amplitude or decay time of NMDAR-mediated EPSCs at SC-CA1 synapse (NT: *n*=12; tGFP-shRNA-Scramble: *n*=12). F) Transfection with tGFP-shRNA-Scramble did not reduce the amplitude of AMPAR-mediated EPSCs at SC-CA1 (NT: *n*=10; tGFP-shRNA-Scramble: *n*=10). All data are represented as mean±s.e.m. **P*<0.05.

As previously mentioned, synaptic transmission is strictly related to dendritic spine shape and density, reflecting specific states of the synapse. Therefore, hippocampal primary neurons were transfected with shRph3A/shScr or treated with TAT-2A-40/TAT-9c and analyzed for dendritic spine density and shape. Importantly, dendritic spine density was dramatically reduced by both silencing and active peptide treatments (Fig.19A-B). TAT-2A-40 treatment also led to a significant reduction in thin spines, but not other types (Fig.9D).

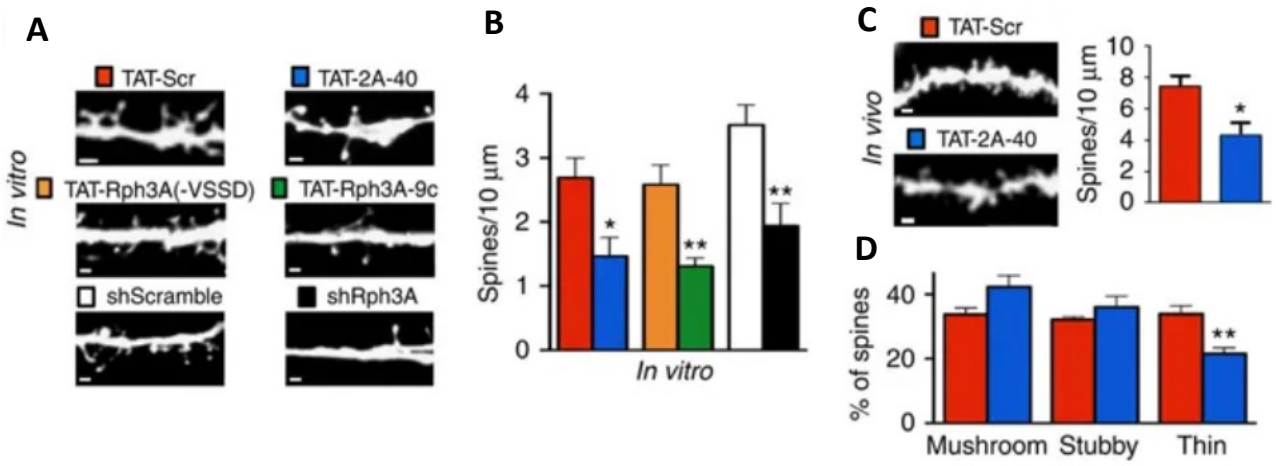

Figure 19. Disruption of GluN2A/Rph3A interaction impairs basal spine density in vitro and in vivo. Representative images show dendrites of *DIV15* hippocampal neurons treated with TAT-Scr (red), TAT-2A-40 (blue), TAT-Rph3A(−VSSD; orange) or TAT-Rph3A-9c (green) or transfected with tGFP-shScramble (white) or tGFP-shRph3A (black) at *DIV9*. (**b**) Bar graph representing the respective spine densities in these neurons (*n*=6–8; unpaired Student's *t*-test). (**c**) Representative images show dendrites of adult mouse CA1 neurons 2 h after injection of either TAT-Scr (red) or TAT-2A-40 (blue), both 3 nmol g^{-1} i.p. Bar graph represents the respective spine densities in these neurons (*n*=5; unpaired Student's *t*-test). (**d**) Bar graph representing the different spine types percentage compared with the total spines (mushroom, stubby and thin; *n*=5; unpaired Student's *t*-test). All data are presented as mean±s.e.m. **P*<0.05, ***P*<0.01, ****P*<0.001. Scale bars, 1 µm.

In vivo disruption of Rph3A/GluN2A/PSD-95 trimeric complex through chronic treatment (9 days from P6 to P14 rat pups, sacrifices at P15) of TAT-2A-40 peptide, similarly led to a decrease in spine density at CA1 region of hippocampus and reduction of NMDA/AMPA currents (Figure 20).

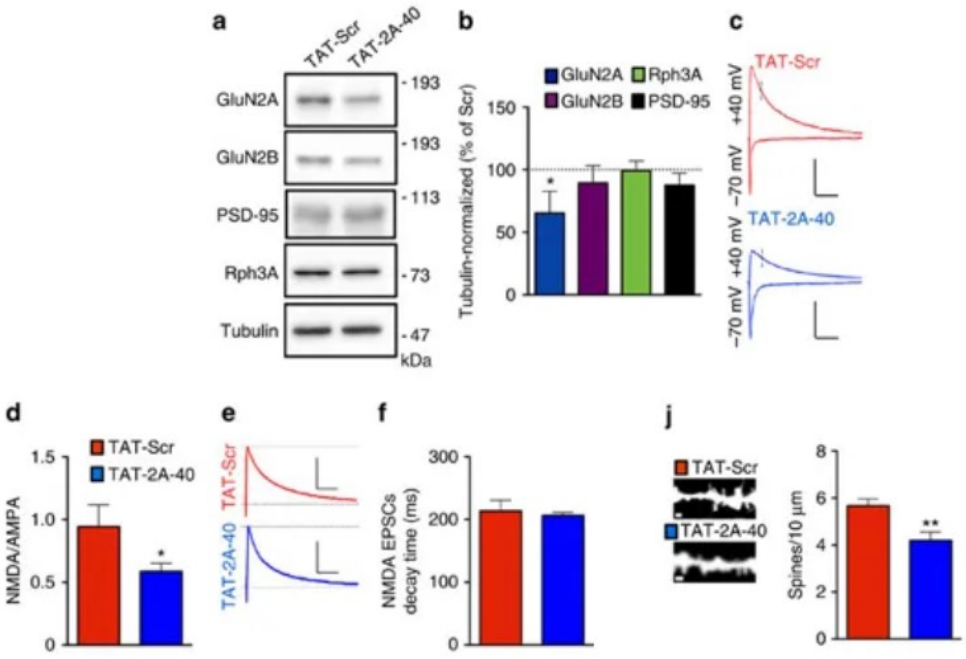

Fig.20 TAT-2A-40 chronic treatment during neurodevelopment reduces NMDAR mediated currents and spine density. A) Western blot analysis of GluN2A, GluN2B, PSD-95, Rph3A and tubulin of TIF from treated rat pups hippocampus. B) Bar graph representing the percentage of tubulin normalized integrated density of GluN2A, GluN2B, Rph3A and PSD-95 WB bands from TIF samples compared with their respective TIF purification TAT-Scr control (*n*=3–5; unpaired Student's *t*-test). C) Sample traces illustrating a decreased NMDA/AMPA in TAT-2A-40-treated animals (blue) compared with TAT-Scr-treated (red) animals at Schaffer collaterals to CA1 pyramidal cell synapses in acute hippocampal slices with 100 pA over 100 ms scale. D) Bar graph summarizes the significant decrease in NMDA/AMPA in TAT-2A-40-treated animals (blue) compared with TAT-Scr-treated (red) animals (*n*=9–12; Mann–Whitney test). E-F) Sample traces (E) and summary bar graph (F) illustrating that the decay time of pharmacologically isolated NMDAR-EPSCs does not differ between TAT-Scr-treated (red) and TAT-2A-40-treated (blue) animals (*n*=10–14) with 40 pA over 100 ms scale. (J) Representative images show dendrites of P15 rat pups CA1 neuron either treated with TAT-Scr (red) or TAT-2A-40 (blue), both 3 nmol g^{-1} s.c. chronically from P6 to P14. Bar graph represents the respective spine densities (*n*=10–11; unpaired Student's *t* test). All data are presented as mean±s.e.m. **P*<0.05, ***P*<0.01, ****P*<0.001. Scale bars, 1 µm.

Overall, these previous results indicated Rph3A is present at the postsynapse and serves as a scaffolding protein for GluN2A/PSD-95/Rph3A protein complex in PSD, stabilizing GluN2A-containing NMDARs at plasmic membrane. Interference with this trimeric complex leads to endocytosis of the receptor reducing GluN2A surface levels at the synapses, altering NMDA mediated currents and reducing spine density both in vitro and in vivo (Stanic et al., 2015).

Modulation of Rph3A/GluN2A protein complex is a pharmacological strategy for Levodopa Induced Dyskinesia

Since synaptic GluN2A/GluN2B ratio is known to play a role in neurotransmission and is altered in several brain disorders such as LID as previously reported (Fabrizio Gardoni & Bellone, 2015), our group also investigated whether Rph3A/GluN2A/PSD-95 protein complex is relevant for synaptic overabundance of GluN2A in this pathological synaptic plasticity condition (Stanic et al., 2017).

In particular, our group first detected Rph3A expression in striatum and further validated the presence of Rph3A in PSD and Rph3A/PSD-95/GluN2A protein complex. Interestingly, Rph3A phosphorylation at S234 modulates its binding to GluN2A and presence in PSD, and is positively coupled to activation of Dopamine-1 receptor (D1) but not D2.

In both striatum from PD patients and primate model of PD, such as Methyl-phenyl-tetrahydropyrine (MPTP) monkey, Rph3A mRNA levels is decreased in spite of equal protein levels.

Furthermore, in striatum from 6OHDA treated rats, an increase in GluN2A/Rph3A protein interaction was detected through IP both in dyskinetic and non-dyskinetic condition. However, increase in Rph3A protein levels in Triton Insoluble Fraction (TIF) was revealed only in dyskinetic ones. Interestingly phosphorylation at S234 was significantly reduced only in dyskinetic animals.

Interference with Rph3A/GluN2A interaction through TAT-2A-40 intrastriatal injection in dyskinetic animals dramatically reduced Abnormal Involuntary Movements (AIMs) for almost 1 week during Levodopa treatments, paralleled by a reduction in S845-GluA1 phosphorylation which is hallmark of dyskinetic striatum. Overall, these results indicate synaptic GluN2A-containing NMDARs at striatum are involved in dyskinetic behavior and Rph3A/GluN2A interaction represent a pharmacological target for treatment of this condition (Stanic et al., 2017).

Rph3A possible role in physiological synaptic plasticity: focus on learning and memory functions

GluN2A-containing NMDARs in learning and memory functions are relevant as previously mentioned (see paragraph GluN2A in synaptic plasticity), and are mostly associated to LTP induction compared to LTD. Furthermore, synaptic GluN2A protein levels increase after learning tasks in hippocampus LTP is characterized by high Ca2+ influx at dendritic spines, and Rph3A is known to display C2 domains which are Ca2+ sensitive. Interestingly as shown in Fig.21, our group has observed Rph3A/GluN2A protein interaction increases almost 3 folds when both Ca2+ and Inositol Triphosphate (IP3) are present (Stanic et al., 2015).

Therefore, modulation of synaptic Rph3A/GluN2A interaction during Ca2+ mediated events such LTP is possible.

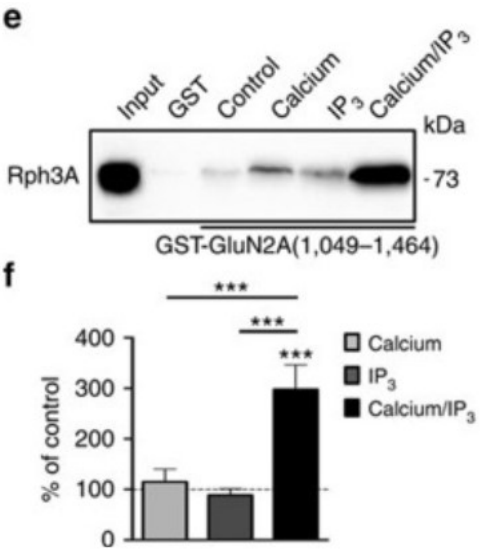

Figure 21. GluN2A/Rph3A interaction increases by copresence of Ca^{2+} and IP3. (adapted from Stanic et al. 2015).

Phosphorylation of Rph3A seems to play a role in LTP, however in a hippocampal region specific fashion. In fact, when inducing LTP Rph3A phosphorylation is much higher at CA3 synaptic terminals compared to CA1 terminals (Castillo et al., 1997). Nevertheless, Rph3A phosphorylation sites also comprehend Tyrosine residues as indicated by Capron in 2007. In particular, LTP induction at CA1 region did not induce T phosphorylation of Rph3A in the first minutes but after 1h, resembling baseline levels after 4h. Furthermore, inhibition of tyrosine kinases prevented late-phase of LTP as well as Rph3A-Tyrosine phosphorylation. However, researches did not investigate which tyrosine residues could play a role in Rph3A sequence (Capron, Wattiez, Sindic, Godaux, & Ris, 2007).

AIMS

As described above, synaptic NMDARs mainly mediate synaptic plasticity pathways, whereas extrasynaptic NMDARs are mostly detrimental for neuronal functions. The balance in synaptic vs. extrasynaptic NMDARs is responsible for adequate glutamatergic neurotransmission, which is altered in several neurological disorders and which is linked to the pathophysiology of brain diseases. In addition, a physiological glutamatergic neurotransmission at hippocampal synapses involves specific ratio of GluN2A/GluN2B subunits of NMDAR. Accordingly, understanding how to modulate qualitative subunit composition of synaptic NMDARs may represent new pharmacological strategies for several CNS disorders (Fabrizio Gardoni and Bellone 2015; Mellone et al. 2015; Franchini et al. 2020).

Our group previously showed Rph3A selectively stabilize GluN2A-containing NMDARs in PSD through a trimeric complex with PSD-95 (Stanic et al., 2015). Silencing Rph3A or disrupting Rph3A/GluN2A interaction both *in vitro* and *in vivo* leads to reduced spine density and synaptic levels of GluN2A-containing NMDARs, thus altering the synaptic ratio between GluN2A and GluN2B-containing NMDARs. Our group also demonstrated how modulation of Rph3A/GluN2A protein complex is relevant in LID conditions, underlining the biological role of this synaptic interaction (Stanic et al., 2017). Furthermore, it is well known GluN2A-containing NMDARs play a key role in learning and memory functions, in particular during potentiation of neurotransmission events such as LTP (Franchini et al. 2020). However, the physiological role of Rph3A in synaptic potentiation and tagging and in learning and memory functions has not been investigated yet.
Therefore, the main aims of this PhD project are:

i.) Elucidating the mechanisms responsible for Rph3A/GluN2A protein interaction
ii.) Investigating the role of GluN2A/Rph3A synaptic interaction
iii.) Evaluating a possible role of Rph3A as a tag for potentiated synapses and in learning and memory.

MATERIALS AND METHODS

1. Cell cultures

Primary hippocampal neuronal cultures

Primary hippocampal neuronal cultures were prepared from embryonic day 18-19 (E18-E19) Sprague-Dawley rat hippocampi (Charles River, Milan, Italy) as previously described (Piccoli et al., 2007). The day before dissection we coated plates and coverslips with PLL 1mg/ml dissolved in Borate Buffer overnight at Room Temperature (RT). Coverslips were previously cleaned with nitric acid, washed in bidistilled water and heat-sterilized in oven. The day of dissection, we removed poli-L-lysine (PLL) and washed with sterile bidistilled water all the plates. We then filled plates with a 37°C plating medium composed by DMEM (Invitrogen) additioned with 10% Horse Serum (Euroclone) and 1% Pen/Strep (Invitrogen) and incubated at 37°C with 5% CO2 in a humidified incubator. We then anestethized and sacrificed a pregnant rat and by cesarean section removed the E18-19 embryos. We collected embryos in a 100mm Petri dish with ice-cold dissection medium (Hank's balanced salt solution, HBSS) and sacrificed embryos by decapitation. Brains were removed, hemispheres separated from cerebellum an under a dissecting microscope we isolated the hippocampi. Hippocampi were collected in a 15mL falcon tube with ice-cold HBSS and under a biological-hood washed four times with the same medium. Next we additioned 500µL of Trypsin 10x (Invitrogen) to 4500µL of HBSS containing the hippocampi, then incubated at 37°C for 13' in a waterbath. After that, hippocampi were washed four times with 37°C pre-warmed plating medium to neutralize trypsine activity. Next we disgregated mechanically with a micropipette the hippocampi in a final volume of 10mL, till the cell suspension becomes cloudy. We then counted cells manually through a Bürker-chamber and plated cells at appropriate density. After 12-16h medium was changed to Neurobasal medium (Gibco) supplemented with 2% B27 (Gibco), 1% Glutamax (Invitrogen) and 1% Pen/Strep.

Neuronal Transfection

Neuronal cultures were transfected between DIV7 and DIV10 using calcium-phosphate method with 1-4µg of plasmid DNA. Insoluble Calcium-phosphate salts coprecipitates with DNA and are then endocyted by the cells. We previously prepared a filter sterilized 2,5M CaCl2 solution in water, and HBS 2x solution. One hour before transfection, cell culture medium was temporary removed and replaced with pre-warmed 37°C Minimal Essential Medium (MEM; Gibco). Plates were then left in the incubator again at 37°C. 30' before transfection we prepared transfection solutions (A and B) to

be mixed according to the following protocol, and waited 25 minutes before adding them to cell culture. In particular, solution A consists of 80µL of HBS 2x while solution B is composed of plasmid DNA, sterile water and 10µL of 2,5M CaCl2 to a final volume of 80µL. The solutions were mixed by pouring drop by drop solution B into solution A on a gently mixing. We then waited 25' minutes before pouring 80µL of DNA precipitates on cell cultures, which were then left in a 37°C incubator for 20 minutes. Next we checked at cell microscope the presence of visible Calcium-Phosphate precipitates. In order to remove all precipitates, we washed cells twice with MEM and left in the incubator for 15' at 37°C. After this interval, we checked again for the presence of Calcium-Phosphate in the culture. If visible precipitates could be found, cells were subjected to another wash as previously. Otherwise, MEM was removed and replaced with the original neurobasal medium collected at the beginning of transfection procedure. Cells were left in the incubator the remaining time till DIV14 was achieved.

COS-7 cell line: Plating and Splitting

All reagents were prewarmed at 37°C in a water bath. Under a biological hood, we removed culture medium and washed twice with PBS (1x) to eliminate serum residues. We then applied 2mL of Trypsin EDTA 1X (Gibco) and left plates in the incubator for 5-6 minutes to promote trypsine activity and therefore cell detachment from the plate surface. We used a micropipette (P1000) to help detachment of cells. We counted cells through a Neubauer cell counter and plated 75000 cells for each well of 12 MW plates.

COS-7 cell line: Lipofectamine Transfection

Lipofectamine transfection was used on COS-7 cell cultures, performed as follows. The day before transfection cells were plated in 12 MW plates for immunostaining. We mixed 1,5µg of DNA in Optimem media containing 1,5µL. of Plus reagent (Invitrogen) at RT for 10 minutes. We then added 4µL of lipofectamine LTX reagent (Invitrogen) to the DNA mixture and incubated for 25 minutes. Next, we changed COS-7 cells medium with DMEM in absence of serum and added DNA mix drop-wise, incubating at 37°C overnight in humidified incubator. The day after, we changed media to DMEM supplemented with 10% FBS and incubated for 24h. We then fixed cells with PFA or collected them for protein quantification.

2. Drug treatments

Chemical-LTP (cLTP) on primary cultures

cLTP was performed on hippocampal primary cultures as previously (Marcello et al., 2013; Oh et al., 2006). In particular, culture medium was removed and replaced by pre-warmed Artificial Cerebrospinal Fluid (ACSF) with MgCl2. Cells were then placed back in the incubator at 37°C for 30'. cLTP induction was developed in 16' by application of Forskolin (50µM), Rolipram (0,1µM) and Picrotoxin (100µM) in ACSF without MgCl2 (pH 7.4-7.5), while control condition consisted of ACSF in presence of MgCl2 and vehicle volume of the corresponding drugs (DMSO, under 1% final concentration). After this span of time, cells were washed once in ACSF+MgCl2 to remove drugs leftover; then cells were incubated with ACSF+MgCl2 for a variable resting period depending on biochemical or imaging experiments (15' for biochemical analysis, 45'-2h for imaging) (Marcello et al., 2013; Otmakhov et al., 2004).

Brain Derived Neurotrophic Factor (BDNF) treatment:

BDNF was resuspendend in sterile water according to the manufacturer instructions. BDNF treatment was used at 50ng/mL in culture medium for 3h at 37°C.

Chemical-LTD (cLTD)

cLTD was performed as previously on hippocampal primary cultures as previously reported (Marcello et al., 2013; Oh et al., 2006). More in detail, cell culture medium was removed and replaced by pre-warmed ACSF + MgCl2 at 37°C. Cells were incubated at 37°C in the incubator for 30' before cLTD induction. cLTD was performed by replacing the media with ACSF+MgCl2 additioned of NMDA 50µM, while control condition was maintained in ACSF+MgCl2. Cells were then incubated at 37°C in the incubator for 10 minutes. After this time frame, cells were washed and incubated with new ACSF+MgCl2 for 20 minutes.

(RS)-3,5-Dihydroxyphenylglycine (DHPG)

DHPG was dissolved according to manufacturer datasheet in water at a stock concentration of 2000x. Cells were incubated with DHPG directly applied in culture media to a final concentration of 50µM for 15', then harvested for biochemical analysis.

SunSET

Puromycin (Sigma) was applied in culture medium to a final concentration of 10µM for 5'. Afterwards, coverslips were washed with PBS Ca/Mg to remove extracellular puromycin and immediately fixed with 4%PFA in PBS+4% sucrose for 10' at RT.

3. Biochemistry

Cell fractionation

Neuronal cultures were washed once with PBS Ca2+/Mg2+, then scraped and lysed in ice-cold lysis buffer consisting of 0.32M Sucrose, 1mM NaF, 0,1mM PMSF, 1mM MgCl2, 1mM Hepes using a glass-glass homogenizer. First, homogenates were centrifuged at 1000 g for 5 minutes at 4°C to pellet nuclear components. Supernatant was then centrifuged at 13000 g for 15 minutes at 4°C. The resultant pellet (P2) represents crude membrane fraction containing both pre and postsynaptic compartments, additioned of other organelles. The post-synaptic fraction is a complex mix of PSD proteins which cannot be solubilized in 0,5%-1% Triton solutions (Triton Insoluble Fraction; Gardoni et al., 2001). Therefore, resuspension of P2 in a triton buffer (Tryton 0,5% for cell cultures, while 1% for tissue processing) additioned with 150mM KCl. We incubated the suspension for 15 minutes on ice and the centrifuged in a ultra-centrifuge at 100000 g for 1h at 4°C. The resultant pellet represents the TIF, which is then resuspended in Hepes 20mM buffer and protease inhibitors.

In case both P2 and TIF from the same sample were analyzed, P2 was first resuspended in Hepes 20mM. An aliquote was immediately frozen and the leftover additioned of 2x Triton-KCl buffer to obtain the desired Triton-KCl final concentration.

All the previous steps were performed in presence of protease inhibitors (Sigma) and phosphatase inhibitors (Roche). Protein concentration was detected through Bio-Rad protein assay reagent (Hercules, CA, USA).

Co-ImmunoPrecipitation assays (Co-IP)

Homogenate/P2 aliquots containing respectively 150-50µg of proteins were incubated overnight at 4°C with primary antibody in RIA buffer containing 50 mM Tris HCl (pH 7.2), 150 mM NaCl, 1% NP-40, 0,2% sodium dodecyl sulphate (SDS), 0,5% deoxycholic acid. As control, a No-IgG sample was prepared in same conditions without the antibody.

The Protein A/G-sepharose beads (Sigma-Aldrich) were added and incubated for additional 2 h, at room temperature, on a wheel. Beads were precipitated by quick centrifugation and washed three times in RIA buffer supplemented with SDS 0,1% and boiled for 10 minutes in β-mercaptoethanol and SDS supplemented sample buffer (VWR). Beads were centrifuged and supernatant loaded in a proper acrylamide gel for SDS-PAGE. For the input lane a 10% of homogenate/P2 samples were used. This allows to monitor the expected molecular weight of immunoprecipitated proteins and verify heir presence in the sample.

Western blotting

We evaluated by spectrophotometer analysis the protein concentration in our samples. Afterwards, we prepared 1µg/µL stock samples with denaturating sample buffer (in presence of SDS and β-mercaptoethanol. We then loaded the same amount of protein in poli-acrylamide gels for SDS-PAGE and performed an electrophoresis for protein separation. Next, we transferred proteins onto a nitrocellulose membrane at 250 mA for 2h in 1x blotting buffer (25mM Tris, 192mM glycine). We then incubated membranes 1h with I-block solution, composed of I-block powder (1g per 500mL solution; Invitrogen) dissolved TBS 1x supplemented with 2mL of Tween20 (Sigma) 20% in water. Membranes were then incubated with primary antibodies for target proteins overnight at 4°C on a shaker plate. Primary antibodies were dissolved in I-block solution.

The day after, membranes were washed three times with TBS 1X added of 1mL Tween20. Membranes were then incubated with respective Horseradish conjugated secondary antibodies for chemiluminescence detection, at a final concentration of 1:5000-1:30000 depending on experimental conditions. Detection adopted the Biorad ECL substrates and for chemiluminescence western blot detection we used the ChemiDoc MP system (Bio-Rad Laboratories).

4. Molecular Biology

Bacterial transformation

We transformed using E.Coli DH5 strain in our protocol. We added 50-200ng of

DNA into 50 µL aliquot of competent cells, then incubated on ice for 30 minutes.

We heat-shocked the cells by leaving them in a temperature-controlled waterbath at 42°C for 30 seconds, and putting them again on ice for 3 minutes. We added 250 µL of S.O.C. Media to bacteria and incubated them for 1h at 37°C with vigorous shaking to allow expression of antibiotic resistance.

Finally, we plated the cells on LB-agar plates with the antibiotic of choice (depending on the plasmids, Ampicillin or Kanamacin) and incubated at 37°C overnight. Day after, colonies were tip-picked and grown in LB overnight for mini/midi/maxi preparations according to manufacturer protocol (Qiagen) and glycerol stocks.

5. Confocal imaging

Immunocytochemistry (ICC)

Hippocampal primary neurons on coverslips were treated at DIV14 and fixed for 10 minutes with 4% paraformaldehyde (PFA)+4% sucrose in PBS solution at RT and then washed with PBS three times. Next, cells were permeabilized with 0.1% Triton-X100
in PBS for 15 minutes and blocked with 5% BSA (VWR) in PBS for 1 h at room temperature.
Primary antibodies for immunostaining were dissolved in 3% BSA in PBS in a humidified chamber at 4°C overnight, followed by three washes in PBS at RT.
Secondary antibodies were applied in 3% BSA in PBS for 1 hour at room
Temperature. After that, coverslips were washed again three times, eventually applied DAPI staining for nuclei (1:50000 in PBS), washed again and finally mounted with Fluoromount media (Sigma) on a glass slide. Glass slides were maintained at 4°C till acquisition with Zeiss LSM 510; Nikon A1 Ti2 system or Zeiss LSM 900 with sequential setting at 1024x1024 pixels resolution.
For all images the signals for each image were kept within the linear range and settings
were consistent between different experimental conditions for an unbiased comparison.

In situ Proximity Ligation Assay (PLA)

PLA was performed in primary cultures as previously reported (Dieck et al., 2015). Cells were fixed with 4% PFA+4% Sucrose in PBS solution for 10
min at RT. Cells were then washed with PBS for three times, permeabilized with 0.1% Triton X-100 in PBS for 15 min at room temperature and blocked with blocking solution from PLA kit (Sigma-Aldrich, Olink Bioscience) at RT on shaker. Neurons were then incubated overnight at 4°C with different couples of antibodies, depending on the protein-protein interaction to be visualized, in Antibody diluent solution provided with PLA kit. The day after, coverslips were washed at RT with the kit buffer A twice for 5 minutes on shaker. Anti-mouse Plus and Anti-Rabbit Minus probes were diluted 1:5 in Antibody diluent and applied on coverslips for 30 minutes at 37°C in dark humid

chamber. Coverslips were then washed with buffer A twice again and incubated for 30' at 37°C in dark humid chamber with ligation solution consisting of Ligase Buffer 1:5, Ligase 1:40 and water. Next, coverslips were washed with Buffer A twice again and incubated 1h and 30' at 37°C in dark humid chamber, with amplification solution made of Polymerase 1:80, amplification buffer 1:5 and water. After that, coverslips were washed with buffer B (provided with the kit) twice for 5' to stop polymerization. Coverslip eventually underwent immunostaining after PLA, for MAP2 or GFP. Coverslips were mounted using Fluoroshield mounting media (Sigma).

Puro-PLA

To detect local protein synthesis, we used Puro-PLA technique as previously described (Li and Gotz, 2017; Dieck et al. 2015). Neurons were incubated for 15 min with 1µM Puromycin at the end of the cLTP protocol. Puromycin inserts in new synthetized polypeptides blocking their elongation. Specific labeling of Puromycin through a monoclonal antibody (Merck #MABE343 1:100) and an antibody against N-terminal portion of a target protein, allows detection with a PLA technique of new synthetized polipeptides. We quantified cluster density in dendrites as a ratio of clusters along dendrite length, marked with MAP2. Somatic density was instead quantified as area of the clusters over the somatic area removing nuclei (labeled with DAPI). Negative controls were considered as Rph3A antibody (Proteintech 1:200 #133961AP).

Spine morphology and density

spine morphology analysis was performed with FIJI freeware software. Stacks were collapsed along Z axis, resulting in a bidimensional image. For each spine the length, width of the head and the neck were measured with straight-line function. Dendrites were also measured to obtain mean spine density as ratio of n. of spines on 10µm of dendrite length.

6. Animals and behavioral tasks

Enriched Environment (EE)

Mice (5 weeks old female, strain C57BL/6J) were obtained from Charles River (Calco, Italy) and were housed in the animal facility of the Department of Pharmacy, Section of Pharmacology and Toxicology, School of Medical and Pharmaceutical Sciences, University of Genoa. After three days, mice were housed for three months in standard or in enriched conditions (see below) and then they

were sacrificed by cervical dislocation and immediately decapitated to collect the brain. Female mice were randomly assigned to two different groups: the untrained mice and the enriched environmental trained mice. Trained animals were housed in a large cage (36 x 54 x 19 cm, 8 animals per cage) containing a variety of objects such as plastic tunnels, climbing ladders, toys in wood and plastic suspended from the ceiling, running wheels, paper, cardboard boxes, and nesting material. Objects were changed every 3 days. Untrained animals were housed in a standard cage with nest. In both cases, the bedding was changed every week. The animals were kept in the enriched environment for three months.

Spatial object recognition

Mice (6 weeks old male, strain C57BL/6J) were obtained from Charles River (Calco, Italy) and were housed in the animal facility of the CNR Institute of Neuroscience, Milano. Spatial object recognition test was performed one week after housing. Object location tests were performed in an arena according to the methods described in (Kenney, Adoff, Wilkinson, & Gould, 2011), with slight modifications. Two visual cues were placed on two adjacent walls of an opaque white Plexiglas cage (58 × 50 × 43 cm) that was dimly lit from above (27 lux). The visual cues consisted of a black and white striped pattern (21 × 29 cm) that was affixed to the center of the northern wall and a black and white checkered pattern (21 × 29 cm) that was placed in the center of the western wall. The objects were counterbalanced across locations. The cage and the objects were thoroughly wiped down with acetic acid (0.1%) before and after all behavioral procedures, which were observed and recorded using a camera mounted above the cage. Climbing or sitting on objects was not scored as object exploration. Twenty-four hours after 10 min habituation to the cage without objects, mice were exposed to the cage where two different objects were placed in the NE and NW corners for a maximum of 20 min or until they had completed 30 s of cumulative objects exploration and the time spent exploring the objects was recorded. Two hours later, the object the mouse had spent more time exploring in the previous session (T1 phase) was moved to the SW corner of the cage, and each mouse was allowed to re-explore the cage (T2 phase). Exploration was defined as a mouse having its nose directed toward the object and within approximately 1 cm of the object. TAT-SCR or TAT-2A40 treatment was done 60 min before T1 phase. Performance was evaluated by calculating a discrimination index (N-F/N+F), where N = the time spent exploring the moved object during T2, and F = the time spent exploring the stationary object during T2. Spontaneous motor activity - Motor function was evaluated in an automated activity cage (43 x 43 x 32 cm; Ugo Basile) placed in a sound-

attenuating room. The cage was fitted with two parallel horizontal and vertical infrared beams located 2 and 4 cm from the floor, respectively. Before the start of the test, each mouse was habituated to the testing room for 1 h. Cumulative horizontal and vertical movement counts were recorded for 10 min. The test was carried out in the same animals submitted to Spatial Object Recognition test, immediately after T2 phase of Spatial Object Recognition test (M. Sala et al., 2011).

Rat hippocampal slices

Adult Sprague-Dawley rats were anesthetized and sacrificed by decapitation. Brain was immediately removed and hippocampi were sliced through a chopper to a 400µm thickness. Slices were selected in a petri with Krebs solution supplied with CO2+O2 under dissection microscope. Only intact slices with visible hippocampal regions were selected for cLTP procedures. In particular, slices were maintained for 45' in ACSF+MgCl2 before cLTP induction (see cLTP).

Pre-embedding immunohistochemistry

Three adult Sprague Dawley male rats were used. After terminal anesthesia was induced by brief inhalation of isoflurane (0.05% in air), followed by an intramuscular injection of ketamine (100 mg kg-1) and xylazine (10 mg kg-1), rats were intracardially perfused with 4% paraformaldehyde (PFA) and 0.1% glutaraldehyde in phosphate buffer saline (PBS, 0.1 M, pH 7.2), and brain sections (100 µm) were cut on a Leica VT1000S vibratome (Leica Microsystems, Milton Keynes, UK. The vibratome sections were collected in PBS and then incubated in 50 mM ammonium chloride in PBS for 20 min at RT. After extensive washing in PBS, antigen retrieval was performed by incubation of the sections in 10 mM sodium citrate, pH 8.4, for 1 h at 80°C. Sections were once more extensively washed with PBS before being blocked in 0.1% (w/v) gelatin in PBS. Sections were incubated with rabbit anti-Rph3A polyclonal antibody (1:100; ab68857, Abcam) in 0.1% (w/v) gelatin, 0.05% Triton X-100 in PBS at 4°C for 48–72 h. Sections were rinsed in PBS, postfixed for 5 min in 4% PFA in PBS, rinsed again, and incubated with biotin-conjugated goat anti-rabbit secondary antibody (1:200) for 12 h in 0.8% bovine serum albumin and 0.2% fish gelatin (Sigma-Aldrich) in PBS at 4°C. The following day, sections were rinsed in PBS, then postfixed in 1% glutaraldehyde in PBS (5 min) and rinsed in PBS followed by ABC Elite Kit (1:200; 2 h at RT) (Vector Laboratories). The peroxidase reaction was revealed by incubating the sections in ImmPACT VIP substrate Kit (Vector Laboratories). Then the sections were osmicated, dehydrated, and flat embedded in Durcupan resin (Sigma-Aldrich). Ultrathin sections (70–90 nm) were countercolored with uranyl acetate and lead citrate. Control

experiments, in which the primary antibody was omitted, resulted in no immunoreactivity. The images were captured with an AMT XR404 megapixel side mounted CDD camera at a magnification between 7900 and 92000. Only identified synapses on dendritic spines of apical dendrites of pyramidal cells in stratum radiatum of CA1 hippocampus were included in the analysis. No tangentially cut synapses were analysed. To determine the spine density (number of spines/µm2), we utilized 28-35 images per animal (7900 magnification, Tot Area: 7841.306µm2) in which we identified the spines and, then, quantified them using the cell counter tool in ImageJ (http://rsb.info.nih.gov/ij). Morphometric parameters such as spine head area, PSD length, and thickness (Moreau et al., 2010) were measured from 500 spines/animal. To determine the head area of spines, we traced the plasma membrane with ImageJ. The average thickness of the PSDs was measured as follow: the cytoplasmic outline of a PSD, including the associated dense material, was traced with ImageJ, and this area was then enclosed by tracing the postsynaptic membrane (length of PSD). The area was then divided by the length of the postsynaptic membrane to derive an average thickness for the PSD. The results are presented as the mean ± SEM. The measurements were all performed by researchers blind to the genotype.

Electrophysiology

C57BL/6J male mice were intraperitoneal injected either with TAT-2A40 or TAT-SCR peptides at 3nmol/g. After 1h mice were anesthetized with isoflurane/O2 and brains were dissected on ice. Hippocampal coronal slices (300 µm) were cut in cold artificial cerebrospinal fluid (ACSF) containing (in mM): 119 NaCl, 2.5 KCl, 1.3 MgCl2, 2.5 CaCl2, 1.0 NaH2PO4, 26.2 NaHCO3 and 11 glucose, bubbled with 95% O2 and 5% CO2. Slices were maintained at room temperature and allowed to recover for 1 hr before being transferred to the recording chamber. The external solutions contained (in mM) 119 NaCl, 2.5 KCl, 2.5 CaCl2, 1.3 MgSO4, 1.0 NaH2PO4, 26.2 NaHCO3, 11 glucose, and 0.1 picrotoxin (pH 7.4) at 37°C and equilibrated with 95% O2 and 5% CO2. Somatic whole-cell voltage-clamp recordings were made from CA1 pyramidal cells using 2–6 ΩM electrodes. The internal solution contained (in mM) 115 CsMeSO4, 20 CsCl2, 10 HEPES, 2.5 MgCl2, 4 NaATP, 0.4 NaGTP, 10 NaCreatine, and 0.6 EGTA (pH 7.2). Cells were held at −70 mV and LTP protocol was induced by pairing the cell at 0 mV at a frequency of 2 Hz for 90 s. Synaptic responses were collected for 25 minutes with a Multiclamp 700B-amplifier (Axon Instruments, Foster City, CA), filtered at 2 kHz, digitized at 5 Hz, and analysed online using Igor Pro software Wavemetrics, Lake Oswego, OR).

7. Antibodies

Anti-Anti-GluN2B phosphor-Tyr1472 Calbiochem (#454583); Anti-phosphoT202/Y204-MAPK 44/42 Cell signaling #9101; anti-ERK 44/42 Cell Signaling #9102; Anti-Puromycin #MABE343 Merck, WB 1:1000; monoclonal anti-PSD-95 (WB 1:1000, ICC 1:100 #K28/43) Neuromab; anti-tGFP ICC 1:300 #AB513, Evrogen; anti-Tubulin (WB 1:30000; #T9026, Sigma), rabbit anti-GluN2A (WB 1:1000 #M264) were purchased from Sigma-Aldrich. Mouse monoclonal anti-Puromycin (WB 1:5000 #MABE343) clone 12D10, rabbit anti-N-term GluA1 (ICC 1:100 MAB2263) and rabbit monoclonal anti-phosphoSer845-GluA1 (WB 1:1000 #04-1073) were purchased from Merck Millipore. Rabbit anti-Rabphilin3A (WB 1:1000 #118003) was purchased from Synaptic System. Rabbit anti-N-term GluN2A (ICC 1:100 480031), rabbit Anti-GluN2B (WB 1:1000 #718600), were purchased from Invitrogen. Secondary antibodies for imaging experiments: goat anti-rabbit-Alexa555 (A-21429; Life Technologies), Alexa-fluor 488 (A-11039) goat anti-chicken, goat anti-mouse-Alexa555 (A-21422), 4',6'-diamidino-2-phenylindole (DAPI, 1:50,000 in PBS, Thermo Fischer Scientific), goat anti-rabbit-Alexa-488 (A-11034).

8. Ethical authorizations

For Electron microscopy experiments, all procedures were performed according to the requirements of the United Kingdom Animals (Scientific Procedures) Act 1986, Newcastle University AWERB 596. For enriched environment experiments, n. 484 of 2004 and Experimental procedures were in accordance with the European legislation (Directive 2010/63/EU for animal experiments), the ARRIVE guidelines and the 8th Edition of the "Guide for the care and Use in laboratory-animals", and they were approved by the Animal Subjects Review Board of the University of Genoa and by the Italian Ministry of Health (DDL 26/2014 and previous legislation; protocol n. 50/2011-B and 612/2015-PR) and on authorization n.484 of 2004.

9. Quantification and statistical analysis

Western Blot quantification was performed using the software ImageLab (BioRad Laboratories). Protein levels were expressed as relative optical density (OD) normalized on tubulin levels as housekeeping protein. Images acquired with confocal microscope were analyzed with the use of Fiji / Image J software. Statistical analysis was performed with GraphPad Prism7 software and data were presented as mean ± SEM (standard error of the mean). The tests used to assess data significance

are indicated in the figure legends, we used 2-tailed Student t test (a p value less of 0.05 was considered significant) or one-way ANOVA followed by Tukey or Bonferroni's as a post-hoc test. In each result at least three independent experiments were analyzed.

RESULTS

1. Rph3A positive spines are characterized by increased spine head area and PSD size

Rph3A is mostly characterized in the presynaptic compartment, involved in neurotransmitter exocytosis (Burns, Sasaki, Takai, & Augustine, 1998; C. Li et al., 1994; Mizoguchi et al., 1994). Our group previously characterized Rph3A presence in the postsynaptic compartment, in particular at lateral side of PSD (Stanic et al. 2015). We first characterized with pre-embedding immunohistochemistry through electron microscopy (EM) the quantitative distribution of Rph3A at rat CA1 stratum radiatum in basal conditions. As shown in Fig.1, we detected Rph3A presence in almost 50% of dendritic spines (48.275 ± 2.331% of dendritic spines, n = 3632). Noteworthly, Rph3A positive presynaptic terminals showed similar distribution (42.428 ± 2.301% of 3632 presynaptic terminals), without significant association to Rph3A presence at the postsynapse (data not shown)

We then questioned whether Rph3A+ spines could display different morphological parameters. From morphological analysis, Rph3A+ spines show a significant increase in spine head area (Fig.1C, 1D), PSD length (Fig.1E, 1F) and PSD thickness (Fig.1G, 1H) compared to Rph3A- ones (see Fig.1 and also table 1). These results indicate an abundance of Rph3A in PSD of more mature spines in static conditions.

However, synapses undergo continuous rearrangement during synaptic plasticity events, so we investigated the modulation of Rph3A presence in PSD during potentiation of neurotransmission, such as LTP.

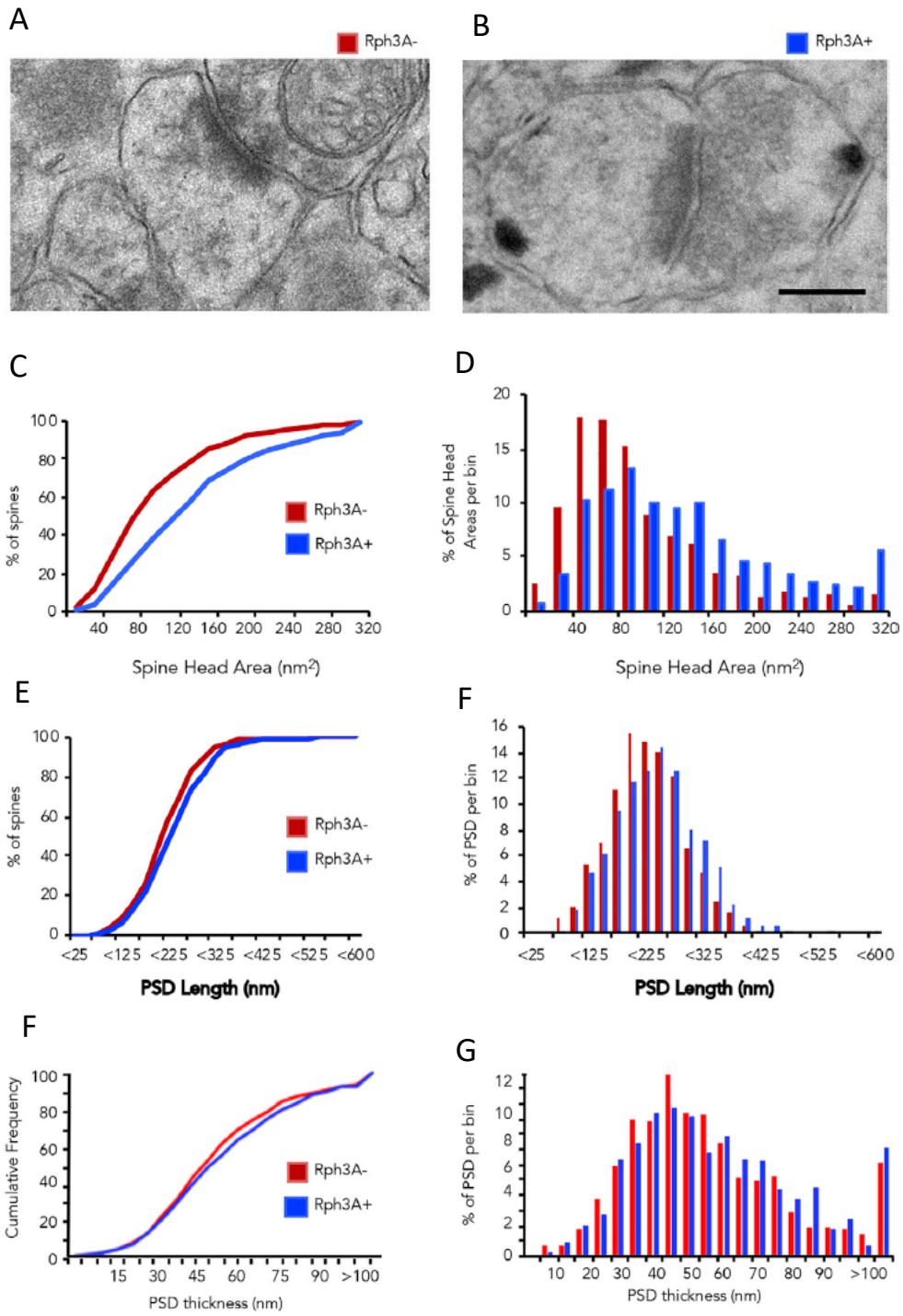

Fig. 1. Morphological Analysis of Rph3A-Positive and Rph3A-Negative Dendritic Spines.

Representative electron micrographs of stratum radiatum CA1 region of Rph3A negative (A, left image; Rph3A-) and positive (B, right image; Rph3A+) spinous synapses, respectively. Scale bar, 125 nm. C-D) Shifted distribution of spine head area toward bigger values in Rph3A+ spines (blue; n = 689/1,500, 3 rats) compared with Rph3A_ spines (red; n = 811/1,500, 3 rats; $p < 0.001$, Mann-Whitney Rank Sum Test). E-F) Shifted distribution of PSD length toward bigger values in Rph3A+ spines (blue; n = 689/1,500, 3 rats) compared with Rph3A_ spines (red; n = 811/1,500, 3 rats; $p < 0.001$, Mann-Whitney Rank Sum Test). G-H) Shifted distribution of PSD thickness toward bigger values in Rph3A+ spines (blue; n = 689/1,500, 3 rats) compared with Rph3A_ spines (red; n = 811/1,500, 3 rats; $p < 0.05$; Mann-Whitney Rank Sum Test).

Table 1. Morphological Analysis of Rph3a+ and Rph3A− Dendritic Spines (n = 3 Rats, 500 Spines/Rat).

Labeling	Rph3A− Spines (n = 811/1,500)	Rph3A+ Spines (n = 689/1,500)	p Value (Rph3A+ versus Rph3A−)
PSD length (nm)	215 ± 2.38	232 ± 2.87	<0.001
PSD thickness (nm)	54.5 ± 0.96	56.7 ± 1.06	0.049
Spine Head Area (nm^2)	99.9 ± 2.40	143 ± 3.54	<0.001

2. cLTP increases GluN2A and Rph3A protein levels in PSD

GluN2A levels are well known to increase at excitatory PSDs after LTP induction (Barria & Malinow, 2002; Bellone & Nicoll, 2007; Grosshans et al., 2002), thus we wondered whether also Rph3A was driven to PSD after LTP. Therefore, we used a validated chemical-LTP protocol (cLTP; Marcello et al. 2013; Otmakhov et al. 2004) on hippocampal primary cultures, based on increased PKA activity through Forskolin (enhancer of AC activity), Rolipram (Phosphodiesterase inhibitor) and Picrotoxin (GABA-A receptor antagonist). As internal control of this treatment, we verified augmented levels in phosphorylation at S845 of GluA1-containing AMPAR (**p<0,01; Fig. 2A), which is a hallmark of LTP (Esteban et al. 2003; Hu et al. 2007; Makino et al. 2011; Oh et al. 2006). As expected, we detected increased levels of phosphor-S845-GluA1 AMPARs in TIF after cLTP (**p<0,01, Fig. 2A). According to literature GluN2A protein levels were increased after cLTP (**p<0,01; Fig.2B; Baez, Cercato, and Jerusalinsky 2018). Interestingly, also Rph3A levels was increased in the same fraction after cLTP (*p<0,5; Fig.2B).

To better elucidate whether summon of Rph3A was specific for potentiation of neurotransmission, we verified in parallel through a NMDA-dependent chemical-Long-Term Depression (cLTD) protocol applied on hippocampal primary cultures (Marcello et al., 2013) Rph3A and GluN2A presence in TIF. As shown in Fig.2C, cLTD did not resemble the same effects of LTP and we could not infer any difference in GluN2A and Rph3A protein levels at the postsynapse.

Next, we investigated whether also in vivo improved neurotransmission was leading to Rph3A-GluN2A summon in PSD. Enriched environment is well known to promote neuronal plasticity with BDNF expression, and accumulation of GluN2A at synapses (Philpot, Cho, & Bear, 2007; Philpot, Espinosa, & Bear, 2003; Philpot, Sekhar, Shouval, & Bear, 2001; Sawtell et al., 2003; Yashiro, 2005). We fractionated hippocampi from adult rats housed in enriched environment (EE) or standard home cages (CTRL) to obtain TIF, then evaluated Rph3A and GluN2A protein levels through Western Blot (Fig. 2D). Of relevance, also in EE condition we detected

increased Rph3A and GluN2A levels in PSD (*p<0,05).

These results, indicate improvement in neurotransmission is required for Rph3A and GluN2A summon in PSD both *in vitro* and *in vivo* (Fig. 2).

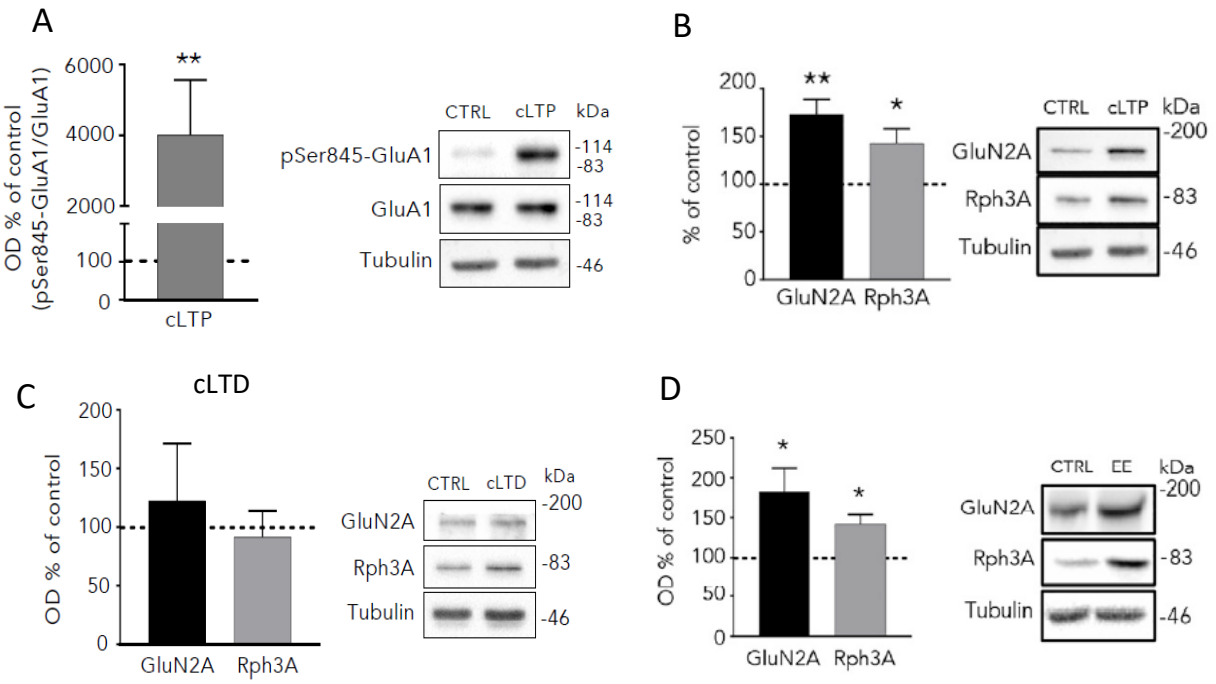

Fig.2. Potentiation of Neurotransmission drives Rph3A and GluN2A in PSD.

Bar chart (left) and Western Blot (WB) represenatitive blots (right) of protein levels in TIF from different synaptic plasticity protocols used in vitro and in vivo. Molecular weight markers are indicated on the right. A) Application of cLTP on hippocampal primary cultures significantly increases phosphorylation in S845 of GluA1 subunit of AMPAR compared to control (CTRL) **p<0,01, n=9 paired t-test. B) cLTP fosters increase in Rph3A and GluN2A protein levels in TIF. n=9; *p<0,05; **p<0,01 paired t-test. C) NMDA-dependent chemical-LTD (cLTD) protocol did not augment or reduce GluN2A and Rph3A levels in TIF. n=3, paired t-test. D) Enriched Environment (EE) housing of mice increases hippocampal GluN2A and Rph3A protein levels in TIF compared to standard cage (CTRL). *p<0,05 unpaired t-test. All data are expressed as mean ± SEM.

3. cLTP increases number of Rph3A+ spines

We then wondered whether the increase in Rph3A presence in TIF was associated to augmented Rph3A+ spines. Therefore, after cLTP application on hippocampal primary cultures transfected with GFP, we quantified positive spines for Rph3A through confocal microscopy. Noteworthly, the number of spines in basal conditions displaying Rph3A were almost 18% in confocal imaging acquisitions. This amount is less than

half of the amount detected through EM in hippocampus as previously shown (paragraph 1 of Results). This can probably be ascribed to the different techniques and resolution obtained with the two instruments. Noteworthly, Rph3A+ spines significantly increased from ~18% to ~30% after cLTP (**p<0,01 Fig.3). More in detail, we also investigated morphological characteristics of these Rph3A+ spines. Interestingly, Rph3A presence significantly increases only in mushroom spines, which are the more mature and stable ones (Fig.3B; *p<0,05 unpaire t test; Grutzendler, Kasthuri, and Gan 2002; Trachtenberg et al. 2002), while no difference was observed for Rph3A presence in thin or stubby spines.

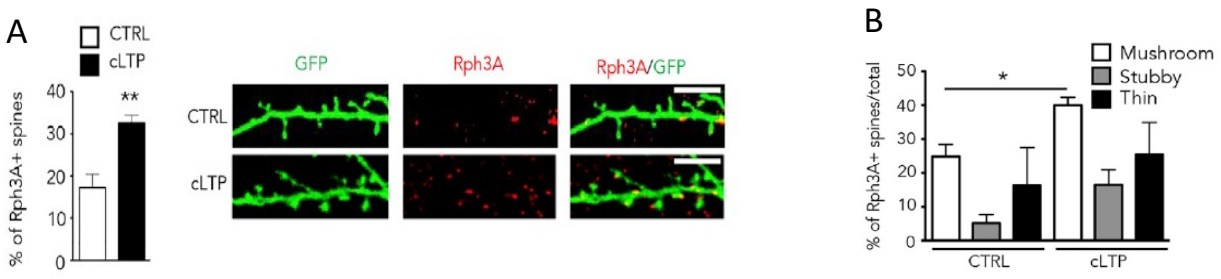

Fig.3 cLTP protocol augments Rph3A presence in mature spines. A) Bar chart and representative pictures of Rph3A immunostaining (red) on GFP-transfected (green) hippocampal primary cultures with or without cLTP. After cLTP, Rph3A+ spines significantly increase. *p<0,05; scale bar 5µm. B) morphological analysis of Rph3A+ spines with or without cLTP. Rph3A presence after cLTP increases selectively only in mushroom spines but not stubby or thin. *p<0,05.

4. cLTP increases Rph3A/GluN2A/PSD-95 protein complex formation

From these observations, we could only speculate GluN2A and Rph3A increase in PSD was also accompanied by formation of new GluN2A/Rph3A/PSD-95 trimeric complex. Therefore, we used Proximity Ligation Assay in situ (PLA, see materials and methods) to detect GluN2A/Rph3A and Rph3A/PSD-95 interaction before and after cLTP on GFP transfected neurons. As shown from Fig.4, cLTP application was able to increase significantly Rph3A/GluN2A interaction and Rph3A/PSD-95 complex formation (**p<0,01; *p<0,05).

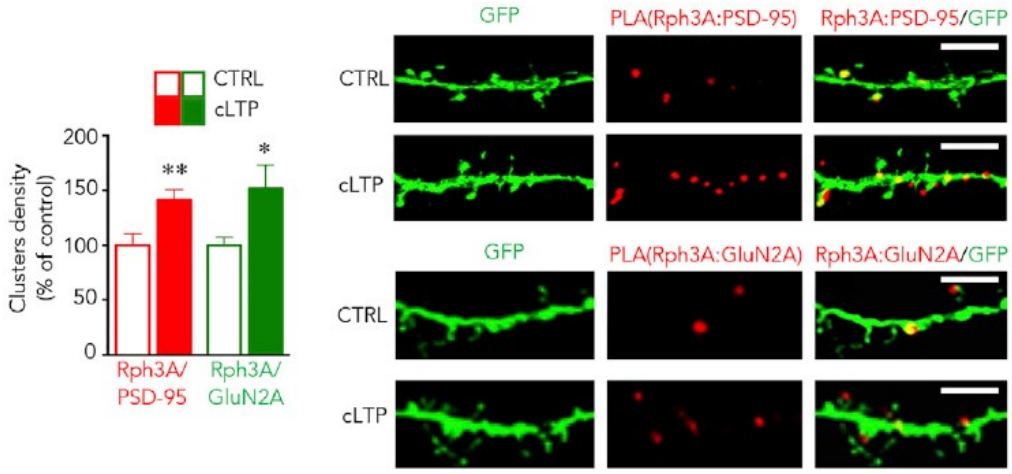

Fig.4. cLTP increases Rph3A/GluN2A/PSD-95 trimeric complex. Bar chart and representative images of PLA clusters density (red) on GFP-transfected hippocampal primary cultures, with or without cLTP. cLTP application significantly augmented Rph3A:PSD95 and Rph3A:GluN2A PLA clusters. *p<0,05; **p<0,01. All data are expressed as mean ± SEM.

5. cLTP induces Rph3A trafficking to PSD

Given these results, we also investigated whether Rph3A increase in PSD was due to trafficking or protein synthesis. Therefore, we induced cLTP on hippocampal primary cultures in presence or absence of Anisomycin (40µM in the last 15' of resting; cLTP+ANI), which is a wide used protein synthesis inhibitor. As shown in Fig.5A, we could not find statistical significance comparing cLTP+ANI and control, nevertheless we almost reached same protein levels of cLTP. Interestingly, cLTP+ANI did not show significant difference compared to cLTP. Due to no significant differences between cLTP and cLTP+ANI in Rph3A protein levels, we addressed this question of local protein synthesis through the Puro-PLA assay (Dieck et al. 2015; see materials and methods). By applying in the last resting phase of LTP Puromycin (1µM), we blocked polypeptide elongation and performed a PLA between an antibody for Puromycin and an antibody for the N-terminal fragment of Rph3A. In this way, the clusters detected as PLA signal represent newly synthetized Rph3A. As shown in Fig.5B, we could not infer any difference in cluster density among somatic or dendritic compartment before and after cLTP, indicating Rph3A is probably trafficked to the synapse upon LTP induction and not due to augmented de novo protein synthesis.

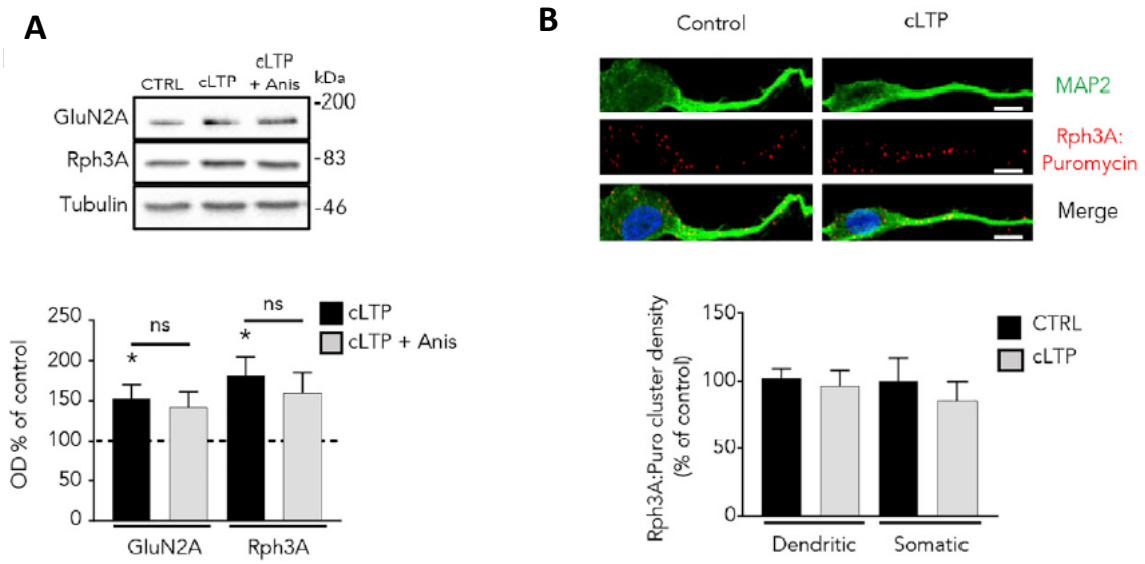

Fig.5 Rph3A is trafficked to the synapse upon cLTP application. A) Bar chart and representative blots of Western Blot analysis for Rph3A and GluN2A protein levels after cLTP in presence or absence of Anisomycin (40µM; cLTP+Anis). cLTP increased as previously shown GluN2A and Rph3A TIF levels (CTRL vs cLTP; *p<0,05; n=8; one-way ANOVA). In presence of Anisomycin we could not infer differences in Rph3A or GluN2A levels compared to CTRL or cLTP. B) Bar chart and representative pictures of Puro-PLA cluster density for Rph3A with or without cLTP on GFP transfected neurons. Anlalysis of Rph3A:Puromycin cluster density in the soma or dendrites did not reveal significant differences between CTRL or cLTP conditions (n=39-43, scale bar 10µm). All data are expressed as mean ± SEM.

6. Rph3A interaction with GluN2A is independent of Phosphorylation at Y1387 at GluN2A-CTD

Several mechanisms can be ascribed for promotion of GluN2A/Rph3A protein complex in PSD after cLTP. In particular, the Y1387 site is present along GluN2A interaction domain for Rph3A (1349-1389, Stanic et al. 2015) and its phosphorylation was previously associated to forward trafficking of the receptor at synapses (Salter & Kalia, 2004; M. Yang & Leonard, 2001). We first evaluated in COS-7 cells whether expression of surface mutant GluN2A-super ecliptic pHluorin (SEP) mimicking phosphorylation at Y1387 possibly affected RFP-Rph3A/GluN2A colocalization. As shown in Fig.6A, no differences in colocalization with RFP-Rph3A could be inferred between mutant Y1387E-GluN2A-SEP compared to WT-GluN2A-SEP, indicating phosphorylation at Y1387 does not alter Rph3A capability to interact with GluN2A. However, this experiment is in COS-7 cell line and furthermore is in static condition. Therefore, we investigated the role of GluN2A-Y1387 phosphorylation in hippocampal primary cultures after cLTP. In particular, we could not detect differences in

Y1387 phosphorylation levels of GluN2A subunit in TIF after cLTP (Fig.6B), suggesting Rph3A interaction after cLTP is independent of GluN2A phosphorylation at Y1387.

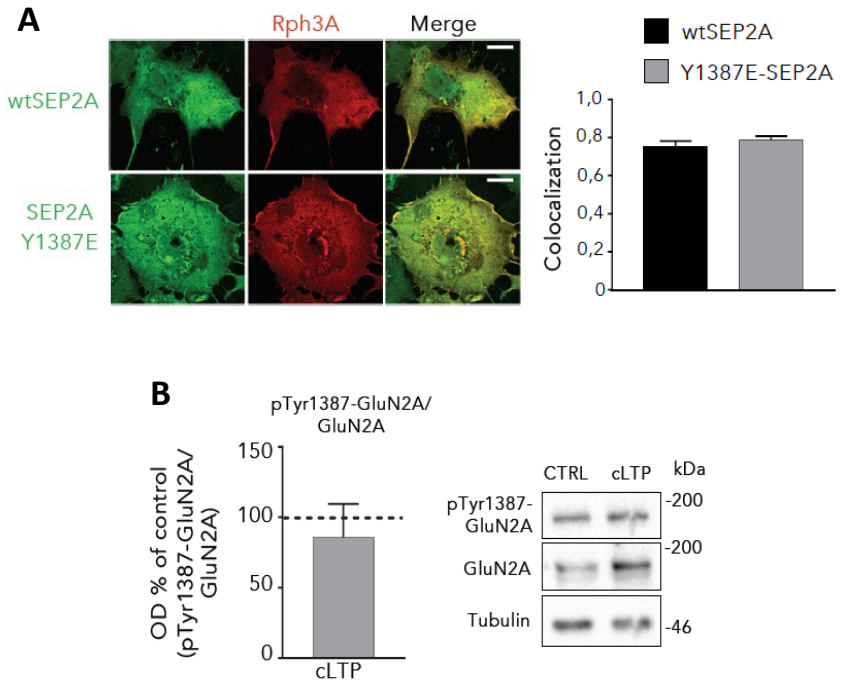

Fig.6 Tyrosine-1387 (Y1387) is not involved in Rph3A/GluN2A interaction. A) representative confocal pictures and bar chart of colocalization analysis in COS-7 cell line transfected with RFP-Rph3A and WT-GluN2A-SEP (wtSEP2A) or mutant Y1387E-GluN2A-SEP (SEP2A-Y1387E). No significant differences in wtSEP2A or SEP2A-Y1387E were detected for colocalization with RFP-Rph3A. n=13, t-test, scale bar 10µm. B) Bar graph and representative blots of phosphor-Y1387-GluN2A (pTyr1387-GluN2A) levels normalized on total GluN2A in TIF from hippocampal primary cultures undergone cLTP. No differences could be inferred with cLTP in pTyr1387-GluN2A levels at postsynapse. n=3, t-test. All data are expressed as mean ± SEM.

7. Phospholypase-C (PLC) activation mediates Rph3A/GluN2A interaction in PSD

Rph3A was previously characterized for the presence of C2 domains which are able to interact with Inositol Triphosphate (IP3) and Ca2+ (Ferrer-Orta et al., 2017; Montaville et al., 2008). The interaction of Ca2+ and IP3 with C2A domain of Rph3A is reciprocally modulated (Ferrer-Orta et al., 2017; Montaville et al., 2008). Notably, Ca2+ specifically interacts with CBL3 loop of Rph3A and affects conformational rearrangements for IP3 binding (Coudevylle, Montaville, Leonov, Zweckstetter, & Becker, 2008; Guillen et al., 2013). Of relevance, our group previously reported when both Ca2+ and IP3 are present, Rph3A-GluN2A interaction is dramatically increased compared to the presence of single components (Stanic et al., 2015).

It is well known IP3 and Ca2+ are downstream Phospholipase C (PLC) activity. In particular, PLC cleaves Phosphatidyl-inositol-biphosphate (PIP2) in IP3 and Dyacilglycerol (DAG); subsequently IP3 promotes Calcium-induced-calcium release from the Endoplasmic Reticulum (ER), indicating a potential upstream role

of PLC in Rph3A/GluN2A complex formation. In particular, PLC signaling is triggered by GPCR or Tyrosine-Kinase Receptor (Trk); more in detail, in the hippocampus PLCβ1 and PLCγ are prominent PLC isoforms associated respectively to group I mGluRs (mGluR1 and mGluR5) and the Tyrosine-Kinase Receptor B (TrkB) for Brain Derived Neurotrophic Factor (BDNF) (Chuang, Bianchi, Kim, Shin, & Wong, 2001; Gottschalk et al., 1999; Hannan et al., 2001). As previously mentioned group I mGluRs is generally associated with LTD induction in hippocampus (Oliet et al., 1997), however literature suggest these receptor play a modulation role for potentiation of neurotransmission by priming LTP conditions (A. Cohen et al., 1998; Mellentin et al., 2007; Van Dam et al., 2004). At mature hippocampal synapses, group I mGluRs is predominantly located postsynaptically (Berridge & Irvine, 1984). We decided to activate group I mGluR by applying DHPG (50µM) for 15 minutes in culture media. Then cells were immediately harvested and fractionated to obtain homogenate, P2 and TIF. To validate DHPG treatments, we evaluated phosphorylation of Extracellular Regulated Kinase (ERK) in homogenate of samples, which as expected was increased by DHPG application (**p<0,01 Fig.7A). After DHPG treatment we were also able to detect Rph3A and GluN2A increase in TIF (*p<0,05; Fig.7B). We further investigated through Co-IP from P2 fraction, whether this increase was accompanied by augmented GluN2A/Rph3A interaction. Noteworthly, DHPG treatment increased Rph3A/GluN2A interaction significantly (***p<0,001; Fig.7C).

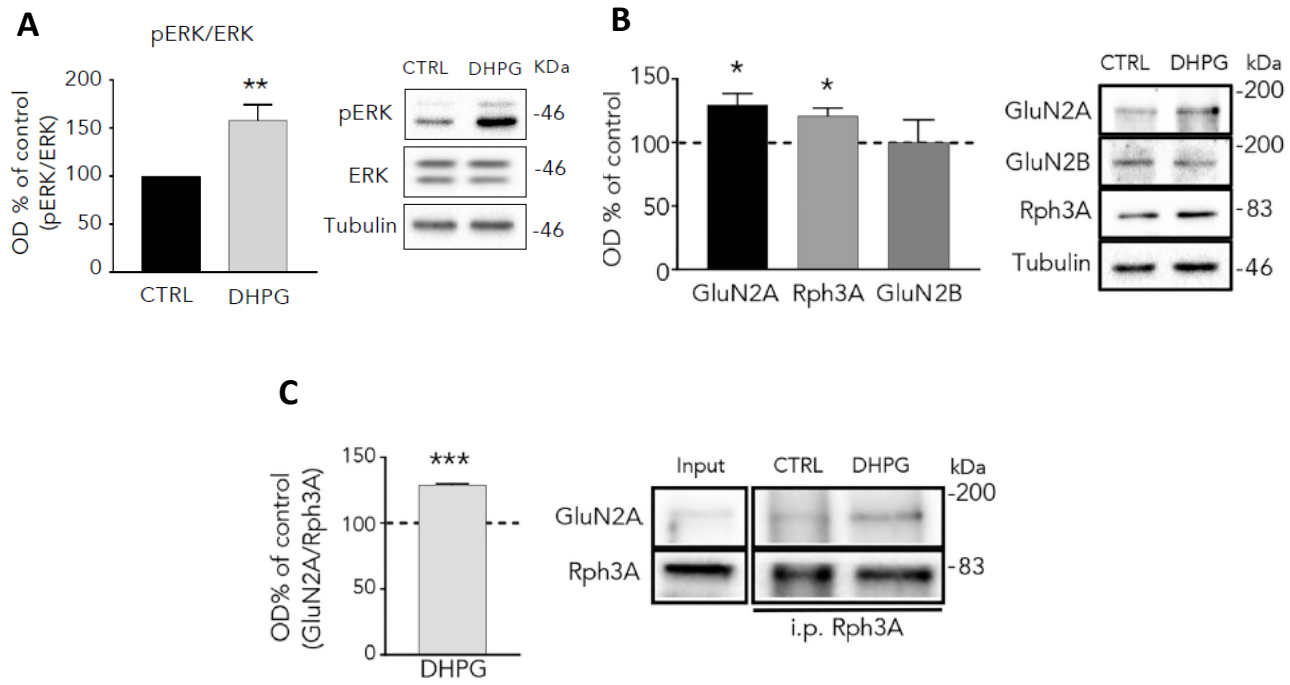

Fig.7 Group I mGluR positively modulates Rph3A synaptic localization and interaction with GluN2A-containing NMDARs. A) Bar chart and representative blots of ERK and phosphor-ERK (pERK) in Homogenate from DHPG (50µM) treated hippocampal primary cultures. DHPG increased significantly pERK/ERK levels compared to control (CTRL) and was used as internal control for treatment validation. **p<0,01 paired t-test n=9. B) Bar graph and representative blots of Rph3A, GluN2A and GluN2B protein levels in TIF from DHPG treatment of hippocampal primary cultures. DHPG treatment was able to increase Rph3A and GluN2A postsynaptic levels but not GluN2B. +p<0,05, paired t-test n=5. C) Western Blot analysis and representative pictures of Co-Ip of Rph3A with GluN2A from P2 of hippocampal primary cultures treated with DPHG. DHPG treatment augmented significantly Rph3A/GluN2A interaction ***p<0,001; paired t-test n=4.

8. BDNF-induced synaptic plasticity promotes Rph3A summon in PSD

BDNF mediates activity-induced modifications of brain circuits through TrkB activation, and is also able to promote LTP through protein synthesis (Bramham & Messaoudi, 2005; Bramham & Wells, 2007; Reichardt, 2006). To verify whether also TrkB-PLCγ pathway could be involved in Rph3A synaptic localization, we applied BDNF (50ng/mL) for 3h in culture media, then harvested cells and fractionated to obtain homogenate and TIF. It is well known TrkB downstream signaling promotes Fyn Kinase activity and GluN2B subunit phosphorylation at Y1472 (Salter & Kalia, 2004); therefore, we validated BDNF treatment by verifying phospho-Y1472-GluN2B levels in homogenate (data not shown). Accordingly, BDNF treatment was able to increase phospho-Y1472-GluN2B levels, and this increase was paralleled by augmented Rph3A levels in TIF (*p<0,05; Fig.8). BDNF-induced synaptic plasticity represents another mechanism responsible for Rph3A presence in PSD. Considering also the results ovrained with group I mGluR, PLC signaling plays a pivotal role in Rph3A/GluN2A presence in PSD.

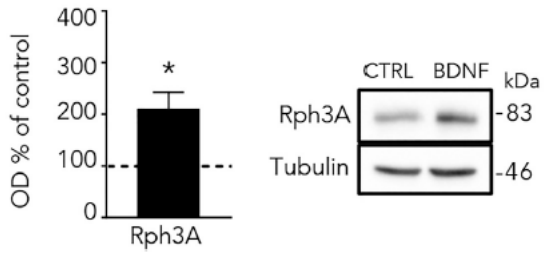

Fig.8 BDNF treatment augments Rph3A levels in TIF. Bar graph and representative blot of Rph3A in TIF from hippocampal primary cultures with or without BDNF treatment (50ng/mL) for 3h. BDNF augmented Rph3A protein levels in TIF compared to control. *p<0,05; paired t-test. All data are expressed as mean ± SEM.

9. Silencing Rph3A impairs cLTP-induced AMPAR and GluN2A-containing NMDAR insertion at plasmic membrane

To better elucidate the role of Rph3A/GluN2A interaction during synaptic plasticity, we silenced Rph3A expression through a specific short-hairpin (tGFP-shRph3A; shRph3A) which we previously showed reduces GluN2A/Rph3A interaction (Stanic et al., 2015); afterwards, we verified GluN2A surface levels with or without cLTP. LTP is known to promote GluN2A synaptic localization (María Verónica Baez et al., 2018), thus in shScramble conditions (shSCR) transfected cultures with LTP as expected we detected a significant increase in GluN2A surface localization (shSCR-CTRL vs shSCR-LTP ***p<0,001; Fig.9A). On the other hand, shRph3A transfected cells displayed an impairment in GluN2A insertion (shSCR-LTP vs shRph3A-LTP ***p<0,001 Fig.9A). This underlies Rph3A-mediated retention of GluN2A-containing NMDARs in PSD is necessary for GluN2A surface localization after cLTP.

It is well-known LTP promotes insertion of GluA1-containing AMPARs at plasmic membranes, as also confirmed by our cLTP protocol (Fig.9A, Joiner et al. 2010; Otmakhov et al. 2004). Therefore, we evaluated whether reducing Rph3A/GluN2A interaction by silencing Rph3A was also affecting GluA1-containing AMPAR membrane insertion. As expected, application of cLTP fostered GluA1 insertion compared to CTRL condition (***p<0,001 Fig.9B). However, silencing Rph3A also aborted GluA1-containing AMPAR insertion at membranes after cLTP (shSCR-LTP vs shRph3A-LTP ***p<0,001; Fig.9B). This indicates GluN2A/Rph3A protein complex in PSD is necessary for molecular modifications induced by LTP, in particular potentiation of neurotransmission.

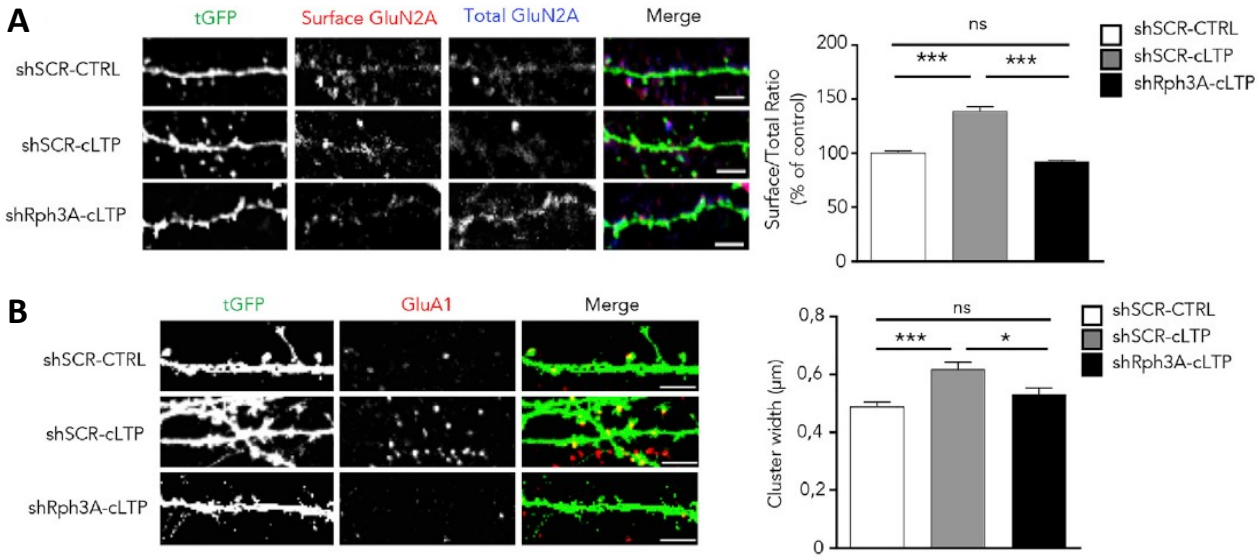

Fig.9 Silencing Rph3A impairs cLTP-induced GluN2A surface staining, GluA1 synaptic localization. Hippocampal primary cultures were transfected with t GFP-shScramble (shSCR) or t GFP-shRph3A (shRph3A) and treated with or without cLTP. A) cLTP lead to increased GluN2A surface levels in shSCR conditions (shSCR-CTRL vs shSCR-cLTP ***p<0,001, one-way ANOVA, Tukey's post-hoc analysis, n=41-46, scale bar 4µm). Analysis of shRph3A-cLTP transfected neurons revealed reduced GluN2A surface levels compared to shSCR-cLTP (shSCR-cLTP vs shRph3A-cLTP ***p<0,001, one-way ANOVA Tukey's post-hoc analysis). B) Bar chart and representative pictures of GluA1 cluster width shows shSCR neurons with significantly increased GluA1 cluster width after cLTP compared to control CTRL (shSCR-CTRL vs shSCR-cLTP ***p<0,001; one-way ANOVA, Tukey's post-hoc analysis n=9-11, scale bar 4µm n=8). Silencing Rph3A impaired cLTP induced GluA1 cluster width increase (shSCR-cLTP vs shRph3A-cLTP *p<0,05 one-way ANOVA Tukey's post-hoc analysis).

10.Silencing Rph3A impairs cLTP-driven increase in spine density

Spine density and spine head width are well-known to increase after LTP (Kopec et al., 2006; Lang et al., 2004; Segal, 2005). Due to previous results suggesting Rph3A/GluN2A complex as relevant for LTP induction, we investigated whether also these parameters were affected by reduction in Rph3A/GluN2A protein complex. Noteworthly, we previously reported shRph3A leads to reduced spine density in basal condition (Stanic et al., 2015). As shown in Fig.10, shSCR-LTP neurons display increased spine density and spine head width compared to shSCR-CTRL neurons (shSCR-CTRL vs shSCR-LTP **p<0,01 Fig.4.1C). Noteworthly, when we silenced Rph3a we could not induce increase in spine density by cLTP, indicating Rph3A/GluN2A complex mediates intracellular signaling associated to LTP-dependent spinogenesis (shSCR-LTP vs shRph3A-LTP *p<0,05; Fig.10. In parallel, spine head width was increased by LTP in shSCR neurons (shSCR-CTRL vs shSCR-LTP *p<0,05; Fig.10). However, silencing Rph3A did not significantly changed this parameter in respect to shSCR-CTRL or shSCR-LTP conditions (Fig.10).

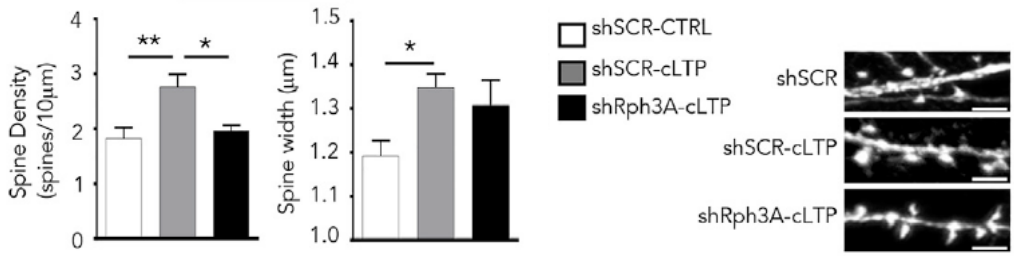

Fig.10 Silencing Rph3A impairs cLTP-induced structural features. Dendritic spine morphology after cLTP revealed in shSCR neurons increased spine density and spine head width (shSCR-CTRL vs shSCR-cLTP **p<0,01; *p<0,05 one-way ANOVA Tukey's post-hoc n=). However, in shRph3A transfected neurons after cLTP no increase in spine number was observed, as well for spine head width (shSCR-cLTP vs shRph3A-cLTP *<0,05 one-way ANOVA Tukey's post-hoc analysis n=8 scale bar 4µm). All data are expressed as mean ± SEM.

11. Interfering with PLC activity impairs cLTP-induced molecular and morphological features.

PLC is known to participate in LTP modulation (Seol et al., 2007). Due to previous results showing PLC activation by group I mGluR and TrkB is relevant for Rph3A/GluN2A protein interaction, we modulated Rph3A/GluN2A complex formation by interfering with PLC during cLTP. In particular, we used a highly validate PLC inhibitor (U3122, 1µM) maintained during all the steps of cLTP protocol on hippocampal primary cultures. We then fractionated cultures to obtain TIF and analyzed Rph3A and GluN2A protein levels through Western Blot. Consistently with previous results, vehicle-LTP treated cultures display increased Rph3A and GluN2A protein levels in TIF (***p<0,001; *p<0,05 Fig.11A). Interestingly, inhibition of PLC activity through U73122 reduced Rph3A and GluN2A protein levels compared to vehicle-LTP (LTP) (LTP vs LTP+U73122; *p<0,05 Fig.11A).

Similarly, to previous experiments of this chapter with shRph3A, we also investigated whether U73122 treatment was affecting structural consequences of LTP. Therefore, we analyzed spine density after cLTP in presence or absence of U73122. According to previous experiments, cLTP protocol increased spine density (***p<0,001; Fig.11B), which was reverted by U73122 treatment (**p<0,01; Fig.11B). This indicates PLC activity promotes Rph3A/GluN2A protein complex and consequent molecular and structural features of LTP.

Overall, these results show Rph3A/GluN2A protein complex is driven at the postsynapse by cLTP in vitro, through PLC activity. Furthermore, these data show Rph3A importance in LTP-induced molecular and structural features of synaptic plasticity, such as dendritic spine formation and trafficking of AMPARs at plasmic membranes.

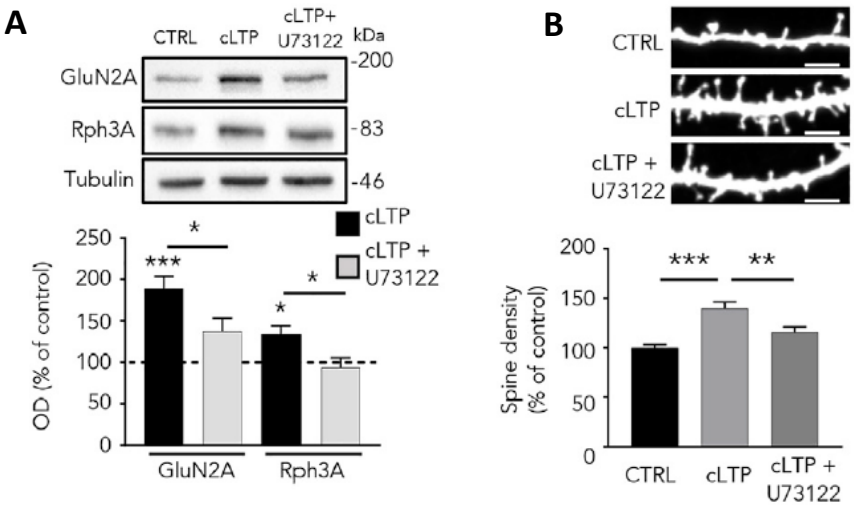

Fig.11 interfering with PLC activity impairs cLTP-induced molecular and morphological consequences. Hippocampal primary cultures underwent cLTP in presence or absence of PLC-inhibitor U73122 (1µM). A) Bar chart and representative blots of Rph3A and GluN2A levels in TIF. cLTP is able to increase both Rph3A and GluN2A protein postsynaptic levels (CTRL vs cLTP ***p<0,001; *p<0,05 one-way ANOVA Bonferroni post-hoc analysis n=5-7) but in presene of U73122 (cLTP-U73122) this effect was completely reversed (cLTP vs cLTP+U73122 *p<0,05 one-way ANOVA Bonferroni post-hoc analysis). B) Dendritic spine density was significantly increased in GFP transfected neurons after cLTP (CTRL vs cLTP ***p<0,001 one-way ANOVA Bonferroni post-hoc analysis n=25 scale bar 4µm). When cLTP was performed with U73122 the increase in spine density was no more observed (cLTP vs cLTP+U73122 **p<0,01; one-way ANOVA Bonferroni post-hoc analysis). All data are expressed as mean ± SEM.

12. Disruption of Rph3A/GluN2A protein interaction is necessary for electrophysiological induced LTP in CA1 region of hippocampus

TAT-cell permeable peptides (CPPs) represent a useful pharmacological tool for investigation of protein-protein interaction. In particular, CPP are able to cross plasmic membrane and also the Blood Brain Barrier (BBB), allowing their use not only in vitro but also in vivo. In particular, TAT-2A-40 mimicking GluN2A CTD domain of interaction for Rph3A, was previously validate by our group both in vitro and in vivo, and reported to reduce GluN2A/GluN2B synaptic ratio and spine density (Stanic et al., 2015, 2017) which is in accordance to the other approaches where GluN2A/Rph3A protein complex was disrupted. After peptide injection intraperitoneally (i.p.), it is able to reach active concentrations in the brain in 1h, and the permanence of the peptide in the brain is for more than 24h depending on the concentration used (Stanic et al., 2015, 2017).

Given previous results in vitro where GluN2A/Rph3A complex disruption was leading to impaired LTP-induced molecular and structural consequences, we decided to verify whether also in vivo Rph3A/GluN2A interaction was relevant for LTP and hippocampal cognitive functions.

In particular, we injected C57BL/6J intraperitoneally (i.p.) with 3nmol/g of either TAT-2A-40 or TAT-Scramble (TAT-SCR) peptides 1h before sacrifice. Next, brain was immediately removed and sliced for electrophysiological recording of LTP in CA1 hippocampal region. Noteworthly, TAT-2A-40 treatment completely aborted LTP induction compared to TAT-scramble peptide (**p<0,01; Fig.5.1A-C), suggesting the presence of this complex at synapses is necessary for LTP initiation.

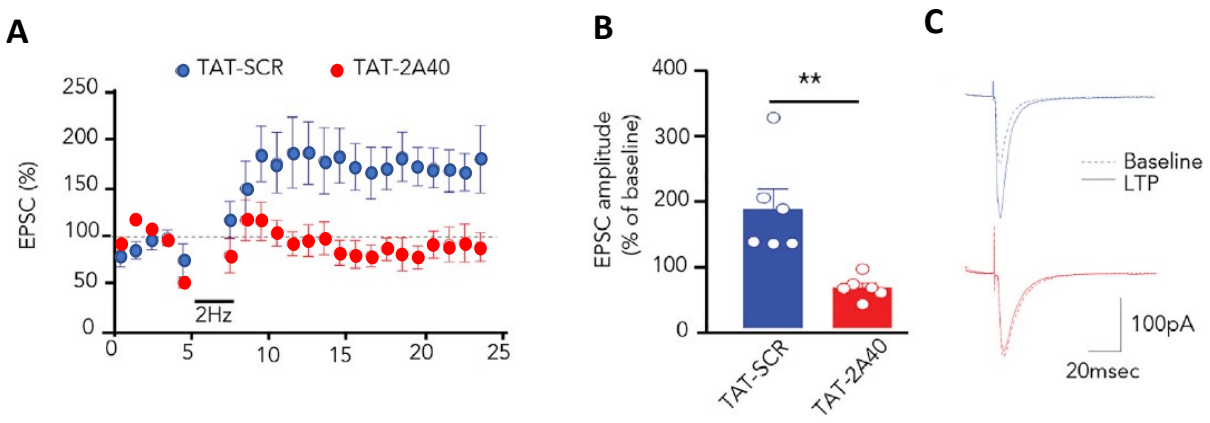

Fig.12 Disruption of Rph3A/GluN2A protein complex aborts LTP induction in CA1 region of hippocampus. Somatic whole-cell voltage-clamp recordings were made from CA1 pyramidal cells using 2–6 UM electrodes. The internal solution contained (in mM) 115 CsMeSO4, 20 CsCl2, 10 HEPES, 2.5 MgCl2, 4 NaATP, 0.4 NaGTP, 10 NaCreatine, and 0.6 EGTA (pH 7.2). Synaptic responses were collected with a Multiclamp 700B amplifier (Axon Instruments, Foster City, CA, USA), filtered at 2 kHz, digitized at 5 kHz, and analyzed online using Igor Pro Software (Wavemetrics, Lake Oswego, OR, USA). All data are expressed as mean ± SEM. Cells were held at _70 mV, and LTP protocol was induced by pairing the cell at 0 mV at a frequency of 2 Hz for 90 s. The amplitude of TAT-2A40 treated animals, as well as LTP kinetic, was completely impaired compared with TAT-SCR (AMPLITUDE, **p < 0.01, unpaired t test). All data are expressed as mean ± SEM.

13. Disruption of Rph3A/GluN2A interaction impairs spatial learning

It is well known learning functions depend on adequate LTP induction and maintainance through specific brain circuits. In particular, hippocampal spatial memory depends on correct neurotransmission in hippocampus (Morris et al., 1986, 1982), and is associated with peculiar changes in GluN2A/GluN2B synaptic levels (María Verónica Baez et al., 2018). Given the result of LTP abortion by disruption of Rph3A/GluN2A interaction, we considered to test mice in a highly validated chronic hippocampal dependent spatial memory test, such as spatial object displacement task. We injected animals with 3nmol/g of TAT-2A-40 or TAT-scramble peptide i.p. 1h before the test. Animals were also tested for possible effects of treatments on locomotor activity, which has an impact on the outcome of behavioral performance. After locomotion analysis, animals were sacrificed, and hippocampi collected and frozen for molecular analysis. In particular we fractionated hippocampi to obtain Homogenate and TIF.

As shown in Fig.13, both groups of animals showed similar exploration of objects in T1 phase (TAT-SCR: Object 1 = 11.7 G 1.0; Object 2 = 12.4 G 0.96. TAT-2A40: Object 1 = 12.9 G 0.82; Object 2 = 13.7 G 0.75). During T2 phase two-way ANOVA revealed differences among groups (treatment effect: $F(1,36) = 4.269$, $p < 0.05$; object effect: $F(1,36) = 8.79$, $p = 0.0053$; interaction treatment x object: $F(1,36) = 12.28$, $p = 0.001$). Post hoc analysis revealed that the mean exploration time of the displaced object was significantly higher than that of the stationary object after treatment with TAT-SCR (Figure 5E; $$$p < 0.001 versus the corresponding stationary object). No difference could be inferred between exploration time of the two objects after TAT-2A-40 treatment (Fig.13). Furthermore, no locomotion alteration was detected in horizontal and vertical movements (Horizontal counts: $t18 = 1.252$, $p = 0.23$, Figure 5F; Vertical counts:$t18 = 0.325$, $p = 0.74$, Fig.5.3C-D). Result of this behavioral task was not related to locomotion alterations of the treatment, since no significant variation of motor activity was detected (Fig.5.3C-D). Furthermore, we verified whether CPP treatment was effective in reduction of GluN2A synaptic levels. Noteworthly, GluN2A/GluN2B ratio was reduced in TIF from TAT-2A-40 treated mice, without affecting GluN1 subunit levels. Since synaptic NMDAR subunit ratio is important for correct synaptic plasticity events (María Verónica Baez et al., 2018; Fabrizio Gardoni & Bellone, 2015; Mellone et al., 2015) we derive reduction of GluN2A/GluN2B subunit ratio by disruption of Rph3A/GluN2A protein complex through TAT-2A-40 impairs hippocampal dependent spatial learning.

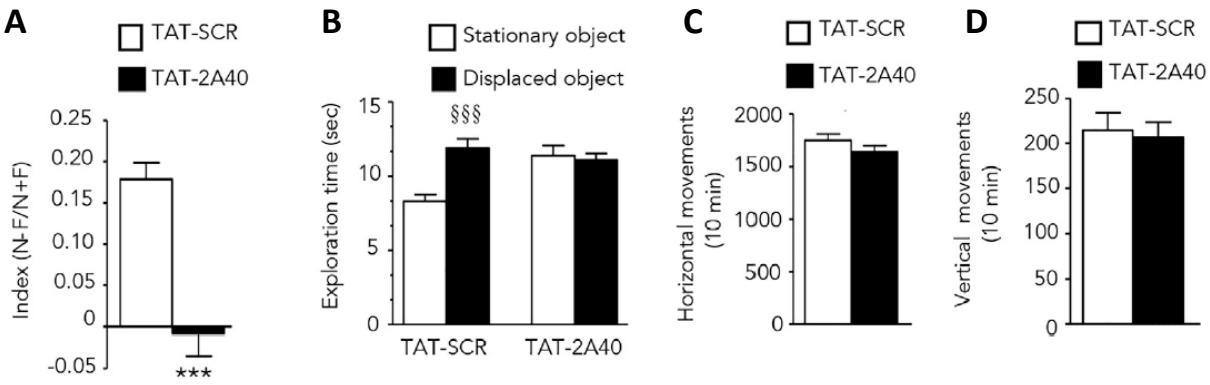

Fig.13 Rph3A/GluN2A protein complex is necessary for spatial learning in spatial object displacement. C57BL/6J were treated with 3nmol/g of TAT-Scr or TAT-2A-40 i.p. 1h before the task. After spatial learning task animals also underwent locomotion monitoring through counts of vertical and horizonal movements. A-B) Mean discrimination index and mean exploration time evaluated in the Spatial Object Recognition test, 60 min after treatment; ***p < 0.001 versus TAT-SCR Student's t test; §§§p < 0.001 versus corresponding stationary object, TAT-SCR; two-way ANOVA followed by Bonferroni test. (C-D) Cumulative mean of horizontal (C) and vertical (D) counts evaluated for 10 min in an automated activity cage. N = 10 animals for each group. All data are expressed as mean ± SEM.

14. TAT-2A-40 treatment reduces synaptic GluN2A/GluN2B ratio without affecting NMDAR assembly

We previously mentioned that at hippocampal glutamatergic synapses, neurotransmission efficacy relies on specific balance in GluN2A/GluN2B subunits (María Verónica Baez et al., 2018; Fabrizio Gardoni & Bellone, 2015; Paoletti et al., 2013). TAT-2A-40 was previously characterized by our group in the reduction of Rph3A/GluN2A/PSD-95 interaction (Stanic et al., 2015). To verify whether the results of behavioral tests could be ascribed to impaired NMDA receptor assembly in PSD, we fractionated hippocampi of mice tested in spatial object recognition task and detected GluN1/GluN2A/GluN2B subunit levels in TIF. As shown in Fig.14, the GluN2A/GluN2B ratio was significantly decreased in TAT-2A-40 treated animals, compared to control (*p<0,05 unpaired t-test n=5). However, no differences in GluN1 were observed among groups, suggesting TAT-2A-40 administration mobilized GluN2A-containing NMDAR synaptic pool without affecting the overall receptor levels in PSD.

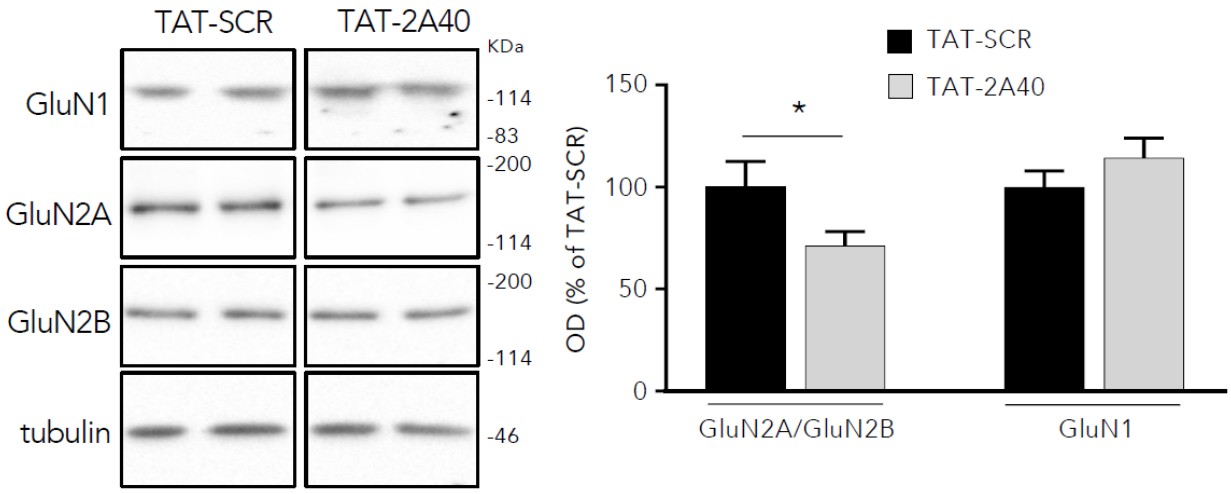

Fig.14 TAT-2A-40 treated mice display lower GluN2A/GluN2B ratio at hippocampal synapses without influence on overall synaptic NMDAR levels. Representative blots and bar chart of GluN1, GluN2A, GluN2B levels detected through Western Blot from hippocampi of mice treated with TAT-2A-40 or TAT-Scr peptide (3nmol/g i.p.) 1h before spatial object displacement. As shown in the graph, GluN2A/GluN2B levels were significantly reduced in TAT-2A-40 group compared to TAT-Scr (+p<0,05; unpaired t-test n=5), but GluN1 levels were unaltered

15. Rph3A+ spines accumulate newly synthetized proteins

We have previously shown in this thesis as well as in previous work from the lab (Stanic et al., 2015), that silencing Rph3A as well as disrupting Rph3A/GluN2A protein complex leads to reduced spine density both in basal and stimulated conditions. The enrichment of Rph3A in mature spines as shown in Figure 1 of this section, led us to investigate whether Rph3A could represent a tag for potentiated synapses. Since stable synapses need support of newly synthetized proteins to maintain molecular and structural features necessary for neurotransmission, we decided to investigate whether Rph3A+ spines displayed accumulation of newly synthetized proteins. For this purpose, we used Puromycin treatment 10µM for 5' at the end of cLTP protocol on GFP transfected hippocampal primary cultures. LTP is well known to promote both local and somatic protein synthesis (Redondo et al., 2010). We then performed an ICC for Rph3A and Puromycin to detect newly synthetized proteins in Rph3A+ and Rph3A- spines. As shown in Fig.15A-B, both in control and cLTP conditions we could observe a significantly increase in newly synthetized proteins in Rph3A+ spines (***p<0,001, paired t-test; CTRL n=14; cLTP n=16). This result indicates Rph3A+ spines are associated to preferential pathways for potentiation of synaptic transmission both in basal and stimulated conditions.

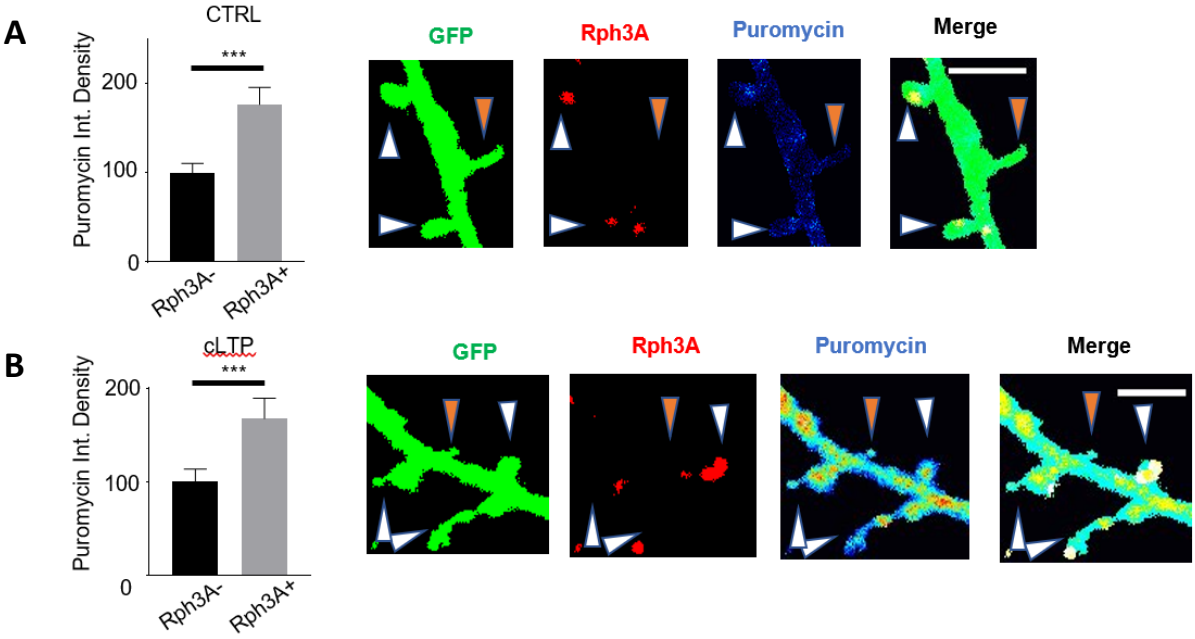

Fig.15 Rph3A+ spines are associated with accumulation of newly synthetized proteins. Hippocampal primary cultures were transfected with GFP, underwent cLTP protocol and in the last 5 minutes Puromycin (10µM) was applied to cultures. A-B) Bar graph and representative pictures of immunostaining for Rph3A (red), newly synthetized proteins with Puromycin (Blue) and GFP (green) in control (CTRL) (A) and cLTP (B) conditions. White arrows indicate Rph3A+ spines, orange arrows Rph3A- negative spines. Integrated intensity of Puromycin in Rph3A+ spines representing newly synthetized proteins, was increased in both CTRL and cLTP conditions. ***p<0,001; unpaired t-test Scale bars 2µm, CTRL n=14; cLTP n=16. All data are expressed as mean ± SEM.

16. Rph3A/MyoVA/GluA1 protein complex detection in hippocampus

Potentiation of spine responsiveness and neurotransmission during LTP in hippocampus relies on AMPAR insertion in PSD. Myosins are molecular motors involved in vesicle trafficking both forward and backward the synapse. A specific association of Myosins to vesicles is reported in literature (Brozzi et al., 2012; Correia et al., 2008; Fili & Toseland, 2020; Folci et al., 2016; Hammer & Sellers, 2012; J. Li, Lu, & Zhang, 2016), and seems to be dictated by complex pattern of markers on the target vesicle and the target region, which still needs to be flly clarified. Interestingly, Myosins have been associated with trafficking of AMPAR at the synapse, were also Rab proteins are involved (Correia et al., 2008; Folci et al., 2016). We previously mentioned Rph3A/MyoVA interaction was characterized in a study about granules secretion in vitro (Brozzi et al., 2012). In 2008, Correia and colleagues observed MyoVA was responsible for synapse delivery of GluA1-containing AMPARs during synaptic plasticity, such as LTP (Correia et al., 2008). Therefore, we deided to investigate whether i) a GluA1/Rph3A/MyoVA could be present in hippocampus, ii) Rph3A/GluA1/MyoVA complex could be modulated by potentiation of neurotransmission such as cLTP.

We first obtained evidence of Rph3A/MyoVA/GluA1 interaction from Co-IP by immunoprecipitation of Rph3A, MyoVa and GluA1 in P2 fraction of hippocampus (Fig.16).

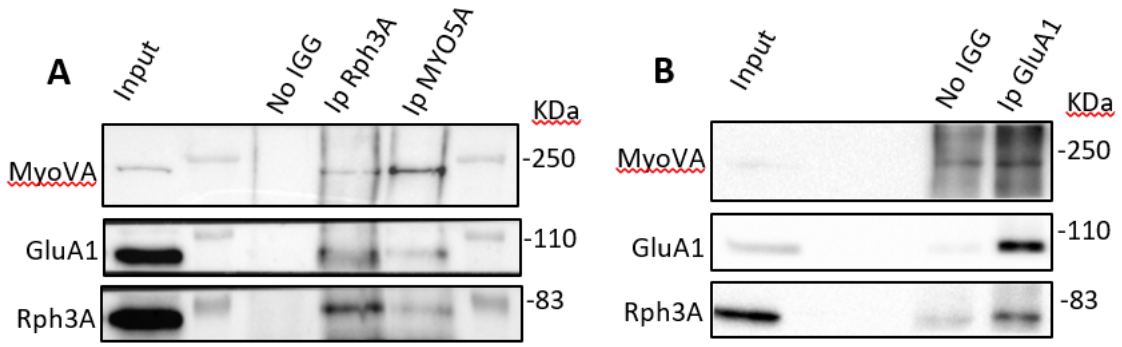

Fig.16 MyoVA/Rph3A/GluA1 protein complex detection in hippocampus. Representative blots of Co-IPs from P2 fraction of rat hippocampus by single immunoprecipitation of Rph3A, MyoVA (A) and GluA1 (B).

In 2012, Brozzi and colleagues described Rph3A/MyoVA interaction dependence on Ca^{2+} driving granules exocytosis. Thus, we questioned whether Rph3A/MyoVA/GluA1 interaction could be modulated by Ca^{2+} triggered synaptic potentiation by LTP.

17. Rph3A/MyoVA interaction is modulated by cLTP

We applied cLTP protocol to fresh hippocampal slices and considered as endpoint 5 minutes, due to the possible quick increase in Ca^{2+} driven by the treatment. We immediately froze slices and then fractionated

to obtain P2 in which we verified phosphorylation at S845 of GluA1 subunit of AMPAR as internal control of cLTP treatment. We then performed immunoprecipitation of MyoVA and evaluated rates of interaction with Rph3A and GluA1 (Fig. 17).

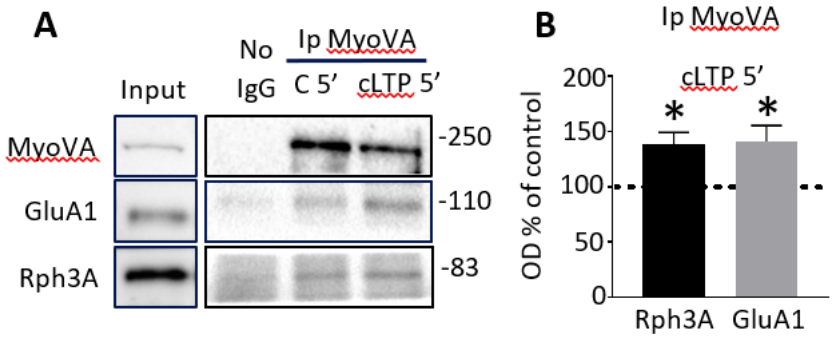

Fig. 17 Rph3A/MyoVA/GluA1 protein complex increases after cLTP. A) Representative blots of MyoVA, Rph3A and GluA1 after MyoVA immunoprecipitation from P2 fraction of hippocampal slices undergone 5 minutes of cLTP. B) Bar graph displaying significant increase of both Rph3A and GluA1 interaction with MyoVA after cLTP compared to control.

18. Rph3A synaptic localization is affected by synapse-to-nucleus communication

It is likely that in vivo only a subset of spines undergoes potentiation and shrinkage upon synaptic plasticity. Synaptic potentiation not only relies on pre-existing pools of in situ proteins and mRNAs available for immediate synaptic modification; but also on somatic and epigenetic mechanisms responsible for the long term maintenance of these synaptic characteristics. Synapse activation always leads to differences membrane potential sensed by the soma and eventually converted to action potential at the axon initial segment. However, this event is common to all excitatory synapses; thus neuronal cells need more specific signals to recognize which synaptic connections should be maintained and which should be eliminated. Recently, synapse-to-nucleus communication through so called "synapse-to-nucleus messengers" seems relevant for integration of synaptic neurotransmission with core neuronal compartments (Marcello et al., 2018). Even though augmented Ca2+ concentrations in the nucleus obtained after synaptic plasticity are considered as synapse-to-nucleus mediator (Bengtson & Bading, 2012), the promiscuity of Ca2+ signaling by activating a plethora of enzymes does not *per se* fully explain this process of synapse-nucleus integration. Interestingly, among synapse-to-nucleus mediators several proteins associated to glutamatergic neurotransmission have been discovered (Marcello et al., 2018). These messengers exploit an importin-dependent transport from the synapse along dendritic cytoskeleton to reach nuclear compartment. In particular, importin-α recognizes specific nuclear localization signal (NLS) domains on cargo proteins; then the consequent binding allows the transport to the nucleus (Lange et al., 2007). The role in synaptic plasticity

of these protein messengers have been elucidated and associated to synaptic rearrangement (Dinamarca et al., 2016; Karpova et al., 2013; Panayotis et al., 2015).

However, how neurons convey back to specific synapses the product of plasticity-induced somatic changes has never been investigated.

Our group has previously defined the importin-α dependent transport of RNF10 is realized through its NLS2 domain (Dinamarca et al., 2016). Accordingly, the usage of NLS2 peptide interferes with importin-mediated transport of RNF10 to the nucleus (Dinamarca et al., 2016). Therefore, we decided to elucidate a possible correlation of Rph3A synaptic localization with synapse-to-nucleus communication by impairing importin-mediated RNF10 transport and then applying synaptic potentiation. We applied 24h before cLTP (30' resting, 16' cLTP induction, 15' final resting) NLS2 or TAT-peptide (as a control, 10uM; Dinamarca et al. 2016) to hippocampal primary cultures, then fractionated samples to obtain TIF and homogenate fractions, which were analyzed through Western Blot. In the same experimental conditions, we also analyzed through Airyscan super-resolution Rph3A/PSD-95 spine localization. As shown in Fig. 18A, Rph3A postsynaptic presence was negatively affected by NLS2-peptide treatment, suggesting synape-to-nucleus communication induced by potentiation of neurotransmission is also relevant for Rph3A summon in PSD and stabilization of GluN2A-containing NMDARs. In the same experimental conditions, we also performed a TIF analysis of Rph3A and GluN2A from hippocampal primary cultures. As reported in Figure 18B, NLS2 treatment impaired Rph3A presence at the postsynapse.

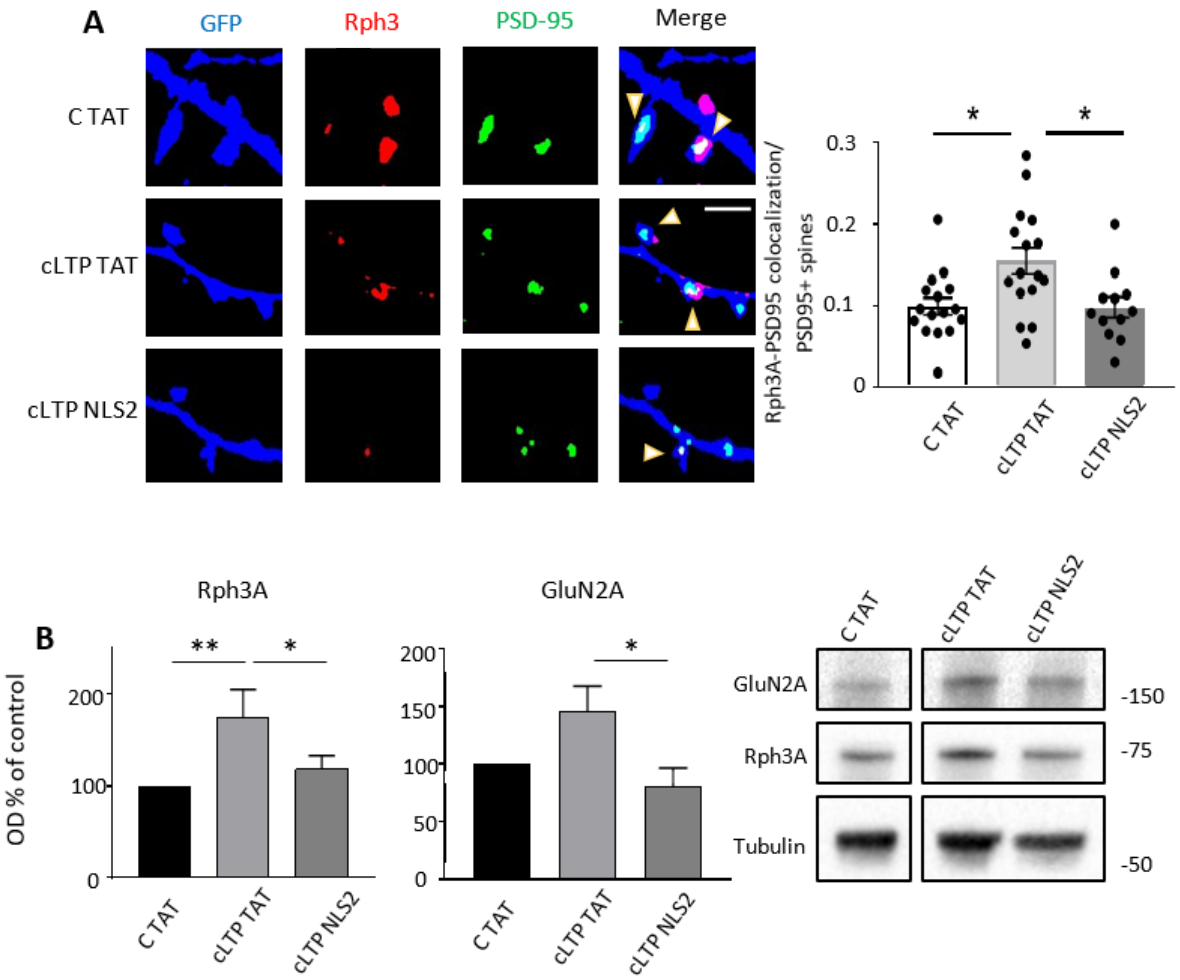

Fig. 18 Impairment of synapse to nucleus communication reduces Rph3A/PSD95 spine localization after cLTP and Rph3A recruitment to the synapse. A) Representative pictures and graph of Rph3A/PSD95 spine clusters (yellow arrows) before (C TAT) and after cLTP in presence of TAT (cLTP TAT) or NLS2 (cLTP NLS2) peptide (10uM for 24h). *p<0,05 One-way ANOVA Tukey's post-hoc. n=12-16 neurons, scale bar 2um. B) Representative blots of Rph3A and GluN2A protein levels in TIF fraction before and after cLTP in presence of NLS2 peptide treatment (10uM for 24h). *p<0,05; **p<0,01. For GluN2A RM one-way ANOVA n=8; for Rph3A **p<0,01 Friedman's test n=9.

DISCUSSION

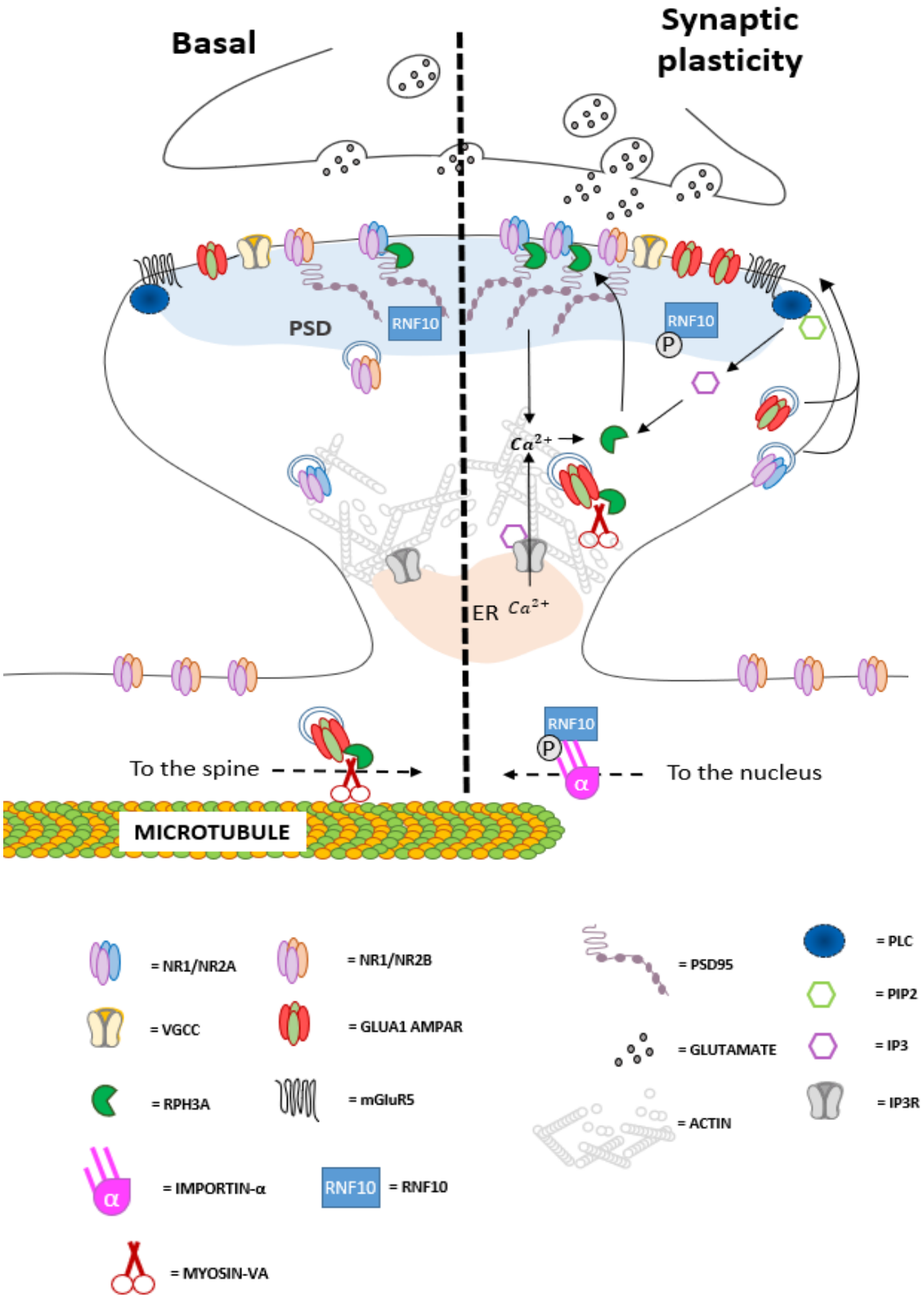

Fig. 1. Schematic representation of Rph3A role at the postsynapse derived from our results. Rph3A increases at the postsynapse after potentiation of neurotransmission stabilizing GluN2A-containing NMDARs, and probably promoting the delivery of GluA1 containing AMPARs in PSD. Rph3A synaptic localization is affected by RNF10 translocation to the nucleus.

At glutamatergic synapses activation of different NMDAR pools accounts for different forms of synaptic plasticity. Furthermore, modulation of NMDAR subunit composition induces a detailed regulation of synaptic transmission and synaptic plasticity thus leading to modulation of higher brain functions. It is also widely established synaptic GluN2A/GluN2B ratio is relevant for physiological and pathological synaptic plasticity. Noteworthly, GluN2A/GluN2B ratio is altered in several neurodegenerative diseases and associated to disease pathophysiology and symptoms outbreak (Q. Chen et al., 2007; Fabrizio Gardoni & Bellone, 2015; Mellone et al., 2015).

In the hippocampus, synaptic GluN2A-containing NMDARs are needed for potentiation of neurotransmission during activity-dependent synaptic plasticity, such as LTP (María Verónica Baez et al., 2018). Notably, different studies reported how interfering with GluN2A expression or activity affects LTP and cognitive functions (Bannerman et al., 2008; Ge et al., 2010; X. H. Zhang et al., 2013). We have previously reported that Rph3A, a Rab-effector protein, is located at dendritic spines where it interacts with GluN2A and PSD-95 promoting stabilization of GluN2A-containing NMDARs at synapse. Disruption of this trimeric complex in basal condition reduces GluN2A surface levels and localization in PSD, notably accompanied by reduced spine density both *in vitro* and *in vivo* (Stanic et al., 2015). Interestingly, Rph3A interaction with GluN2A is improved by the concomitant presence of Ca^{2+} and IP3 (Stanic et al., 2015), which are also key elements in the potentiation of synaptic transmission (Fernández De Sevilla, Núñez, Borde, Malinow, & Buño, 2008).

Based on these previous studies, in the present PhD project we aimed at investigating the physiological role of Rph3A/GluN2A/PSD-95 trimeric complex. To this, we used different synaptic plasticity protocols *in vitro* on hippocampal primary cultures to elucidate the molecular mechanisms modulating Rph3A/GluN2A interaction. Moreover, we confirmed the role of Rph3A/GluN2A/PSD-95 complex *in vivo* on cognitive behavior.

It is well known mushroom spines represent the more mature and stable connections between neural cells, displaying higher spine head area. Interestingly, we detected Rph3A presence in about 50% of hippocampal CA1 dendritic spines in basal conditions and its presence was associated with augmented with PSD thickness, length and spine head area, indicating Rph3A+ spines could be more stable and potentiated synapses.

Spine stability is regulated by efficient protein turnover and delivery of plasticity related proteins (Frey & Morris, 1998; Morris, 2006). Interestingly, Rph3A+ spines displayed a preferential accumulation of newly synthetized proteins compared to Rph3A- ones, suggesting Rph3A as a marker of synaptic potentiation. Noteworthly, the number of Rph3A+ spines increases after induction of cLTP and are characterized by a mushroom shape, which indicate high maturation degree and low plasticity ability (Grutzendler et al., 2002; Trachtenberg et al., 2002). After cLTP but not cLTD, Rph3A/GluN2A synaptic levels are increased, paralleled by augmented Rph3A/GluN2A/PSD-95 protein complex formation, stabilizing GluN2A-containing NMDARs in

PSD. We also ruled out Rph3A/GluN2A interaction is not only promoted by high calcium concentrations at dendritic spines induced by LTP (Mellentin et al., 2007), but also by IP3 presence resulting from PLC activity. As shown by different approaches (short-hairpin, CPPs), Rph3A/GluN2A complex formation is not only necessary for molecular LTP consequences promoting fast iGluRs re-organization at dendritic spines, but also for morphological changes in dendritic spine density, which occurs in later time. This suggests the involvement of not only Ca^{2+} ions in GluN2A-mediated synaptic plasticity, but also of the whole signalosome associated to Rph3A/GluN2A/PSD-95 complex.

It is well known GluN2A-CTD displays several binding partners, and each of them is relevant for peculiar aspects of synaptic plasticity (Franchini et al. 2020). Even if we did not investigated this aspect, it is probable GluN2A-containing NMDARs binding Rph3A also interact with other kinases/mediators important for synaptic plasticity, and the consequent lack of receptor complex is associated to their lack of activation/recruitment in PSD after LTP, probably participating in the observed impairments. To support this hypothesis, we recorded electrophysiological LTP in vivo on hippocampal slices of animals treated with TAT-2A-40 or TAT-Scramble CPPs, disrupting Rph3A/GluN2A interaction. Noteworthly, LTP was completely aborted in TAT-2A-40 treated animals. Moreover, in the same experimental conditions, mice failed the spatial object recognition task, and this was associated to reduced GluN2A/GluN2B synaptic ratio.

Overall these results clarify GluN2A importance in synaptic plasticity observed in previous studies where GluN2A-containing NMDARs were pharmacologically blocked (X. H. Zhang et al., 2013) or genetically altered with lack of CTD (Bannerman et al., 2008). Due to Rph3A presence at pre and postsynapse, furthermore the still not known redundancy of Rab-effectors in neurotransmission, Rph3A-KO mouse model did not display any impairment in LTP and cognitive functions (Schlüter et al., 1999).

As for the molecular recruitment of receptors after cLTP, this reorganization can be attributed to several events such as i) fast lateral mobilization between synaptic and extrasynaptic sites (Bellone & Nicoll, 2007) ii) trafficking of vesicles and exocytosis (Correia et al., 2008) iii) local protein synthesis from Endoplasmic Reticulum and local mRNA pools (Dieck et al., 2015). We therefore investigated MyoVA function as molecular motor transporting GluA1-containing AMPAR from microtubule cytoskeleton of dendrites to actin cytoskeleton in dendritic spines (Correia et al., 2008). It was already shown Rph3A/MyoVA interaction is modulated by Ca^{2+} concentrations (Brozzi et al., 2012), therefore we investigated whether i) Rph3A/MyoVA/GluA1 were part of a protein complex ii) Rph3A/MyoVA/GluA1 interaction could be modulated by cLTP in hippocampal slices and in hippocampal primary cultures. Noteworthly, we report for the first time Rph3A/MyoVA/GluA1 co-immunoprecipitate from P2 hippocampal fraction and their interaction is increased in the first minutes after cLTP. This leads us to elucidate in the future GluA1/MyoVA interaction and how this is modulated in absence of Rph3A through shRph3A. Furthermore, to clarify the role

of Rph3A in GluA1 trafficking at the synapse, we planned to perform FRAP of SEP-GluA1 at dendritic spines of RFP-shScramble or RFP-shRph3A transfected neurons before and after cLTP.

Finally, in the present work we addressed whether Rph3A trafficking in PSD could be modulated by synapse-to-nucleus transport of a synaptonuclear protein messenger, RNF10. While synapse-to-nucleus messengers are mediators of neurotransmission from the synapse to the soma, we investigated whether Rph3A synaptic localization could represent a "soma-to-synapse" mechanism for spine potentiation. Interestingly, specific blockade of RNF10 synapse-to-nucleus communication through NLS2 peptide impairs LTP-dependent Rph3A recruitment in PSD as shown by both ICC and western blot from hippocampal primary cultures. We also analyzed homogenate levels of Rph3A after treatment to verify a possible impact of NLS2 peptide on Rph3A protein synthesis by the treatment, but no differences compared to TAT-control group were detected, indicating NLS2 effect does not impact Rph3A genetic expression. A useful tool in this respect would be the RNF10-KO mouse model available in our lab, as a model to study the role of synapse-to-nucleus communication and its consequences on Rph3A postsynaptic roles. Furthermore, in the same experimental conditions (NLS2 or TAT-peptides) we could address whether not only Rph3A but also GluA1 trafficking at synapses is affected, and if this is the case whether MyoVA/GluA1/Rph3A protein complex is involved in these events.

Overall, our results show that Rph3A is part of the trimeric GluN2A/PSD-95/Rph3A complex and promotes GluN2A-containing NMDAR synaptic signaling which is necessary for potentiation of neurotransmission, such as LTP induction. In particular, impairment of Rph3A/GluN2A is detrimental for both molecular and morphological consequences of LTP, which is in turn reflected by failure in cognitive functions such as hippocampal dependent spatial learning. The modulation of Rph3A/GluN2A/PSD-95 complex is probably correlated to an increase in Ca^{2+} ions as previously described (Brozzi et al., 2012; Correia et al., 2008).

Moreover, Rph3A seems involved also in AMPA receptor trafficking to the PSD through a complex with MyoVA and GluA1 subunit of AMPA receptors. We speculate that Rph3A is dragged to the active spines through MyoVA/GluA1 protein complex, thus promoting the delivery of AMPARs in PSD and is then recruited for GluN2A-containing NMDAR synaptic retention. These results indicate that Rph3A may play a role in the modulation of dendritic spine responsiveness, providing an improved neurotransmission at specific synapses. Finally, Rph3A synaptic localization seems also to be affected by the GluN2A subunit associated synapse-to-nucleus messenger RNF10.

In conclusion, understanding Rph3A postsynaptic roles may lead to different lines of pharmacological intervention for neurological disorders where not only synaptic NMDAR subunits are unbalanced, as previously demonstrated by our group (Stanic et al., 2017), but also for modulation of AMPAR trafficking and dendritic spine potentiation.

REFERENCES

Akazawa, C., Shigemoto, R., Bessho, Y., Nakanishi, S., & Mizuno, N. (1994). Differential expression of five N-methyl-D-aspartate receptor subunit mRNAs in the cerebellum of developing and adult rats. *Journal of Comparative Neurology*, *347*(1), 150–160. https://doi.org/10.1002/cne.903470112

Baez, María Verónica, Cercato, M. C., & Jerusalinsky, D. A. (2018). NMDA receptor subunits change after synaptic plasticity induction and learning and memory acquisition. *Neural Plasticity*, *2018*. https://doi.org/10.1155/2018/5093048

Baez, Maria Veronica, Oberholzer, M. V., Cercato, M. C., Snitcofsky, M., Aguirre, A. I., & Jerusalinsky, D. A. (2013). NMDA Receptor Subunits in the Adult Rat Hippocampus Undergo Similar Changes after 5 Minutes in an Open Field and after LTP Induction. *PLoS ONE*, *8*(2), e55244. https://doi.org/10.1371/journal.pone.0055244

Bagni, C., Tassone, F., Neri, G., & Hagerman, R. (2012). Fragile X syndrome: Causes, diagnosis, mechanisms, and therapeutics. *Journal of Clinical Investigation*, *122*(12), 4314–4322. https://doi.org/10.1172/JCI63141

Bajaj, G., Hau, A. M., Hsu, P., Gafken, P. R., Schimerlik, M. I., & Ishmael, J. E. (2014). Identification of an atypical calcium-dependent calmodulin binding site on the C-terminal domain of GluN2A. *Biochemical and Biophysical Research Communications*, *44*(4), 588–594. https://doi.org/10.1016/j.bbrc.2014.01.111

Balleine, B. W., & O'Doherty, J. P. (2010, January). Human and rodent homologies in action control: Corticostriatal determinants of goal-directed and habitual action. *Neuropsychopharmacology*. https://doi.org/10.1038/npp.2009.131

Banke, T. G., Dravid, S. M., & Traynelis, S. F. (2005). Protons trap NR1/NR2B NMDA receptors in a nonconducting state. *Journal of Neuroscience*, *25*(1), 42–51. https://doi.org/10.1523/JNEUROSCI.3154-04.2005

Bannerman, D. M., Niewoehner, B., Lyon, L., Romberg, C., Schmitt, W. B., Taylor, A., … Rawlins, J. N. P. (2008). NMDA receptor subunit NR2A is required for rapidly acquired spatial working memory but not incremental spatial reference memory. *Journal of Neuroscience*, *28*(14), 3623–3630. https://doi.org/10.1523/JNEUROSCI.3639-07.2008

Barria, A., & Malinow, R. (2002). Subunit-Specific NMDA Receptor Trafficking to Synapses. *Neuron*, *35*(2), 345–353. https://doi.org/10.1016/B978-012369437-9/50015-3

Bassell, G. J., & Warren, S. T. (2008). Fragile X Syndrome: Loss of Local mRNA Regulation Alters Synaptic Development and Function. *Neuron*, *60*(2), 201–214. https://doi.org/10.1016/j.neuron.2008.10.004

Bastrikova, N., Gardner, G. A., Reece, J. M., Jeromin, A., & Dudek, S. M. (2008). Synapse elimination accompanies functional plasticity in hippocampal neurons. *Proceedings of the National Academy of Sciences of the United States of America*, *105*(8), 3123–3127. https://doi.org/10.1073/pnas.0800027105

Bayer, K. U., & Schulman, H. (2001). Regulation of signal transduction by protein targeting: The case for CaMKII. *Biochemical and Biophysical Research Communications*, *289*(5), 917–923. https://doi.org/10.1006/bbrc.2001.6063

Bear, M. F., & Malenka, R. C. (1994). Synaptic plasticity: LTP and LTD. *Current Opinion in Neurobiology*, *4*(3), 389–399. https://doi.org/10.1016/0959-4388(94)90101-5

Bell, K. F. S., & Hardingham, G. E. (2011). The influence of synaptic activity on neuronal health. *Current Opinion in Neurobiology*, *21*(2), 299–305. https://doi.org/10.1016/j.conb.2011.01.002

Bellone, C., & Nicoll, R. A. (2007). Rapid Bidirectional Switching of Synaptic NMDA Receptors. *Neuron*, *55*(5), 779–785. https://doi.org/10.1016/j.neuron.2007.07.035

Bengtson, C. P., & Bading, H. (2012). Nuclear calcium signaling. *Advances in Experimental Medicine and Biology*, *970*. https://doi.org/10.1007/978-3-7091-0932-8_17

Berretta, N., & Jones, R. S. G. (1996). Tonic facilitation of glutamate release by presynaptic N-methyl-D-aspartate autoreceptors in the entorhinal cortex. *Neuroscience*, *75*(2), 339–344. https://doi.org/10.1016/0306-4522(96)00301-6

Berridge, M. J., & Irvine, R. F. (1984). Inositol trisphosphate, a novel second messenger in cellular signal transduction. *Nature*, *312*(5992), 315–321. https://doi.org/10.1038/312315a0

Bezaire, M. J., & Soltesz, I. (2013). Quantitative assessment of CA1 local circuits: Knowledge base for interneuron-pyramidal cell connectivity. *Hippocampus*, *23*(9), 751–785. https://doi.org/10.1002/hipo.22141

Bidoret, C., Ayon, A., Barbour, B., & Casado, M. (2009). Presynaptic NR2A-containing NMDA receptors implement a high-pass filter synaptic plasticity rule. *Proceedings of the National Academy of Sciences of the United States of America*, *106*(33), 14126–14131. https://doi.org/10.1073/pnas.0904284106

Bodhinathan, K., Kumar, A., & Foster, T. C. (2010). Intracellular redox state alters NMDA receptor response during aging through Ca2+/calmodulin-dependent protein kinase II. *Journal of Neuroscience*, *30*(5), 1914–1924. https://doi.org/10.1523/JNEUROSCI.5485-09.2010

Bourne, J. N., & Harris, K. M. (2012). Nanoscale analysis of structural synaptic plasticity. *Current Opinion in Neurobiology*, *22*(3), 372–382. https://doi.org/10.1016/j.conb.2011.10.019

Bramham, C. R., & Messaoudi, E. (2005). BDNF function in adult synaptic plasticity: The synaptic consolidation hypothesis. *Progress in Neurobiology*, *76*(2). https://doi.org/10.1016/j.pneurobio.2005.06.003

Bramham, C. R., & Wells, D. G. (2007). Dendritic mRNA: Transport, translation and function. *Nature Reviews Neuroscience*. https://doi.org/10.1038/nrn2150

Braun, A. P., & Schulman, H. (1995). The Multifunctional Calcium/Calmodulin-Dependent Protein Kinase: From Form to Function. *Annual Review of Physiology*, *57*, 417–445. https://doi.org/10.1146/annurev.ph.57.030195.002221

Brozzi, F., Diraison, F., Lajus, S., Rajatileka, S., Philips, T., Regazzi, R., … Váradi, A. (2012). Molecular mechanism of Myosin Va recruitment to dense core secretory granules. *Traffic*, *13*(1), 54–69. https://doi.org/10.1111/j.1600-0854.2011.01301.x

Burns, M. E., Sasaki, T., Takai, Y., & Augustine, G. J. (1998). Rabphilin-3A : A Multifunctional Regulator of Synaptic Vesicle Traffic. *Journal of General Physiology*, *111*(2), 243–255.

Calabresi, P., Picconi, B., Tozzi, A., & Di Filippo, M. (2007). Dopamine-mediated regulation of corticostriatal synaptic plasticity. *Trends in Neurosciences*, *30*(5), 211–219. https://doi.org/10.1016/j.tins.2007.03.001

Capron, B., Wattiez, R., Sindic, C., Godaux, E., & Ris, L. (2007). Tyrosine phosphorylation of rabphilin during long-lasting long-term potentiation. *Neuroscience Letters*, *414*(3), 257–262. https://doi.org/10.1016/j.neulet.2006.12.031

Caroni, P., Donato, F., & Muller, D. (2012). Structural plasticity upon learning: Regulation and functions. *Nature Reviews Neuroscience*, *13*(7), 478–490. https://doi.org/10.1038/nrn3258

Carrano, N., Samaddar, T., Brunialti, E., Franchini, L., Marcello, E., Ciana, P., … Gardoni, F. (2019). The Synaptonuclear Messenger RNF10 Acts as an Architect of Neuronal Morphology. *Molecular Neurobiology*, *56*(11), 7583–7593. https://doi.org/10.1007/s12035-019-1631-1

Carvill, G. L., Regan, B. M., Yendle, S. C., O'Roak, B. J., Lozovaya, N., Bruneau, N., … Mefford, H. C. (2013).

GRIN2A mutations cause epilepsy-aphasia spectrum disorders. *Nature Genetics*, *45*(9), 1073–1076. https://doi.org/10.1038/ng.2727

Casado, M., Dieudonné, S., & Ascher, P. (2000). Presynaptic N-methyl-D-aspartate receptors at the parallel fiber-Purkinje cell synapse. *Proceedings of the National Academy of Sciences of the United States of America*, *97*(21), 11593–11597. https://doi.org/10.1073/pnas.200354297

Castillo, P. E., Janz, R., Südhof, T. C., Tzounopoulos, T., Malenka, R. C., & Nicoll, R. A. (1997). Rab3A is essential for mossy fibre long-term potentiation in the hippocampus. *Nature*, *388*(6642), 590–593. https://doi.org/10.1038/41574

Cercato, M., Vàzquez, C., Kornisiuk, E., Aquirre, A., Colettis, N., Snitcofsky, M., … Baez, M. (2017). GluN1 and GluN2A NMDA Receptor Subunits Increase in the Hippocampus during Memory Consolidation in the Rat. *Frontiers in Behavioral Neuroscience*, *13*(10), 242.

Chen, B. S., & Roche, K. W. (2007). Regulation of NMDA receptors by phosphorylation. *Neuropharmacology*, *53*(3), 362–368. https://doi.org/10.1016/j.neuropharm.2007.05.018

Chen, N., Moshaver, A., & Raymond, L. A. (1997). Differential sensitivity of recombinant N-methyl-D-aspartate receptor subtypes to zinc inhibition. *Molecular Pharmacology*, *51*(6), 1015–1023. https://doi.org/10.1124/mol.51.6.1015

Chen, Q., He, S., Hu, X. L., Yu, J., Zhou, Y., Zheng, J., … Xiong, Z. Q. (2007). Differential roles of NR2A- and NR2B-containing NMDA receptors in activity-dependent brain-derived neurotrophic factor gene regulation and limbic epileptogenesis. *Journal of Neuroscience*, *27*(3), 542–552. https://doi.org/10.1523/JNEUROSCI.3607-06.2007

Chen, Y. F., Chen, Z. X., Wang, R. H., Shi, Y. W., Xue, L., Wang, X. G., & Zhao, H. (2019). Knockdown of CLC-3 in the hippocampal CA1 impairs contextual fear memory. *Progress in Neuro-Psychopharmacology and Biological Psychiatry*, *89*, 132–145. https://doi.org/10.1016/j.pnpbp.2018.07.004

Chidambaram, S. B., Rathipriya, A. G., Bolla, S. R., Bhat, A., Ray, B., Mahalakshmi, A. M., … Sakharkar, M. K. (2019). Dendritic spines: Revisiting the physiological role. *Progress in Neuro-Psychopharmacology and Biological Psychiatry*, *92*(June), 161–193. https://doi.org/10.1016/j.pnpbp.2019.01.005

Chuang, S. C., Bianchi, R., Kim, D., Shin, H. S., & Wong, R. K. (2001). Group I metabotropic glutamate receptors elicit epileptiform discharges in the hippocampus through PLCbeta1 signaling. *The Journal of Neuroscience*.

Chung, S.-H., Stabila, P., Macara, I. G., & Holz, R. W. (1997). Importance of the Rab3a-GTP Binding Domain for the Intracellular Stability and Function of Rabphilin3a in Secretion. *Journal of Neurochemistry*, *69*(1), 164–173. https://doi.org/10.1046/j.1471-4159.1997.69010164.x

Chung, S. H., Takai, Y., & Holz, R. W. (1995). Evidence that the Rab3a-binding protein, Rabphilin3a, enhances regulated secretion: Studies in adrenal chromaffin cells. *Journal of Biological Chemistry*, *270*(28), 16714–16718. https://doi.org/10.1074/jbc.270.28.16714

Cohen, A., Raymond, C., & Abraham, W. (1998). Priming of long-term potentiation induced by activation of metabotropic glutamate receptors coupled to phospholipase C. *Hippocampus*, *8*(2), 160–170.

Cohen, S. M., Ma, H., Kuchibhotla, K. V., Watson, B. O., Buzsáki, G., Froemke, R. C., & Tsien, R. W. (2016). Excitation-Transcription Coupling in Parvalbumin-Positive Interneurons Employs a Novel CaM Kinase-Dependent Pathway Distinct from Excitatory Neurons. *Neuron*, *90*(2), 292–307. https://doi.org/10.1016/j.neuron.2016.03.001

Colbran, R. J., & Brown, A. M. (2004). Calcium/calmodulin-dependent protein kinase II and synaptic plasticity. *Current Opinion in Neurobiology*. https://doi.org/10.1016/j.conb.2004.05.008

Collingridge, G. L., Peineau, S., Howland, J. G., & Wang, Y. T. (2010). Long-term depression in the CNS. *Nature Reviews Neuroscience*, *11*(7), 459–473. https://doi.org/10.1038/nrn2867

Correia, S. S., Bassani, S., Brown, T. C., Lisé, M. F., Backos, D. S., El-Husseini, A., … Esteban, J. A. (2008). Motor protein-dependent transport of AMPA receptors into spines during long-term potentiation. *Nature Neuroscience*, *11*(4), 457–466. https://doi.org/10.1038/nn2063

Coudevylle, N., Montaville, P., Leonov, A., Zweckstetter, M., & Becker, S. (2008). Structural determinants for Ca2+ and phosphatidylinositol 4,5-bisphosphate binding by the C2A domain of rabphilin-3A. *Journal of Biological Chemistry*. https://doi.org/10.1074/jbc.M804094200

Dailey, M. E., & Smith, S. J. (1996). The dynamics of dendritic structure in developing hippocampal slices. *Journal of Neuroscience*, *16*(9), 2983–2994. https://doi.org/10.1523/jneurosci.16-09-02983.1996

De Ligt, J., Willemsen, M. H., Van Bon, B. W. M., Kleefstra, T., Yntema, H. G., Kroes, T., … Vissers, L. E. L. M. (2012). Diagnostic exome sequencing in persons with severe intellectual disability. *New England Journal of Medicine*, *367*(20), 1921–1929. https://doi.org/10.1056/NEJMoa1206524

De Rubeis, S., & Bagni, C. (2010). Fragile X mental retardation protein control of neuronal mRNA metabolism: Insights into mRNA stability. *Molecular and Cellular Neuroscience*, *43*(1), 43–50. https://doi.org/10.1016/j.mcn.2009.09.013

Desai, N. S., Casimiro, T. M., Gruber, S. M., & Vanderklish, P. W. (2006). Early postnatal plasticity in neocortex of Fmr1 knockout mice. *Journal of Neurophysiology*, *96*(4), 1734–1745. https://doi.org/10.1152/jn.00221.2006

Devinsky, O., Vezzani, A., O'Brien, T. J., Jette, N., Scheffer, I. E., De Curtis, M., & Perucca, P. (2018). Epilepsy. *Nature Reviews Disease Primers*, *4*. https://doi.org/10.1038/nrdp.2018.24

Dieck, S. tom, Kochen, L., Hanus, C., Bartnik, I., Nassim-Assir, B., Merk, K., … Schuman, E. M. (2015). Direct visualization of identified and newly synthesized proteins in situ. *Nature Methods*. https://doi.org/10.1038/nmeth.3319

Dinamarca, M. C., Guzzetti, F., Karpova, A., Lim, D., Mitro, N., Musardo, S., … Di Luca, M. (2016). Ring finger protein 10 is a novel synaptonuclear messenger encoding activation of NMDA receptors in hippocampus. *ELife*, *5:e12430*. https://doi.org/10.7554/eLife.12430.001

Diógenes, M. J., Dias, R. B., Rombo, D. M., Vicente Miranda, H., Maiolino, F., Guerreiro, P., … Outeiro, T. F. (2012). Extracellular alpha-synuclein oligomers modulate synaptic transmission and impair LTP via NMDA-receptor activation. *Journal of Neuroscience*, *32*(34), 11750–11762. https://doi.org/10.1523/JNEUROSCI.0234-12.2012

Doyle, D. A., Lee, A., Lewis, J., Kim, E., Sheng, M., & MacKinnon, R. (1996). Crystal structures of a complexed and peptide-free membrane protein- binding domain: Molecular basis of peptide recognition by PDZ. *Cell*, *85*(7), 1067–1076. https://doi.org/10.1016/S0092-8674(00)81307-0

Dumas, T. C. (2005). Developmental regulation of cognitive abilities: Modified composition of a molecular switch turns on associative learning. *Progress in Neurobiology*, *76*(3), 189–211. https://doi.org/10.1016/j.pneurobio.2005.08.002

Durante, V., De Iure, A., Loffredo, V., Vaikath, N., De Risi, M., Paciotti, S., … Calabresi, P. (2019). Alpha-synuclein targets GluN2A NMDA receptor subunit causing striatal synaptic dysfunction and visuospatial memory alteration. *Brain*, *142*(5), 1365–1385. https://doi.org/10.1093/brain/awz065

Elagabani, M. N., Brisevac, D., Kintscher, M., Pohle, J., Köhr, G., Schmitz, D., & Kornau, H. C. (2016). Subunit-selective N-Methyl-D-aspartate (NMDA) receptor signaling through brefeldin a-resistant arf guanine nucleotide exchange factors BRAG1 and BRAG2 during synapse maturation. *Journal of Biological Chemistry*, *291*(17), 9105–9118. https://doi.org/10.1074/jbc.M115.691717

Esteban, J. A., Shi, S. H., Wilson, C., Nuriya, M., Huganir, R. L., & Malinow, R. (2003). PKA phosphorylation of AMPA receptor subunits controls synaptic trafficking underlying plasticity. *Nature Neuroscience*. https://doi.org/10.1038/nn997

Fayyazuddin, A., Villarroel, A., Le Goff, A., Lerma, J., & Neyton, J. (2000). Four residues of the extracellular N-terminal domain of the NR2A subunit control high-affinity Zn2+ binding to NMDA receptors. *Neuron*, *25*(3), 683–694. https://doi.org/10.1016/S0896-6273(00)81070-3

Fernández De Sevilla, D., Núñez, A., Borde, M., Malinow, R., & Buño, W. (2008). Cholinergic-mediated IP3-receptor activation induces long-lasting synaptic enhancement in CA1 pyramidal neurons. *Journal of Neuroscience*, *28*(6), 1469–1478. https://doi.org/10.1523/JNEUROSCI.2723-07.2008

Ferreira, J. S., Papouin, T., Ladépêche, L., Yao, A., Langlais, V. C., Bouchet, D., … Groc, L. (2017). Co-agonists differentially tune GluN2B-NMDA receptor trafficking at hippocampal synapses. *ELife*, 6:e25492. https://doi.org/10.7554/eLife.25492

Ferrer-Orta, C., Pérez-Sánchez, M. D., Coronado-Parra, T., Silva, C., López-Martínez, D., Baltanás-Copado, J., … Verdaguer, N. (2017). Structural characterization of the Rabphilin-3A–SNAP25 interaction. *Proceedings of the National Academy of Sciences*. https://doi.org/10.1073/pnas.1702542114

Fili, N., & Toseland, C. P. (2020). Unconventional myosins: How regulation meets function. *International Journal of Molecular Sciences*, *21*(1). https://doi.org/10.3390/ijms21010067

Folci, A., Murru, L., Vezzoli, E., Ponzoni, L., Gerosa, L., Moretto, E., … Bassani, S. (2016). Myosin IXa binds AMPAR and regulates synaptic structure, LTP, and cognitive function. *Frontiers in Molecular Neuroscience*, *9*(JAN). https://doi.org/10.3389/fnmol.2016.00001

Franchini, L., Carrano, N., Di Luca, M., & Gardoni, F. (2020). Synaptic gluN2A-containing NMDA receptors: From physiology to pathological synaptic plasticity. *International Journal of Molecular Sciences*, *21*(4). https://doi.org/10.3390/ijms21041538

Franchini, L., Stanic, J., Ponzoni, L., Mellone, M., Carrano, N., Musardo, S., … Gardoni, F. (2019). Linking NMDA Receptor Synaptic Retention to Synaptic Plasticity and Cognition. *IScience*, *19*, 927–939. https://doi.org/10.1016/j.isci.2019.08.036

Freire, M., García-López, P., & García-Marín, V. (2010). Dendritic spines and development: Towards a unifying model of spinogenesis a present day review of cajal's histological slides and drawings. *Neural Plasticity*. https://doi.org/10.1155/2010/769207

Frey, U., & Morris, R. G. M. (1998). Weak before strong: Dissociating synaptic tagging and plasticity-factor accounts of late-LTP. *Neuropharmacology*, *37*(4–5), 545–552. https://doi.org/10.1016/S0028-3908(98)00040-9

Frizelle, P., Chen, P., & Wyllie, D. (2006). Equilibrium constants for (R)-[(S)-1-(4-bromo-phenyl)-ethylamino]-(2,3-dioxo-1,2,3,4-tetrahydroquinoxalin-5-yl)-methyl]-phosphonic acid (NVP-AAM077) acting at recombinant NR1NR2A and NR1NR2B N-methyl-D-aspartate receptors Im. *Molecular Pharmacology*, *70*(3), 1022–1032.

Fujii, R., Okabe, S., Urushido, T., Inoue, K., Yoshimura, A., Tachibana, T., … Takumi, T. (2005). The RNA binding protein TLS is translocated to dendritic spines by mGluR5 activation and regulates spine morphology. *Current Biology*, *15*(6), 587–593. https://doi.org/10.1016/j.cub.2005.01.058

Fukuda, M. (2003). Distinct Rab binding specificity of Rim1, Rim2, Rabphilin, and Noc2: Identification of a critical determinant of Rab3a/Rab27a recognition by Rim2. *Journal of Biological Chemistry*, *278*(17), 15373–15380. https://doi.org/10.1074/jbc.M212341200

Fykse, E., Li, C., & Südhof, T. (1995). Phosphorylation of rabphilin-3A by Ca2+/calmodulin- and cAMP-dependent protein kinases in vitro. *The Journal of Neuroscience : The Official Journal of the Society for*

Neuroscience. https://doi.org/10.1149/2.0711613jes

Gambrill, A. C., & Barria, A. (2011). NMDA receptor subunit composition controls synaptogenesis and synapse stabilization. *Proceedings of the National Academy of Sciences of the United States of America*, *108*(14), 5855–5860. https://doi.org/10.1073/pnas.1012676108

Gardoni, F., Schrama, L. H., Van Dalen, J. J. W., Gispen, W. H., Cattabeni, F., & Di Luca, M. (1999). αCaMKII binding to the C-terminal tail of NMDA receptor subunit NR2A and its modulation by autophosphorylation. *FEBS Letters*, *456*(3), 394–398. https://doi.org/10.1016/S0014-5793(99)00985-0

Gardoni, F., Schrama, L., Kamal, A., Gispen, W., Cattabeni, F., & Di Luca, M. (2001). Hippocampal synaptic plasticity involves competition between Ca2+calmodulin-dependent protein kinase II and postsynaptic density 95 for binding to the NR2A subunit of the NMDA receptor. *Journal of Neuroscience*, *21*(5), 1501–1509. https://doi.org/10.1523/JNEUROSCI.21-05-01501.2001

Gardoni, Fabrizio, & Bellone, C. (2015). Modulation of the glutamatergic transmission by Dopamine: a focus on Parkinson, Huntington and Addiction diseases. *Frontiers in Cellular Neuroscience*, *9*. https://doi.org/10.3389/fncel.2015.00025

Gardoni, Fabrizio, Bellone, C., Cattabeni, F., & Di Luca, M. (2001). Protein Kinase C Activation Modulates α-Calmodulin Kinase II Binding to NR2A Subunit of N-Methyl-D-Aspartate Receptor Complex. *Journal of Biological Chemistry*, *273*(33), 20689–20692. https://doi.org/10.1074/jbc.M009922200

Gardoni, Fabrizio, Picconi, B., Ghiglieri, V., Polli, F., Bagetta, V., Bernardi, G., … Calabresi, P. (2006). A critical interaction between NR2B and MAGUK in L-DOPA induced dyskinesia. *Journal of Neuroscience*, *26*(11), 2914–2922. https://doi.org/10.1523/JNEUROSCI.5326-05.2006

Gardoni, Fabrizio, Sgobio, C., Pendolino, V., Calabresi, P., Di Luca, M., & Picconi, B. (2012). Targeting NR2A-containing NMDA receptors reduces L-DOPA-induced dyskinesias. *Neurobiology of Aging*, *33*(9), 2138–2144. https://doi.org/10.1016/j.neurobiolaging.2011.06.019

Ge, Y., Dong, Z., Bagot, R. C., Howland, J. G., Phillips, A. G., Wong, T. P., & Wang, Y. T. (2010). Hippocampal long-term depression is required for the consolidation of spatial memory. *Proceedings of the National Academy of Sciences of the United States of America*, *107*(38), 16697–16702. https://doi.org/10.1073/pnas.1008200107

Geppert, M., & Südhof, T. C. (1998). RAB3 AND SYNAPTOTAGMIN: The Yin and Yang of Synaptic Membrane Fusion. *Annual Review of Neuroscience*, *21*(1), 75–95. https://doi.org/10.1146/annurev.neuro.21.1.75

Goodfellow, M. J., Abdulla, K. A., & Lindquist, D. H. (2016). Neonatal Ethanol Exposure Impairs Trace Fear Conditioning and Alters NMDA Receptor Subunit Expression in Adult Male and Female Rats. *Alcoholism: Clinical and Experimental Research*, *40*(2), 309–318. https://doi.org/10.1111/acer.12958

Gottschalk, W. A., Jiang, H., Tartaglia, N., Feng, L., Figurov, A., & Lu, B. (1999). Signaling mechanisms mediating BDNF modulation of synaptic plasticity in the hippocampus. *Learning & Memory (Cold Spring Harbor, N.Y.)*. https://doi.org/10.1101/lm.6.3.243

Grau, C., Arató, K., Fernández-Fernández, J. M., Valderrama, A., Sindreu, C., Fillat, C., … Altafaj, X. (2014). DYRK1A-mediated phosphorylation of GluN2A at ser1048 regulates the surface expression and channel activity of GluN1/GluN2A receptors. *Frontiers in Cellular Neuroscience*, *8*(OCT). https://doi.org/10.3389/fncel.2014.00331

Groc, L., Heine, M., Cousins, S. L., Stephenson, F. A., Lounis, B., Cognet, L., & Choquet, D. (2006). NMDA receptor surface mobility depends on NR2A-2B subunits. *Proceedings of the National Academy of Sciences of the United States of America*, *103*(49), 18769–18774. https://doi.org/10.1073/pnas.0605238103

Grosshans, D., Calyton, D., Coultrap, S., & Browning, M. (2002). LTP leads to rapid surface expression of

NMDA but not AMPA receptors in adult rat CA1. *Nature Neuroscience*, *5*(1), 27–33.

Grutzendler, J., Kasthuri, N., & Gan, W. B. (2002). Long-term dendritic spine stability in the adult cortex. *Nature*, *420*(6917), 812–816. https://doi.org/10.1038/nature01276

Guillen, J., Ferrer-Orta, C., Buxaderas, M., Perez-Sanchez, D., Guerrero-Valero, M., Luengo-Gil, G., … C.Corbalan-Garcia, S. (2013). Structural insights into the Ca2+ and PI(4,5)P2 binding modes of the C2 domains of rabphilin 3A and synaptotagmin 1. *Proceedings of the National Academy of Sciences*, *110*(51), 20503–20508. https://doi.org/10.1073/pnas.1316179110

Gupta-Agarwal, S., Jarome, T. J., Fernandez, J., & Lubin, F. D. (2014). NMDA receptor- and ERK-dependent histone methylation changes in the lateral amygdala bidirectionally regulate fear memory formation. *Learning and Memory*, *21*(7), 351–362. https://doi.org/10.1101/lm.035105.114

Hammer, J. A., & Sellers, J. R. (2012). Walking to work: Roles for class v myosins as cargo transporters. *Nature Reviews Molecular Cell Biology*, *13*(1), 13–26. https://doi.org/10.1038/nrm3248

Hannan, A. J., Blakemore, C., Katsnelson, A., Vitalis, T., Huber, K. M., Bear, M., … Kind, P. C. (2001). PLC-β1, activated via mGluRs, mediates activity-dependent differentiation in cerebral cortex. *Nature Neuroscience*. https://doi.org/10.1038/85132

Hanson, J. E., Ma, K., Elstrott, J., Weber, M., Saillet, S., Khan, A. S., … Palop, J. J. (2020). GluN2A NMDA Receptor Enhancement Improves Brain Oscillations, Synchrony, and Cognitive Functions in Dravet Syndrome and Alzheimer's Disease Models. *Cell Reports*, *30*(2), 381-396.e4. https://doi.org/10.1016/j.celrep.2019.12.030

Hardingham, G. (2019). NMDA receptor C-terminal signaling in development, plasticity, and disease. *F1000Research*, *8*, 1547. https://doi.org/10.12688/f1000research.19925.1

Hardingham, G. E., & Bading, H. (2010). Synaptic versus extrasynaptic NMDA receptor signalling: Implications for neurodegenerative disorders. *Nature Reviews Neuroscience*. https://doi.org/10.1038/nrn2911

Harris, K. M., Jensen, F. E., & Tsao, B. (1992). Three-dimensional structure of dendritic spines and synapses in rat hippocampus (CA 1) at postnatal day 15 and adult ages: Implications for the maturation of synaptic physiology and long-term potentiation. *Journal of Neuroscience*. https://doi.org/10.1523/jneurosci.12-08-j0001.1992

Harris, Kristen M, Jensen, F. E., & Tsao, B. (1992). Three-dimensional structure of dendritic spines and synapses in rat hippocampus (CA1) at postnatal day 15 and adult ages: implications for the maturation of synaptic physiology and long-term potentiation. *Journal of Neuroscience*, *12*(7), 2685–2705. https://doi.org/10.1016/j.tcb.2009.06.001

Hawkins, L. M., Prybylowski, K., Chang, K., Moussan, C., Stephenson, F. A., & Wenthold, R. J. (2004). Export from the endoplasmic reticulum of assembled N-methyl-D-aspartic acid receptors is controlled by a motif in the C terminus of the NR2 subunit. *Journal of Biological Chemistry*, *279*(28), 28903–28910. https://doi.org/10.1074/jbc.M402599200

Henley, J. M., & Wilkinson, K. A. (2016). Synaptic AMPA receptor composition in development, plasticity and disease. *Nature Reviews Neuroscience*, *17*(6), 337–350. https://doi.org/10.1038/nrn.2016.37

Hering, H., & Sheng, M. (2001). Dentritic spines: structure, dynamics and regulation. *Nature Reviews Neuroscience*, *2*(12), 80–88. https://doi.org/10.1038/35104061

Hill, T. C., & Zito, K. (2013). LTP-induced long-term stabilization of individual nascent dendritic spines. *Journal of Neuroscience*, *33*(2), 678–686. https://doi.org/10.1523/JNEUROSCI.1404-12.2013

Hirokawa, N. (2006). mRNA transport in dendrites: RNA granules, motors, and tracks. *The Journal of*

Neuroscience : The Official Journal of the Society for Neuroscience, *26*(27), 7139–7142. https://doi.org/10.1523/JNEUROSCI.1821-06.2006

Holz, R. W., Brondyk, W. H., Senter, R. A., Kuizon, L., & Macara, I. G. (1994). Evidence for the involvement of Rab3A in Ca2+-dependent exocytosis from adrenal chromaffin cells. *Journal of Biological Chemistry*, *269*(14), 10229–10234.

Howard, M. A., Elias, G. M., Elias, L. A. B., Swat, W., & Nicoll, R. A. (2010). The role of SAP97 in synaptic glutamate receptor dynamics. *Proceedings of the National Academy of Sciences of the United States of America*, *107*, 3805–3810. https://doi.org/10.1073/pnas.0914422107

Hsieh, H., Boehm, J., Sato, C., Iwatsubo, T., Tomita, T., Sisodia, S., & Malinow, R. (2006). AMPAR Removal Underlies Aβ-Induced Synaptic Depression and Dendritic Spine Loss. *Neuron*, *52*(5), 831–843. https://doi.org/10.1016/j.neuron.2006.10.035

Hu, H., Real, E., Takamiya, K., Kang, M. G., Ledoux, J., Huganir, R. L., & Malinow, R. (2007). Emotion Enhances Learning via Norepinephrine Regulation of AMPA-Receptor Trafficking. *Cell*. https://doi.org/10.1016/j.cell.2007.09.017

Hu, N. W., Klyubin, I., Anwy, R., & Rowan, M. J. (2009). GluN2B subunit-containing NMDA receptor antagonists prevent Aβ-mediated synaptic plasticity disruption in vivo. *Proceedings of the National Academy of Sciences of the United States of America*, *106*(48), 20504–20509. https://doi.org/10.1073/pnas.0908083106

Huber, K. M., Kayser, M. S., & Bear, M. F. (2000). Role for rapid dendritic protein synthesis in hippocampal mGluR- dependent long-term depression. *Science*, *288*(5469), 1254–1256. https://doi.org/10.1126/science.288.5469.1254

Huber, K. M., Roder, J. C., & Bear, M. F. (2001). Chemical induction of mGluR5- and protein synthesis-dependent long-term depression in hippocampal area CA1. *Journal of Neurophysiology*, *86*(1), 321–325. https://doi.org/10.1152/jn.2001.86.1.321

Izumi, Y., & Zorumski, C. F. (2012). NMDA receptors, mGluR5, and endocannabinoids are involved in a cascade leading to hippocampal long-term depression. *Neuropsychopharmacology*, *37*(3), 609–617. https://doi.org/10.1038/npp.2011.243

Jacobs, S., Cui, Z., Feng, R., Wang, H., Wang, D., & Tsien, J. Z. (2014). Molecular and genetic determinants of the NMDA receptor for superior learning and memory functions. *PLoS ONE*, *9*(10). https://doi.org/10.1371/journal.pone.0111865

JG, R., Z, L., & DB, S. (2008). IQGAP1 integrates Ca2+calmodulin and B-Raf signaling. *Journal of Biological Chemistry*, *283*(34), 22972–22982. https://doi.org/10.1074/jbc.M804626200.

Jin, I., Puthanveettil, S., Udo, H., Karl, K., Kandel, E. R., & Hawkins, R. D. (2012). Spontaneous transmitter release is critical for the induction of long-term and intermediate-term facilitation in Aplysia. *Proceedings of the National Academy of Sciences of the United States of America*, *109*(23), 9131–9136. https://doi.org/10.1073/pnas.1206914109

Johnson, J. W., & Ascher, P. (1987). Glycine potentiates the NMDA response in cultured mouse brain neurons. *Nature*, *325*(6104), 529–531. https://doi.org/10.1038/325529a0

Joiner, M. L. A., Lisé, M. F., Yuen, E. Y., Kam, A. Y. F., Zhang, M., Hall, D. D., … Hell, J. W. (2010). Assembly of a B 2-adrenergic receptorGluR1 signalling complex for localized cAMP signalling. *EMBO Journal*, *29*(2), 482–495. https://doi.org/10.1038/emboj.2009.344

Karpova, A., Mikhaylova, M., Bera, S., Bär, J., Reddy, P. P., Behnisch, T., … Kreutz, M. R. (2013). Encoding and transducing the synaptic or extrasynaptic origin of NMDA receptor signals to the nucleus. *Cell*, *152*(5), 1119–1133. https://doi.org/10.1016/j.cell.2013.02.002

Kasai, H., Hayama, T., Ishikawa, M., Watanabe, S., Yagishita, S., & Noguchi, J. (2010). Learning rules and persistence of dendritic spines. *European Journal of Neuroscience*, *32*(2), 241–249. https://doi.org/10.1111/j.1460-9568.2010.07344.x

Kato, M., Sasakii, T., Ohyai, T., Nakanishi, H., Nishioka, H., Imamura, M., & Takai, Y. (1996). Physical and functional interaction of rabphilin-3A with α-actinin. *Journal of Biological Chemistry*, *271*(50), 31775–31778. https://doi.org/10.1074/jbc.271.50.31775

Kellermayer, B., Ferreira, J. S., Dupuis, J., Levet, F., Grillo-Bosch, D., Bard, L., … Groc, L. (2018). Differential Nanoscale Topography and Functional Role of GluN2-NMDA Receptor Subtypes at Glutamatergic Synapses. *Neuron*. https://doi.org/10.1016/j.neuron.2018.09.012

Kemp, N., & Bashir, Z. I. (1997). NMDA receptor-dependent and -independent long-term depression in the CA1 region of the adult rat hippocampus in vitro. *Neuropharmacology*, *36*(3), 397–399. https://doi.org/10.1016/S0028-3908(96)90015-5

Kemp, Nicola, McQueen, J., Faulkes, S., & Bashir, Z. I. (2000). Different forms of LTD in the CA1 region of the hippocampus: Role of age and stimulus protocol. *European Journal of Neuroscience*, *12*(1), 360–366. https://doi.org/10.1046/j.1460-9568.2000.00903.x

Kenney, J. W., Adoff, M. D., Wilkinson, D. S., & Gould, T. J. (2011). NIH Public Access. *Psychopharmacology (Berl)*, *217*(3), 353–365. https://doi.org/10.1007/s00213-011-2283-7.The

Kessels, H. W., Nabavi, S., & Malinow, R. (2013). Metabotropic NMDA receptor function is required for β-amyloid-induced synaptic depression. *Proceedings of the National Academy of Sciences of the United States of America*, *110*(10), 4033–4038. https://doi.org/10.1073/pnas.1219605110

Kholmanskikh, S. S., Koeller, H. B., Wynshaw-Boris, A., Gomez, T., Letourneau, P. C., & Ross, M. E. (2006). Calcium-dependent interaction of Lis1 with IQGAP1 and Cdc42 promotes neuronal motility. *Nature Neuroscience*, *9*(1), 50–57. https://doi.org/10.1038/nn1619

Kim, E., & Sheng, M. (2004). PDZ domain proteins of synapses. *Nature Reviews Neuroscience*, *5*(10), 771–781. https://doi.org/10.1038/nrn1517

Kim, J. H., Anwyl, R., Suh, Y. H., Djamgoz, M. B. A., & Rowan, M. J. (2001). Use-dependent effects of amyloidogenic fragments of β-amyloid precursor protein on synaptic plasticity in rat hippocampus in vivo. *Journal of Neuroscience*, *21*(4), 1327–1333. https://doi.org/10.1523/jneurosci.21-04-01327.2001

Knott, G. W., Holtmaat, A., Wilbrecht, L., Welker, E., & Svoboda, K. (2006). Spine growth precedes synapse formation in the adult neocortex in vivo. *Nature Neuroscience*, *9*(9), 1117–1124. https://doi.org/10.1038/nn1747

Kopec, C. D., Li, B., Wei, W., Boehm, J., & Malinow, R. (2006). Glutamate receptor exocytosis and spine enlargement during chemically induced long-term potentiation. *Journal of Neuroscience*, *26*(7), 2000–2009. https://doi.org/10.1523/JNEUROSCI.3918-05.2006

Kornau, H. C., Schenker, L. T., Kennedy, M. B., & Seeburg, P. H. (1995). Domain interaction between NMDA receptor subunits and the postsynaptic density protein PSD-95. *Science*. https://doi.org/10.1126/science.7569905

Kramár, E. A., Lin, B., Rex, C. S., Gall, C. M., & Lynch, G. (2006). Integrin-driven actin polymerization consolidates long-term potentiation. *Proceedings of the National Academy of Sciences of the United States of America*, *103*(14), 5579–5584. https://doi.org/10.1073/pnas.0601354103

Kumar, A., & Foster, T. C. (2005). Intracellular calcium stores contribute to increased susceptibility to LTD induction during aging. *Brain Research*, *1031*(1), 125–128. https://doi.org/10.1016/j.brainres.2004.10.023

Lang, C., Barco, A., Zablow, L., Kandel, E. R., Siegelbaum, S. A., & Zakharenko, S. S. (2004). Transient expansion of synaptically connected dendritic spines upon induction of hippocampal long-term potentiation. *Proceedings of the National Academy of Sciences of the United States of America*, *101*(47), 16665–16670. https://doi.org/10.1073/pnas.0407581101

Lange, A., Mills, R. E., Lange, C. J., Stewart, M., Devine, S. E., & Corbett, A. H. (2007). Classical nuclear localization signals: Definition, function, and interaction with importin α. *Journal of Biological Chemistry*. https://doi.org/10.1074/jbc.R600026200

Lauterborn, J. C., Rex, C. S., Kramár, E., Chen, L. Y., Pandyarajan, V., Lynch, G., & Gall, C. M. (2007). Brain-derived neurotrophic factor rescues synaptic plasticity in a mouse model of fragile X syndrome. *Journal of Neuroscience*, *27*(40), 10685–10694. https://doi.org/10.1523/JNEUROSCI.2624-07.2007

Lee, J. De, Huang, P. C., Lin, Y. C., Kao, L. Sen, Huang, C. C., Kao, F. J., … Yang, D. M. (2008). In-depth fluorescence lifetime imaging analysis revealing SNAP25A-rabphilin 3A interactions. *Microscopy and Microanalysis*, *14*(6), 507–518. https://doi.org/10.1017/S1431927608080628

Lee, H. Y., Ge, W. P., Huang, W., He, Y., Wang, G. X., Rowson-Baldwin, A., … Jan, L. Y. (2011). Bidirectional regulation of dendritic voltage-gated potassium channels by the fragile X mental retardation protein. *Neuron*, *72*(4), 630–642. https://doi.org/10.1016/j.neuron.2011.09.033

Lemke, J. R., Geider, K., Helbig, K. L., Heyne, H. O., Schütz, H., Hentschel, J., … Syrbe, S. (2016). Delineating the GRIN1 phenotypic spectrum: A distinct genetic NMDA receptor encephalopathy. *Neurology*, *86*(23), 2171–2178. https://doi.org/10.1212/WNL.0000000000002740

Lemke, J. R., Lal, D., Reinthaler, E. M., Steiner, I., Nothnagel, M., Alber, M., … Von Spiczak, S. (2013). Mutations in GRIN2A cause idiopathic focal epilepsy with rolandic spikes. *Nature Genetics*, *45*(9), 1067–1072. https://doi.org/10.1038/ng.2728

Lesca, G., Rudolf, G., Bruneau, N., Lozovaya, N., Labalme, A., Boutry-Kryza, N., … Szepetowski, P. (2013). GRIN2A mutations in acquired epileptic aphasia and related childhood focal epilepsies and encephalopathies with speech and language dysfunction. *Nature Genetics*, *45*(9), 1061–1066. https://doi.org/10.1038/ng.2726

Li, B., Chen, N., Luo, T., Otsu, Y., Murphy, T. H., & Raymond, L. A. (2002). Differential regulation of synaptic and extrasynaptic NMDA receptors. *Nature Neuroscience*, *5*(9), 833–834. https://doi.org/10.1038/nn912

Li, B. S., Sun, M. K., Zhang, L., Takahashi, S., Ma, W., Vinade, L., … Pant, H. C. (2001). Regulation of NMDA receptors by cyclin-dependent kinase-5. *Proceedings of the National Academy of Sciences of the United States of America*, *98*(22), 12742–12747. https://doi.org/10.1073/pnas.211428098

Li, C., Takei, K., Geppert, M., Daniell, L., Stenius, K., Chapman, E. R., … Südhof, T. C. (1994). Synaptic targeting of rabphilin-3A, a synaptic vesicle Ca2+/phospholipid-binding protein, depends on rab3A/3C. *Neuron*, *13*(4), 885–898. https://doi.org/10.1016/0896-6273(94)90254-2

Li, J., Lu, Q., & Zhang, M. (2016). Structural Basis of Cargo Recognition by Unconventional Myosins in Cellular Trafficking. *Traffic*, *17*(8), 822–838. https://doi.org/10.1111/tra.12383

Li, S., Hong, S., Shepardson, N. E., Walsh, D. M., Shankar, G. M., & Selkoe, D. (2009). Soluble Oligomers of Amyloid β Protein Facilitate Hippocampal Long-Term Depression by Disrupting Neuronal Glutamate Uptake. *Neuron*, *62*(6), 788–801. https://doi.org/10.1016/j.neuron.2009.05.012

Li, S., Jin, M., Koeglsperger, T., Shepardson, N. E., Shankar, G. M., & Selkoe, D. J. (2011). Soluble a β oligomers inhibit long-term potentiation through a mechanism involving excessive activation of extrasynaptic NR2B-containing NMDA receptors. *Journal of Neuroscience*, *31*(18), 6627–6638. https://doi.org/10.1523/JNEUROSCI.0203-11.2011

Li, S., Tian, X., Hartley, D. M., & Feig, L. A. (2006). Distinct roles for Ras-guanine nucleotide-releasing factor 1 (Ras-GRF1) and Ras-GRF2 in the induction of long-term potentiation and long-term depression. *Journal of Neuroscience*, *26*(6), 1721–1729. https://doi.org/10.1523/JNEUROSCI.3990-05.2006

Li, Z., Okamoto, K. I., Hayashi, Y., & Sheng, M. (2004). The importance of dendritic mitochondria in the morphogenesis and plasticity of spines and synapses. *Cell*, *119*(6), 873–887. https://doi.org/10.1016/j.cell.2004.11.003

Lim, D., Mapelli, L., Canonico, P. L., Moccia, F., & Genazzani, A. A. (2018). Neuronal activity-dependent activation of astroglial calcineurin in mouse primary hippocampal cultures. *International Journal of Molecular Sciences*, *19*(10). https://doi.org/10.3390/ijms19102997

Lim, I. A., Hall, D. D., & Hell, J. W. (2002). Selectivity and promiscuity of the first and second PDZ domains of PSD-95 and synapse-associated protein 102. *Journal of Biological Chemistry*, *277*(24), 21697–21711. https://doi.org/10.1074/jbc.M112339200

Lisman, J. (1989). A mechanism for the Hebb and the anti-Hebb processes underlying learning and memory. *Proceedings of the National Academy of Sciences of the United States of America*, *86*(23), 9574–9578. https://doi.org/10.1073/pnas.86.23.9574

Lonart, G., & Südhof, T. C. (1998). Region-specific phosphorylation of rabphilin in mossy fiber nerve terminals of the hippocampus. *Journal of Neuroscience*, *18*(2), 634–640. https://doi.org/10.1523/jneurosci.18-02-00634.1998

Lu, W., Shi, Y., Jackson, A. C., Bjorgan, K., During, M. J., Sprengel, R., … Nicoll, R. A. (2009). Subunit Composition of Synaptic AMPA Receptors Revealed by a Single-Cell Genetic Approach. *Neuron*, *62*(2), 254–268. https://doi.org/10.1016/j.neuron.2009.02.027

Lu, W. Y., Man, H. Y., Ju, W., Trimble, W. S., MacDonald, J. F., & Wang, Y. T. (2001). Activation of synaptic NMDA receptors induces membrane insertion of new AMPA receptors and LTP in cultured hippocampal neurons. *Neuron*, *29*(1), 243–254. https://doi.org/10.1016/S0896-6273(01)00194-5

Lundbye, C. J., Toft, A. K. H., & Banke, T. G. (2018). Inhibition of GluN2A NMDA receptors ameliorates synaptic plasticity deficits in the Fmr1−/y mouse model. *Journal of Physiology*, *596*(20), 5017–5031. https://doi.org/10.1113/JP276304

Luo, T., Wu, W. H., & Chen, B. S. (2011). NMDA receptor signaling: Death or survival? *Frontiers in Biology*, *6*(6), 468–476. https://doi.org/10.1007/s11515-011-1187-6

Ma, H., Groth, R. D., Cohen, S. M., Emery, J. F., Li, B., Hoedt, E., … Tsien, R. W. (2014). γcaMKII shuttles Ca2+/CaM to the nucleus to trigger CREB phosphorylation and gene expression. *Cell*. https://doi.org/10.1016/j.cell.2014.09.019

Majewska, A. K., Newton, J. R., & Sur, M. (2006). Remodeling of synaptic structure in sensory cortical areas In Vivo. *Journal of Neuroscience*, *26*(11), 3021–3029. https://doi.org/10.1523/JNEUROSCI.4454-05.2006

Makino, Y., Johnson, R. C., Yu, Y., Takamiya, K., & Huganir, R. L. (2011). Enhanced synaptic plasticity in mice with phosphomimetic mutation of the GluA1 AMPA receptor. *Proceedings of the National Academy of Sciences*. https://doi.org/10.1073/pnas.1105261108

Malenka, R. C., & Bear, M. F. (2004). LTP and LTD: An embarrassment of riches. *Neuron*, *44*(1), 5–21. https://doi.org/10.1016/j.neuron.2004.09.012

Malinow, R., & Malenka, R. C. (2002). AMPA Receptor Trafficking and Synaptic Plasticity. *Annual Review of Neuroscience*, *25*(1), 103–126. https://doi.org/10.1146/annurev.neuro.25.112701.142758

Maltese, M., Stanic, J., Tassone, A., Sciamanna, G., Ponterio, G., Vanni, V., … Pisani, A. (2018). Early

structural and functional plasticity alterations in a susceptibility period of DYT1 dystonia mouse striatum. *ELife*, *7*, e33331. https://doi.org/10.7554/eLife.33331

Marcello, E., Di Luca, M., & Gardoni, F. (2018). Synapse-to-nucleus communication: from developmental disorders to Alzheimer's disease. *Current Opinion in Neurobiology*, *48*, 160–166. https://doi.org/10.1016/j.conb.2017.12.017

Marcello, E., Musardo, S., Vandermeulen, L., Pelucchi, S., Gardoni, F., Santo, N., … Di Luca, M. (2019). Amyloid-β Oligomers Regulate ADAM10 Synaptic Localization Through Aberrant Plasticity Phenomena. *Molecular Neurobiology*, *56*(10), 7136–7143. https://doi.org/10.1007/s12035-019-1583-5

Marcello, E., Saraceno, C., Musardo, S., Vara, H., De La Fuente, A. G., Pelucchi, S., … Di Luca, M. (2013). Endocytosis of synaptic ADAM10 in neuronal plasticity and Alzheimer's disease. *Journal of Clinical Investigation*. https://doi.org/10.1172/JCI65401

Maselli, R. A., Vázquez, J., Schrumpf, L., Arredondo, J., Lara, M., Strober, J. B., … Ferns, M. (2018). Presynaptic congenital myasthenic syndrome with altered synaptic vesicle homeostasis linked to compound heterozygous sequence variants in RPH3A. *Molecular Genetics and Genomic Medicine*, *6*(3), 434–440. https://doi.org/10.1002/mgg3.370

Matta, J. A., Ashby, M. C., Sanz-Clemente, A., Roche, K. W., & Isaac, J. T. R. (2011). MGluR5 and NMDA Receptors Drive the Experience- and Activity-Dependent NMDA Receptor NR2B to NR2A Subunit Switch. *Neuron*. https://doi.org/10.1016/j.neuron.2011.02.045

Mayer, M. L., & Vyklicky, L. (1989). The action of zinc on synaptic transmission and neuronal excitability in cultures of mouse hippocampus. *The Journal of Physiology*, *415*, 315–365. https://doi.org/10.1113/jphysiol.1989.sp017725

Mayer, Mark L. (2017). The Challenge of Interpreting Glutamate-Receptor Ion-Channel Structures. *Biophysical Journal*, *113*(10), 2143–2151. https://doi.org/10.1016/j.bpj.2017.07.028

McGuinness, L., Taylor, C., Taylor, R. D. T., Yau, C., Langenhan, T., Hart, M. L., … Emptage, N. J. (2010). Presynaptic NMDARs in the Hippocampus Facilitate Transmitter Release at Theta Frequency. *Neuron*, *68*(6), 1109–1127. https://doi.org/10.1016/j.neuron.2010.11.023

McKiernan, C. J., Stabila, P. F., & Macara, I. G. (1996). Role of the Rab3A-binding domain in targeting of rabphilin-3A to vesicle membranes of PC12 cells. *Molecular and Cellular Biology*, *16*(9), 4985–4995. https://doi.org/10.1128/mcb.16.9.4985

Mellentin, C., Jahnsen, H., & Abraham, W. C. (2007). Priming of long-term potentiation mediated by ryanodine receptor activation in rat hippocampal slices. *Neuropharmacology*, *52*(1), 118–125. https://doi.org/10.1016/j.neuropharm.2006.07.009

Mellone, M., Stanic, J., Hernandez, L. F., Iglesias, E., Zianni, E., Longhi, A., … Gardoni, F. (2015). NMDA receptor GluN2A/GluN2B subunit ratio as synaptic trait of levodopa-induced dyskinesias: from experimental models to patients. *Frontiers in Cellular Neuroscience*, *9*(July 6), 245. https://doi.org/10.3389/fncel.2015.00245

Meredith, R. M., Holmgren, C. D., Weidum, M., Burnashev, N., & Mansvelder, H. D. (2007). Increased Threshold for Spike-Timing-Dependent Plasticity Is Caused by Unreliable Calcium Signaling in Mice Lacking Fragile X Gene Fmr1. *Neuron*, *54*(4), 627–638. https://doi.org/10.1016/j.neuron.2007.04.028

Mignogna, M. L., Giannandrea, M., Gurgone, A., Fanelli, F., Raimondi, F., Mapelli, L., … D'Adamo, P. (2015). The intellectual disability protein RAB39B selectively regulates GluA2 trafficking to determine synaptic AMPAR composition. *Nature Communications*, *6*(6504). https://doi.org/10.1038/ncomms7504

Mizoguchi, A., Yano, Y., Hamaguchi, H., Yanagida, H., Ide, C., Zahraoui, A., … Takai, Y. (1994). Localization of

Rabphilin-3A on the synaptic vesicle. *Biochemical and Biophysical Research Communications*, *202*(3), 1235–1243. https://doi.org/10.1006/bbrc.1994.2063

Mizui, T., Sekino, Y., Yamazaki, H., Ishizuka, Y., Takahashi, H., Kojima, N., … Shirao, T. (2014). Myosin II ATPase activity mediates the long-term potentiation-induced exodus of stable F-actin bound by drebrin a from dendritic spines. *PLoS ONE*, *9*(1). https://doi.org/10.1371/journal.pone.0085367

Monfils, M. H., & Teskey, G. C. (2004). Induction of long-term depression is associated with decreased dendritic length and spine density in layers III and V of sensorimotor neocortex. *Synapse*, *53*(2), 114–121. https://doi.org/10.1002/syn.20039

Montaville, P., Coudevylle, N., Radhakrishnan, A., Leonov, A., Zweckstetter, M., & Becker, S. (2008). The PIP2 binding mode of the C2 domains of rabphilin-3A. *Protein Science*, *17*(6), 1025–1034. https://doi.org/10.1110/ps.073326608

Monyer, H., Burnashev, N., Laurie, D. J., Sakmann, B., & Seeburg, P. H. (1994). Developmental and regional expression in the rat brain and functional properties of four NMDA receptors. *Neuron*, *12*(3), 529–540. https://doi.org/10.1016/0896-6273(94)90210-0

Moreau, M. M., Piguel, N., Papouin, T., Koehl, M., Durand, C. M., Rubio, M. E., … Sans, N. (2010). The Planar Polarity Protein Scribble1 Is Essential for Neuronal Plasticity and Brain Function. *Journal of Neuroscience*. https://doi.org/10.1523/JNEUROSCI.6007-09.2010

Morris, R. G. M. (2006). Elements of a neurobiological theory of hippocampal function: The role of synaptic plasticity, synaptic tagging and schemas. *European Journal of Neuroscience*, *23*(1), 2829–2846. https://doi.org/10.1111/j.1460-9568.2006.04888.x

Morris, R. G. M., Anderson, E., Lynch, G. S., & Baudry, M. (1986). Selective impairment of learning and blockade of long-term potentiation by an N-methyl-D-aspartate receptor antagonist, AP5. *Nature*, *319*(6056), 774–776. https://doi.org/10.1038/319774a0

Morris, R. G. M., Garrud, P., Rawlins, J. N. P., & O'Keefe, J. (1982). Place navigation impaired in rats with hippocampal lesions. *Nature*, *297*(5868), 681–683. https://doi.org/10.1038/297681a0

Ng, D., Pitcher, G. M., Szilard, R. K., Sertié, A., Kanisek, M., Clapcote, S. J., … McInnes, R. R. (2009). Neto1 is a novel CUB-domain NMDA receptor-interacting protein required for synaptic plasticity and learning. *PLoS Biology*, *7*(2), e41. https://doi.org/10.1371/journal.pbio.1000041

Niswender, C. M., & Conn, P. J. (2010). Metabotropic Glutamate Receptors: Physiology, Pharmacology, and Disease. *Annual Review of Pharmacology and Toxicology*, *50*(1), 295–322. https://doi.org/10.1146/annurev.pharmtox.011008.145533

Nong, Y., Huang, Y. Q., Ju, W., Kalia, L. V., Ahmadian, G., Wang, Y. T., & Salter, M. W. (2003). Glycine binding primes NMDA receptor internalization. *Nature*, *422*(6929), 302–307. https://doi.org/10.1038/nature01497

Norris, C. M., Halpain, S., & Foster, T. C. (1998). Reversal of age-related alterations in synaptic plasticity by blockade of L-type Ca2+ channels. *Journal of Neuroscience*, *18*(9), 3171–3179. https://doi.org/10.1523/jneurosci.18-09-03171.1998

Ogden, K. K., Chen, W., Swanger, S. A., McDaniel, M. J., Fan, L. Z., Hu, C., … Yuan, H. (2017). Molecular Mechanism of Disease-Associated Mutations in the Pre-M1 Helix of NMDA Receptors and Potential Rescue Pharmacology. *PLoS Genetics*, *13*(1), e1006536. https://doi.org/10.1371/journal.pgen.1006536

Oh, M. C., Derkach, V. A., Guire, E. S., & Soderling, T. R. (2006). Extrasynaptic membrane trafficking regulated by GluR1 serine 845 phosphorylation primes AMPA receptors for long-term potentiation. *Journal of Biological Chemistry*. https://doi.org/10.1074/jbc.M509677200

Ohya, T., Sasaki, T., Kato, M., & Takai, Y. (1998). Involvement of rabphilin3 in endocytosis through interaction with rabaptin5. *Journal of Biological Chemistry*, *273*(1), 613–617. https://doi.org/10.1074/jbc.273.1.613

Okuyama, T., Kitamura, T., Roy, D. S., Itohara, S., & Tonegawa, S. (2016). Ventral CA1 neurons store social memory. *Science*, *353*(6307), 1536–1541. https://doi.org/10.1126/science.aaf7003

Oliet, S. H. R., Malenka, R. C., & Nicoll, R. A. (1997). Two distinct forms of long-term depression coexist in CA1 hippocampal pyramidal cells. *Neuron*, *18*(6), 969–982. https://doi.org/10.1016/S0896-6273(00)80336-0

Ostroff, L. E., Fiala, J. C., Allwardt, B., & Harris, K. M. (2002). Polyribosomes redistribute from dendritic shafts into spines with enlarged synapses during LTP in developing rat hippocampal slices. *Neuron*, *35*(3), 535–545. https://doi.org/10.1016/S0896-6273(02)00785-7

Otmakhov, N., Khibnik, L., Otmakhova, N., Carpenter, S., Riahi, S., Asrican, B., & Lisman, J. (2004). Forskolin-Induced LTP in the CA1 Hippocampal Region Is NMDA Receptor Dependent. *Journal of Neurophysiology*, *91*(5), 1955–1962. https://doi.org/10.1152/jn.00941.2003

Paillé, V., Picconi, B., Bagetta, V., Ghiglieri, V., Sgobio, C., Di Filippo, M., … Calabresi, P. (2010). Distinct levels of dopamine denervation differentially alter striatal synaptic plasticity and NMDA receptor subunit composition. *Journal of Neuroscience*, *30*(42), 14182–14193. https://doi.org/10.1523/JNEUROSCI.2149-10.2010

Panayotis, N., Karpova, A., Kreutz, M. R., & Fainzilber, M. (2015). Macromolecular transport in synapse to nucleus communication. *Trends in Neurosciences*, *38*(2), 108–116. https://doi.org/10.1016/j.tins.2014.12.001

Paoletti, P., Ascher, P., & Neyton, J. (1997). High-affinity zinc inhibition of NMDA NR1-NR2A receptors. *Journal of Neuroscience*, *17*(15), 5711–5725. https://doi.org/10.1523/jneurosci.17-15-05711.1997

Paoletti, P., Bellone, C., & Zhou, Q. (2013). NMDA receptor subunit diversity: Impact on receptor properties, synaptic plasticity and disease. *Nature Reviews Neuroscience*, *14*(6), 383–400. https://doi.org/10.1038/nrn3504

Paradee, W., Melikian, H. E., Rasmussen, D. L., Kenneson, A., Conn, P. J., & Warren, S. T. (1999). Fragile X mouse: Strain effects of knockout phenotype and evidence suggesting deficient amygdala function. *Neuroscience*, *94*(1), 185–192. https://doi.org/10.1016/S0306-4522(99)00285-7

Park, D., Bae, S., Yoon, T. H., & Ko, J. (2018). Molecular mechanisms of synaptic specificity: Spotlight on hippocampal and cerebellar synapse organizers. *Molecules and Cells*, *41*(5), 373–380. https://doi.org/10.14348/molcells.2018.0081

Pasciuto, E., & Bagni, C. (2014). SnapShot: FMRP mRNA targets and diseases. *Cell*, *158*(6), 1446-1446.e1.

Persoon, C. M., Hoogstraaten, R. I., Nassal, J. P., van Weering, J. R. T., Kaeser, P. S., Toonen, R. F., & Verhage, M. (2019). The RAB3-RIM Pathway Is Essential for the Release of Neuromodulators. *Neuron*, *104*(6), 1065–1080. https://doi.org/10.1016/j.neuron.2019.09.015

Peters, A., & Kaiserman-Abramof, I. R. (1970). The small pyramidal neuron of the rat cerebral cortex. The perikaryon, dendrites and spines. *American Journal of Anatomy*, *127*(4), 321–355. https://doi.org/10.1002/aja.1001270402

Philpot, B. D., Cho, K. K. A., & Bear, M. F. (2007). Obligatory Role of NR2A for Metaplasticity in Visual Cortex. *Neuron*. https://doi.org/10.1016/j.neuron.2007.01.027

Philpot, B. D., Espinosa, J. S., & Bear, M. F. (2003). Evidence for altered NMDA receptor function as a basis for metaplasticity in visual cortex. *Journal of Neuroscience*, *23*(13), 5583–5588.

https://doi.org/23/13/5583 [pii]

Philpot, B. D., Sekhar, A. K., Shouval, H. Z., & Bear, M. F. (2001). Visual experience and deprivation bidirectionally modify the composition and function of NMDA receptors in visual cortex. *Neuron*. https://doi.org/10.1016/S0896-6273(01)00187-8

Piccoli, G., Verpelli, C., Tonna, N., Romorini, S., Alessio, M., Nairn, A. C., … Sala, C. (2007). Proteomic analysis of activity-dependent synaptic plasticity in hippocampal neurons. *Journal of Proteome Research*. https://doi.org/10.1021/pr0701308

Picconi, B., Centonze, D., Håkansson, K., Bernardi, G., Greengard, P., Fisone, G., … Calabresi, P. (2003). Loss of bidirectional striatal synaptic plasticity in L-DOPA-induced dyskinesia. *Nature Neuroscience*, *6*(5), 501–506. https://doi.org/10.1038/nn1040

Piguel, N. H., Fievre, S., Blanc, J. M., Carta, M., Moreau, M. M., Moutin, E., … Sans, N. (2014). Scribble1/AP2 complex coordinates NMDA receptor endocytic recycling. *Cell Reports*, *9*(2), 712–727. https://doi.org/10.1016/j.celrep.2014.09.017

Pin, J. P., Galvez, T., & Prézeau, L. (2003). Evolution, structure, and activation mechanism of family 3/C G-protein-coupled receptors. *Pharmacology and Therapeutics*, *98*(3), 325–354. https://doi.org/10.1016/S0163-7258(03)00038-X

Prescott, I. A., Liu, L. D., Dostrovsky, J. O., Hodaie, M., Lozano, A. M., & Hutchison, W. D. (2014). Lack of depotentiation at basal ganglia output neurons in PD patients with levodopa-induced dyskinesia. *Neurobiology of Disease*, *71*, 24–33. https://doi.org/10.1016/j.nbd.2014.08.002

Pylypenko, O., Hammich, H., Yu, I. M., & Houdusse, A. (2018). Rab GTPases and their interacting protein partners: Structural insights into Rab functional diversity. *Small GTPases*, *9*(1–2), 22–48. https://doi.org/10.1080/21541248.2017.1336191

Quartarone, A., & Hallett, M. (2013). Emerging concepts in the physiological basis of dystonia. *Movement Disorders*, *28*(7), 958–967. https://doi.org/10.1002/mds.25532

Rao-Ruiz, P., Yu, J., Kushner, S. A., & Josselyn, S. A. (2019). Neuronal competition: microcircuit mechanisms define the sparsity of the engram. *Current Opinion in Neurobiology*. https://doi.org/10.1016/j.conb.2018.10.013

Rastaldi, M. P., Armelloni, S., Berra, S., Li, M., Pesaresi, M., Poczewski, H., … D'Amico, G. (2003). Glomerular podocytes possess the synaptic vesicle molecule Rab3A and its specific effector rabphilin-3A. *American Journal of Pathology*, *163*(3), 889–899. https://doi.org/10.1016/S0002-9440(10)63449-9

Redondo, R. L., Kim, J., Arons, A. L., Ramirez, S., Liu, X., & Tonegawa, S. (2014). Bidirectional switch of the valence associated with a hippocampal contextual memory engram. *Nature*, *513*(7518), 426–430. https://doi.org/10.1038/nature13725

Redondo, R. L., Okuno, H., Spooner, P. A., Frenguelli, B. G., Bito, H., & Morris, R. G. M. (2010). Synaptic tagging and capture: Differential role of distinct calcium/calmodulin kinases in protein synthesis-dependent long-term potentiation. *Journal of Neuroscience*, *30*(14), 4981–4989. https://doi.org/10.1523/JNEUROSCI.3140-09.2010

Reichardt, L. F. (2006). Neurotrophin-regulated signalling pathways. *Philosophical Transactions of the Royal Society B: Biological Sciences*, *361*(1473), 1545–1564. https://doi.org/10.1098/rstb.2006.1894

Reiner, O., Sapoznik, S., & Sapir, T. (2006). Lissencephaly 1 linking to multiple diseases: Mental retardation, neurodegeneration, schizophrenia, male sterility, and more. *NeuroMolecular Medicine*, *8*(4), 547–565. https://doi.org/10.1385/NMM:8:4:547

Ryan, T. J., Kopanitsa, M. V., Indersmitten, T., Nithianantharajah, J., Afinowi, N. O., Pettit, C., … Komiyama,

N. H. (2013). Evolution of GluN2A/B cytoplasmic domains diversified vertebrate synaptic plasticity and behavior. *Nature Neuroscience*, *16*(1), 25–32. https://doi.org/10.1038/nn.3277

Ryu, J., Futai, K., Feliu, M., Weinberg, R., & Sheng, M. (2008). Constitutively active Rap2 transgenic mice display fewer dendritic spines, reduced extracellular signal-regulated kinase signaling, enhanced long-term depression, and impaired spatial learning and fear extinction. *Journal of Neuroscience*, *28*(33), 8178–8188. https://doi.org/10.1523/JNEUROSCI.1944-08.2008

S, S., & Colbran RJ. (1998). Autophosphorylation-dependent targeting of calcium calmodulin-dependent protein kinase II by the NR2B subunit of the N-methyl- D-aspartate receptor. *Journal of Biological Chemistry*, *273*(33), 20689–20692. https://doi.org/10.1074/jbc.273.33.20689

Sakagami, H., Sanda, M., Fukaya, M., Miyazaki, T., Sukegawa, J., Yanagisawa, T., … Kondo, H. (2008). IQ-ArfGEF/BRAG1 is a guanine nucleotide exchange factor for Arf6 that interacts with PSD-95 at postsynaptic density of excitatory synapses. *Neuroscience Research*, *60*(2), 199–212. https://doi.org/10.1016/j.neures.2007.10.013

Sala, C., & Segal, M. (2014). Dendritic spines: The locus of structural and functional plasticity. *Physiological Reviews*, *94*(1), 141–188. https://doi.org/10.1152/physrev.00012.2013

Sala, M., Braida, D., Lentini, D., Busnelli, M., Bulgheroni, E., Capurro, V., … Chini, B. (2011). Pharmacologic rescue of impaired cognitive flexibility, social deficits, increased aggression, and seizure susceptibility in oxytocin receptor null mice: A neurobehavioral model of autism. *Biological Psychiatry*. https://doi.org/10.1016/j.biopsych.2010.12.022

Salter, M. W., & Kalia, L. V. (2004). SRC kinases: A hub for NMDA receptor regulation. *Nature Reviews Neuroscience*, *5*(4), 317–328. https://doi.org/10.1038/nrn1368

Sawtell, N. B., Frenkel, M. Y., Philpot, B. D., Nakazawa, K., Tonegawa, S., & Bear, M. F. (2003). NMDA receptor-dependent ocular dominance plasticity in adult visual cortex. *Neuron*. https://doi.org/10.1016/S0896-6273(03)00323-4

Schlüter, O. M., Schmitz, F., Jahn, R., Rosenmund, C., & Südhof, T. C. (2004). A complete genetic analysis of neuronal Rab3 function. *Journal of Neuroscience*, *24*(29), 6629–6637. https://doi.org/10.1523/JNEUROSCI.1610-04.2004

Schlüter, O. M., Schnell, E., Verhage, M., Tzonopoulos, T., Nicoll, R. A., Janz, R., … Südhof, T. C. (1999). Rabphilin knock-out mice reveal that rabphilin is not required for rab3 function in regulating neurotransmitter release. *Journal of Neuroscience*, *19*(14), 5834–5846. https://doi.org/10.1523/jneurosci.19-14-05834.1999

Schreiber, J. A., Müller, S. L., Westphälinger, S. E., Schepmann, D., Strutz-Seebohm, N., Seebohm, G., & Wünsch, B. (2018). Systematic variation of the benzoylhydrazine moiety of the GluN2A selective NMDA receptor antagonist TCN-201. *European Journal of Medicinal Chemistry*, *158*, 259–269. https://doi.org/10.1016/j.ejmech.2018.09.006

Seeburg, P. H., Burnashev, N., Köhr, G., Kuner, T., Sprengel, R., & Monyer, H. (1995). The NMDA Receptor Channel: Molecular Design of a Coincidence Detector. In *Proceedings of the 1993 Laurentian Hormone Conference* (pp. 19–34). Recent progress in hormone research. https://doi.org/10.1016/b978-0-12-571150-0.50006-8

Segal, M. (2005). Dendritic spines and long-term plasticity. *Nature Reviews Neuroscience*, *6*(4), 277–284. https://doi.org/10.1038/nrn1649

Selamat, W., Jamari, I., Wang, Y., Takumi, T., Wong, F., & Fujii, R. (2009). TLS interaction with NMDA R1 splice variant in retinal ganglion cell line RGC-5. *Neuroscience Letters*, *450*(2), 163–166. https://doi.org/10.1016/j.neulet.2008.12.014

Seol, G. H., Ziburkus, J., Huang, S. Y., Song, L., Kim, I. T., Takamiya, K., … Kirkwood, A. (2007). Neuromodulators Control the Polarity of Spike-Timing-Dependent Synaptic Plasticity. *Neuron*, *55*(6), 919–929. https://doi.org/10.1016/j.neuron.2007.08.013

Sheng, M., Cummings, J., Roldan, L. A., Jan, Y. N., & Jan, L. Y. (1994). Changing subunit composition of heteromeric NMDA receptors during development of rat cortex. *Nature*, *368*(6467), 144–147. https://doi.org/10.1038/368144a0

Sheng, M., & Sala, C. (2001). PDZ Domains and the Organization of Supramolecular Complexes. *Annual Review of Neuroscience*, *24*(1), 1–29. https://doi.org/10.1146/annurev.neuro.24.1.1

Shipton, O. A., & Paulsen, O. (2014). GluN2A and GluN2B subunit-containing NMDA receptors in hippocampal plasticity. *Philosophical Transactions of the Royal Society B: Biological Sciences*. https://doi.org/10.1098/rstb.2013.0163

Shirataki, H., Kaibuchi, K., Sakoda, T., Kishida, S., Yamaguchi, T., Wada, K., … Takai, Y. (1993). Rabphilin-3A, a putative target protein for smg p25A/rab3A p25 small GTP-binding protein related to synaptotagmin. *Molecular and Cellular Biology*, *13*(4), 2061–2068. https://doi.org/10.1128/mcb.13.4.2061

Shohami, E., & Biegon, A. (2014). Novel Approach to the Role of NMDA Receptors in Traumatic Brain Injury. *CNS & Neurological Disorders - Drug Targets*, *13*(4), 567–573.

Shouval, H. Z., Bear, M. F., & Cooper, L. N. (2002). A unified model of NMDA receptor-dependent bidirectional synaptic plasticity. *Proceedings of the National Academy of Sciences of the United States of America*, *99*(16), 10831–11836. https://doi.org/10.1073/pnas.152343099

Sibarov, D. A., Bruneau, N., Antonov, S. M., Szepetowski, P., Burnashev, N., & Giniatullin, R. (2017). Functional properties of human NMDA receptors associated with epilepsy-related mutations of GluN2A subunit. *Frontiers in Cellular Neuroscience*, (11), 155. https://doi.org/10.3389/fncel.2017.00155

Siegel, S. J., Brose, N., Janssen, W. G., Gasic, G. P., Jahn, R., Heinemann, S. F., & Morrison, J. H. (1994). Regional, cellular, and ultrastructural distribution of N-methyl-D- aspartate receptor subunit 1 in monkey hippocampus. *Proceedings of the National Academy of Sciences of the United States of America*, *91*(2), 564–568. https://doi.org/10.1073/pnas.91.2.564

Sjöström, P. J., Turrigiano, G. G., & Nelson, S. B. (2003). Neocortical LTD via coincident activation of presynaptic NMDA and cannabinoid receptors. *Neuron*, *39*(4), 641–654. https://doi.org/10.1016/S0896-6273(03)00476-8

Snyder, E. M., Nong, Y., Almeida, C. G., Paul, S., Moran, T., Choi, E. Y., … Greengard, P. (2005). Regulation of NMDA receptor trafficking by amyloid-β. *Nature Neuroscience*. https://doi.org/10.1038/nn1503

Snyder, E. M., Philpot, B. D., Huber, K. M., Dong, X., Fallon, J. R., & Bear, M. F. (2001). Internalization of ionotropic glutamate receptors in response to mGluR activation. *Nature Neuroscience*, *4*(11), 1079–1085. https://doi.org/10.1038/nn746

Stahl, B., Von Mollard, G. F., Walch-Solimena, C., & Jahn, R. (1994). GTP cleavage by the small GTP-binding protein Rab3A is associated with exocytosis of synaptic vesicles induced by α-latrotoxin. *Journal of Biological Chemistry*, *269*(40), 24770–24776.

Stanic, J., Carta, M., Eberini, I., Pelucchi, S., Marcello, E., Genazzani, A. A., … Gardoni, F. (2015). Rabphilin 3A retains NMDA receptors at synaptic sites through interaction with GluN2A/PSD-95 complex. *Nature Communications*, *6*, 10181. https://doi.org/10.1038/ncomms10181

Stanic, J., Mellone, M., Napolitano, F., Racca, C., Zianni, E., Minocci, D., … Gardoni, F. (2017). Rabphilin 3A: A novel target for the treatment of levodopa-induced dyskinesias. *Neurobiology of Disease*, *108*, 54–64. https://doi.org/10.1016/j.nbd.2017.08.001

Sun, Y., Xu, Y., Cheng, X., Chen, X., Xie, Y., Zhang, L., … Gao, Z. (2018). The differences between GluN2A and GluN2B signaling in the brain. *Journal of Neuroscience Research*, *96*(8), 1430–1433. https://doi.org/10.1002/jnr.24251

Swanger, S. A., Chen, W., Wells, G., Burger, P. B., Tankovic, A., Bhattacharya, S., … Yuan, H. (2016). Mechanistic Insight into NMDA Receptor Dysregulation by Rare Variants in the GluN2A and GluN2B Agonist Binding Domains. *American Journal of Human Genetics*, *99*(6), 1261–1280. https://doi.org/10.1016/j.ajhg.2016.10.002

Tackenberg, C., Grinschgl, S., Trutzel, A., Santuccione, A. C., Frey, M. C., Konietzko, U., … Nitsch, R. M. (2013). NMDA receptor subunit composition determines beta-amyloid-induced neurodegeneration and synaptic loss. *Cell Death and Disease*, *4:e608*. https://doi.org/10.1038/cddis.2013.129

Texidó, L., Martín-Satué, M., Alberdi, E., Solsona, C., & Matute, C. (2011). Amyloid β peptide oligomers directly activate NMDA receptors. *Cell Calcium*, *49*(3), 184–190. https://doi.org/10.1016/j.ceca.2011.02.001

Tian, X., Gotoh, T., Tsuji, K., Lo, E. H., Huang, S., & Feig, L. A. (2004). Developmentally regulated role for Ras-GRFs in coupling NMDA glutamate receptors to Ras, Erk and CREB. *EMBO Journal*, *23*(7), 1567–1575. https://doi.org/10.1038/sj.emboj.7600151

Tomita, S., Sekiguchi, M., Wada, K., Nicoll, R. A., & Bredt, D. S. (2006). Stargazin controls the pharmacology of AMPA receptor potentiators. *Proceedings of the National Academy of Sciences of the United States of America*, *103*(26), 10064–10067. https://doi.org/10.1073/pnas.0603128103

Trachtenberg, J. T., Chen, B. E., Knott, G. W., Feng, G., Sanes, J. R., Welker, E., & Svoboda, K. (2002). Long-term in vivo imaging of experience-dependent synaptic plasticity in adult cortex. *Nature*, *420*(6917), 788–794. https://doi.org/10.1038/nature01273

Traynelis, S. F., & Cull-Candy, S. G. (1991). Pharmacological properties and H+ sensitivity of excitatory amino acid receptor channels in rat cerebellar granule neurones. *The Journal of Physiology*, *443*, 727–763. https://doi.org/10.1113/jphysiol.1991.sp018453

Traynelis, Stephen F., & Cull-Candy, S. G. (1990). Proton inhibition of N-methyl-D-aspartate receptors in cerebellar neurons. *Nature*, *345*(6273), 347–350. https://doi.org/10.1038/345347a0

Traynelis, Stephen F., Wollmuth, L. P., McBain, C. J., Menniti, F. S., Vance, K. M., Ogden, K. K., … Dingledine, R. (2010). Glutamate receptor ion channels: Structure, regulation, and function. *Pharmacological Reviews*. https://doi.org/10.1124/pr.109.002451

Van Dam, E. J. M., Kamal, A., Artola, A., De Graan, P. N. E., Gispen, W. H., & Ramakers, G. M. J. (2004). Group I metabotropic glutamate receptors regulate the frequency-response function of hippocampal CA1 synapses for the induction of LTP and LTD. *European Journal of Neuroscience*, *19*(1), 112–118. https://doi.org/10.1111/j.1460-9568.2004.03103.x

Velíšek, L., Dreier, J. P., Stanton, P. K., Heinemann, U., & Moshé, S. L. (1994). Lowering of extracellular pH suppresses low-Mg2+-induces seizures in combined entorhinal cortex-hippocampal slices. *Experimental Brain Research*, *101*, 44–52. https://doi.org/10.1007/BF00243215

Vieira, M., Yong, X. L. H., Roche, K. W., & Anggono, V. (2020). Regulation of NMDA glutamate receptor functions by the GluN2 subunits. *Journal of Neurochemistry*. https://doi.org/10.1111/jnc.14970

Villemure, E., Volgraf, M., Jiang, Y., Wu, G., Ly, C. Q., Yuen, P. W., … Sellers, B. D. (2016). GluN2A-selective pyridopyrimidinone series of nmdar positive allosteric modulators with an improved in vivo profile. *ACS Medicinal Chemistry Letters*, *8*(1), 84–89. https://doi.org/10.1021/acsmedchemlett.6b00388

Vissel, B., Krupp, J. J., Heinemann, S. F., & Westbrook, G. L. (2001). A use-dependent tyrosine dephosphorylation of NMDA receptors is independent of ion flux. *Nature Neuroscience*, *4*(6), 587–

596. https://doi.org/10.1038/88404

Vitureira, N., & Goda, Y. (2013). The interplay between hebbian and homeostatic synaptic plasticity. *Journal of Cell Biology*, *203*(2), 175–186. https://doi.org/10.1083/jcb.201306030

Volgraf, M., Sellers, B., Jiang, Y., Wu, G., Ly, C., Villemure, E., … Schwarz, J. (2016). Discovery of GluN2A-Selective NMDA Receptor Positive Allosteric Modulators (PAMs) Tuning Deactivation Kinetics via Structure-Based Design. *Journal of Medicinal Chemistry*, *59*(6), 2760–2779.

Wagatsuma, A., Okuyama, T., Sun, C., Smith, L. M., Abe, K., & Tonegawa, S. (2017). Locus coeruleus input to hippocampal CA3 drives single-trial learning of a novel context. *Proceedings of the National Academy of Sciences of the United States of America*, *115*(2), E310–E316. https://doi.org/10.1073/pnas.1714082115

Wang, Jian, Liu, S. H., Fu, Y. P., Wang, J. H., & Lu, Y. M. (2003). Cdk5 activation induces hippocampal CA1 cell death by directly phosphorylating NMDA receptors. *Nature Neuroscience*, *6*(10), 1039–1047. https://doi.org/10.1038/nn1119

Wang, Jiejie, Lv, X., Wu, Y., Xu, T., Jiao, M., Yang, R., … Qiu, S. (2018). Postsynaptic RIM1 modulates synaptic function by facilitating membrane delivery of recycling NMDARs in hippocampal neurons. *Nature Communications*, *9*(1). https://doi.org/10.1038/s41467-018-04672-0

Warming, H., Pegasiou, C. M., Pitera, A. P., Kariis, H., Houghton, S. D., Kurbatskaya, K., … Vargas-Caballero, M. (2019). A primate-specific short GluN2A-NMDA receptor isoform is expressed in the human brain. *Molecular Brain*, *12*(1). https://doi.org/10.1186/s13041-019-0485-9

Williams, J. M., Mason-Parker, S. E., Abraham, W. C., & Tate, W. P. (1998). Biphasic changes in the levels of N-methyl-D-aspartate receptor-2 subunits correlate with the induction and persistence of long-term potentiation. *Molecular Brain Research*, *60*(1), 21–27. https://doi.org/10.1016/S0169-328X(98)00154-5

Wollmuth, L. P. (2018). Ion permeation in ionotropic glutamate receptors: still dynamic after all these years. *Current Opinion in Physiology*, *2*, 36–41. https://doi.org/10.1016/j.cophys.2017.12.003

Wollmuth, L. P., Kuner, T., & Sakmann, B. (1998). Adjacent asparagines in the NR2-subunit of the NMDA receptor channel control the voltage-dependent block by extracellular Mg 2+. *Journal of Physiology*, *506*(1), 13–32. https://doi.org/10.1111/j.1469-7793.1998.013bx.x

Xia, J., Zhang, X., Staudinger, J., & Huganir, R. L. (1999). Clustering of AMPA receptors by the synaptic PD domain-containing protein PICK1. *Neuron*, *22*(1), 179–187. https://doi.org/10.1016/S0896-6273(00)80689-3

Xu, X. X., & Luo, J. H. (2018). Mutations of N-Methyl-D-Aspartate Receptor Subunits in Epilepsy. *Neuroscience Bulletin*, *34*(3), 549–565. https://doi.org/10.1007/s12264-017-0191-5

Yang, M., & Leonard, J. P. (2001). Identification of mouse NMDA receptor subunit NR2A C-terminal tyrosine sites phosphorylated by coexpression with v-Src. *Journal of Neurochemistry*. https://doi.org/10.1046/j.1471-4159.2001.00255.x

Yang, Y., Wang, X. Bin, Frerking, M., & Zhou, Q. (2008). Spine expansion and stabilization associated with long-term potentiation. *Journal of Neuroscience*, *28*(22), 5740–5751. https://doi.org/10.1523/JNEUROSCI.3998-07.2008

Yashiro, K. (2005). Visual Deprivation Modifies Both Presynaptic Glutamate Release and the Composition of Perisynaptic/Extrasynaptic NMDA Receptors in Adult Visual Cortex. *Journal of Neuroscience*. https://doi.org/10.1523/JNEUROSCI.4362-05.2005

Yi, F., Mou, T. C., Dorsett, K. N., Volkmann, R. A., Menniti, F. S., Sprang, S. R., & Hansen, K. B. (2016).

Structural Basis for Negative Allosteric Modulation of GluN2A-Containing NMDA Receptors. *Neuron*, *91*(6), 1316–1329. https://doi.org/10.1016/j.neuron.2016.08.014

Yin, H. H., & Knowlton, B. J. (2006). The role of the basal ganglia in habit formation. *Nature Reviews Neuroscience*, *7*(6), 464–476. https://doi.org/10.1038/nrn1919

Yoshimura, A., Fujii, R., Watanabe, Y., Okabe, S., Fukui, K., & Takumi, T. (2006). Myosin-Va Facilitates the Accumulation of mRNA/Protein Complex in Dendritic Spines. *Current Biology*, *16*(23), 2345–2351. https://doi.org/10.1016/j.cub.2006.10.024

Zalutsky, R. A., & Nicoll, R. A. (1990). Comparison of two forms of long-term potentiation in single hippocampal neurons. *Science*, *248*(4963), 1619–1624. https://doi.org/10.1126/science.2114039

Zhai, S., Ark, E. D., Parra-Bueno, P., & Yasuda, R. (2013). Long-distance integration of nuclear ERK signaling triggered by activation of a few dendritic spines. *Science*. https://doi.org/10.1126/science.1245622

Zhan, J. Q., Zheng, L. L., Chen, H. B., Yu, B., Wang, W., Wang, T., … Yang, Y. J. (2018). Hydrogen sulfide reverses aging-associated amygdalar synaptic plasticity and fear memory deficits in rats. *Frontiers in Neuroscience*, *12*(JUN). https://doi.org/10.3389/fnins.2018.00390

Zhang, X. H., Liu, S. S., Yi, F., Zhuo, M., & Li, B. M. (2013). Delay-dependent impairment of spatial working memory with inhibition of NR2B-containing NMDA receptors in hippocampal CA1 region of rats. *Molecular Brain*. https://doi.org/10.1186/1756-6606-6-13

Zhang, X. M., Yan, X. Y., Zhang, B., Yang, Q., Ye, M., Cao, W., … Luo, J. H. (2015). Activity-induced synaptic delivery of the GluN2A-containing NMDA receptor is dependent on endoplasmic reticulum chaperone Bip and involved in fear memory. *Cell Research*, *25*(7), 818–836. https://doi.org/10.1038/cr.2015.75

Zhang, Y., Luan, Z., Liu, A., & Hu, G. (2001). The scaffolding protein CASK mediates the interaction between rabphilin3a and β-neurexins. *FEBS Letters*, *497*(2–3), 99–102. https://doi.org/10.1016/S0014-5793(01)02450-4

Zhao, M. G., Toyoda, H., Ko, S. W., Ding, H. K., Wu, L. J., & Zhuo, M. (2005). Deficits in trace fear memory and long-term potentiation in a mouse model for fragile X syndrome. *Journal of Neuroscience*, *25*(32), 7385–7392. https://doi.org/10.1523/JNEUROSCI.1520-05.2005

Zheng, F., Gingrich, M. B., Traynelis, S. F., & Conn, P. J. (1998). Tyrosine kinase potentiates NMDA receptor currents by reducing tonic zinc inhibition. *Nature Neuroscience*, *1*(3), 185–191. https://doi.org/10.1038/634

Zhou, Q., Homma, K. J., & Poo, M. M. (2004). Shrinkage of dendritic spines associated with long-term depression of hippocampal synapses. *Neuron*, *44*(5), 749–757. https://doi.org/10.1016/j.neuron.2004.11.011

Track of PhD records:

List of Publications:

- "Synaptic GluN2A-Containing NMDA receptors: from physiology to pathological synaptic plasticity" **Franchini L***; Carrano N*; Di Luca M; Gardoni F. (*equal contribution) *Int. J. Mol. Sci.* 2020, *21*, 1538. **I.F: 4,556**

- "Linking NMDA Receptor synaptic retention to synaptic plasticity and cognition." **Franchini L***, Stanic J*, Ponzoni L, Mellone M, Carrano N, Musardo S, Zianni E, Olivero G, Marcello E, Pittaluga A, Sala M, Bellone C, Racca C, Di Luca M, Gardoni F. (*equal contribution) *iScience.* 2019 Sept 27 https://doi.org/10.1016/j.isci.2019.08.036 **I.F: 4,447 cited: 2**

- "The synaptonuclear messenger RNF10 acts as an architect of neuronal morphology." Carrano N, Samaddar T, Brunialti E, **Franchini L**, Marcello E, Ciana P, Mauceri D, Di Luca M, Gardoni F. *Mol Neurobiol.* 2019 May 8 doi: 10.1007/s12035-019-1631-1 **I.F: 4,500 cited: 2**

- *Manuscript in preparation*. "Overexpression of CYP46A1 leads to sex-specific effects on synaptic functions in aged mice." Latorre M, Rodriguez Rodriguez P, **Franchini L**, Parrado C, Björkem I, Merino Serrais P, Cedazo-Minguez A and Maioli S.

Seminars and Conferences:

- 12th FENS Forum (11th-15th July 2020) – poster presentation *"Elucidating Rabphilin-3A role in NMDA synaptic retention and Dendritic spine potentiation"*

- Spring School in Chiesa in Valmalenco (25th-28th June 2020) – oral communication

- Neuroscience School of Advanced Studies – Learning and Memory course (7th-14th September 2019, Venice)

- 7th European Synapse Meeting (2nd – 4th September 2019, Lousanne); Poster presentation: "*Linking NMDA receptor synaptic retention to synaptic plasticity and cognition*"

- Spring School in Chiesa in Valmalenco (10th-14th April 2019) – oral communication on *"Rabphilin 3A modulates structural and functional synaptic plasticty through interaction with GluN2A/PSD95 complex*"

- 11th FENS Forum 2018 (7-11 July 2018, Berlin); poster presentation: "*Rabphilin 3A modulates structural and functional synaptic plasticty through interaction with GluN2A/PSD95 complex*"

- Spring School in Chiesa in Valmalenco (12-15 April 2018) oral communication "*Rabphilin 3A modulates structural and functional synaptic plasticty through interaction with GluN2A/PSD95 complex*"
- 6th European Synapse Meeting (4-6 December 2017, Milan)

- XXI SIF seminar on Pharmacolgoy for PhD students, Fellows, post doc and Specialist Trainees (19-22 September 2018, Bresso (MI)); poster presentation: "*Rabphilin 3A modulates structural and functional synaptic plasticty through interaction with GluN2A/PSD95 complex*"

Prizes and Scholarships:

- Winner of a Department Scholarship to prepare experimental degree thesis abroad (2.700€).

- Best poster award (500€) in XXI Seminar on Pharmacology for PhD students, Fellows, post docs and Specialist Trainees (19-22 September); from Italian Society of Pharmacology (SIF).
- Winner of Erasmus Traineeship 2018 for internship at Heidelberg University, Daniela Mauceri's Laboratory.

Memberships:

- Società Italiana di Neuroscienze (SINS)
- Socio Junior of Società Italian di Farmacologia (SIF)
- Federation of European Neuroscience Society (FENS)

Extra-activities:

Participation to Meet me tonight 2018 edition